Coordination Chemistry Reviews 253 (2009) 1056–1098

Contents lists available at ScienceDirect

Coordination Chemistry Reviews

journal homepage: www.elsevier.com/locate/ccr

Review

Chemistry of selena macrocycles

Arunashree Panda*

Department of Chemistry, Birla Institute of Technology and Science, Pilani-Goa Campus, Goa 403 726, India

Contents

Abbreviations: SSeTPP, tetraphenyl-21-selena-23-thiaporphyrin; Se2TPP, tetraphenyl-21,23-diselenaporphyrin; $PyPySe_2$, 2,11-diselena[3,3] (2,6) pyridinophane; Sebc, 3H-1,4,5,7-tetrahydro-2,6-benzodiselenonine; 14S4, 1,4,8,11-tetrathiacyclotetradecane; 16S4, 1,5,9,13-tetrathiacyclohexadecane; 15S5, 1,4,7,10,13-pentathiacyclopentadecane; 16S6, 1,3,6,9,11,14-hexathiacyclohexadecane; 18S6, 1,4,7,10,13,16-hexathiacyclooctadecane; 8Se2, 1,5-diselenacyclooctane; 14Se4, 1,4,8,11-tetraselenacyclotetradecane; 16Se4, 1,5,9,13-tetraselenacyclohexadecane; 24Se6, 1,5,9,13,17,21-hexaselenacyclotetracosane; 12Se3, 1,5,9-triselenacyclododecane; 20Se5, 1,5,9,13,17-pentaselenacycloicosane; $Me_4$8Se2, 3,3,7,7-tetramethyl-1,5-diselenacyclooctane; $Me_6$12Se3, 3,3,7,7,11,11-hexamethyl-1,5,9-triselenacyclododecane; $Me_8$16Se4, 3,3,7,7,11,11,15,15-octamethyl-1,5,9,13-tetraselenacyclohexadecane; 8Se2(OH), 1,5-diselenacyclooctane-3-ol; 16Se4(OH), 1,5,9,13-tetraselenacyclohexadecane-3-ol; 16Se4(OH)2, 1,5,9,13-tetraselenacyclohexadecane-3,11-diol; Naphtho-8Se2, 3,4-dihydro-2H-naphtho[1,8-*bc*]-1,5-diselenocine; Naphtho-12Se3, 3,4,7,8-tetrahydro-2H,6H-naphtho-[1,8-*bc*]-1,5,9-triselenacyclododecine; Dinaphtho-16Se4, 9,10,20,21-tetrahydro-8H,19H-dinaphtho[1',8'-*jk* ;1,8-*bc*][1,5,9,13]tetraselenacyclohexadecine; Dic, (2-pyridylmethyleneamino)benzo-15-crown-5; Dic-Se, 4'-(2-pyridylmethyleneamino)benzo-10-selena-15-crown-5; Benzo-15Se2O3, 11,12-benzo-1,4,7-trioxa-10,13-diselenacyclopentadecane; 9O2Se, 1-selena-4,7-dioxacyclononane; 18O4Se2, 1,10-diselena-4,17,13,16-tetraoxacyclooctadecane; 15-US-5, (*Z,Z,Z,Z,Z*)-1,4,7,10,13-pentaselenacyclopentadeca-2,5,8,11,14-pentaene; 18-US-6, (*Z,Z,Z,Z,Z,Z*)-1,4,7,10,13,16-hexaselenacyclooctadeca-2,5,8,11,14,17-hexaene; 21-US-7, (*Z,Z,Z,Z,Z,Z,Z*)-1,4,7,10,13,16,19-heptaselenacycloheneicosa-2,5,8,11,14,17,20-heptaene; 24-US-8, (*Z,Z,Z,Z,Z,Z,Z,Z*)-1,4,7,10,13,16,19,22-octaselenacyclotetracosa-2,5,8,11,14,17,20,23-octaene; 27-US-9, (*Z,Z,Z,Z,Z,Z,Z,Z,Z*)-1,4,7,10,13,16,19,22,25-nonaselenacycloheptacosa-2,5,8,11,14,17,20,23,26-nonaene.

* Tel.: +91 832 2580389; fax: +91 832 2557033.
E-mail address: panda_arunashree@yahoo.com.

0010-8545/$ – see front matter
doi:10.1016/j.ccr.2008.07.006

ARTICLE INFO

Article history:
Received 14 March 2008
Accepted 7 July 2008
Available online 16 July 2008

Keywords:
Selenium
Macrocyles
Cyclophanes
Coronands
Schiff base

ABSTRACT

The synthesis, structure and coordination chemistry of macrocyclic selenoethers with d-block and p-block elements reported since 1978 are described. Small cyclic selenoether 1,5-diselenacyclooctane (**8Se2**) and 3H-1,4,5,7-tetrahydro-2,6-benzodiselenonine (**sebc**) will be included for comparison. This report will not cover selenium-containing porphyrins.

1. Introduction

The design and synthesis of macrocycles of highly selective receptors for metal cations have continued to develop since the pioneering work of Pedersen [1], Lehn [2] and Cram [3] involving the preparation of cation selective crown ethers, cryptands and spherands. Macrocycles containing oxygen and sulfur as donor atoms have been extensively studied and are subjects of numerous reviews. Surprisingly, the investigation of this type of chemistry with the corresponding third and fourth row analogue is not well documented though this is a subject of growing interest. Incorporation of the larger Se and Te would lead to a change in size of the cage cavity and hence allow for some interesting coordination behavior. In addition the greater σ-donating ability of Se and Te would facilitate the complexation of a variety of metal ions. ^{77}Se and ^{125}Te NMR also provide an additional tool for the investigation of conformations in the solution which is absent for its lighter congeners oxygen and sulfur [4–8].

This topic has been included in several review articles by Hope and Levason (recent developments in the coordination chemistry of selenoether and telluroether ligands) [4] and Litvinov and Dyachenko (selenium-containing heterocycles) [5] and Levason et al. (macrocyclic thio-, seleno-, and telloroether ligands) [6] and Levason and Reid (recent developments in the chemistry of selenoethers and telluroethers) [7]. However, in view of the remarkable progress of this chemistry in recent years, it justifies to be detailed in an individual review article. The main focus of this review will be to present a comprehensive review on selenium macrocycle since 1988. However, the larger ring selenides reported before that will also be included. Selenium porphyrin derivatives will be excluded from the present discussion though tetraphenyl-21-selena-23-thiaporphyrin (**SSeTPP**) and tetraphenyl-21,23-diselenaporphyrin (**Se2TPP**) will be discussed briefly since these were the first large rings containing selenium atom.

In 1978, Ulman et al. [9] reported the synthesis of tetraphenyl-21-selena-23-thiaporphyrin (**1a**) and tetraphenyl-21,23-diselenaporphyrin (**1b**). The distance between the two selenium atoms is very short (2.85 Å) in **Se2TPP**. These are the first examples of large rings containing Se-atoms. The structural analysis of these molecules shows a chemical bonding interaction between the heteroatoms, which increases in the order S, Se and Te. This interaction, often called inner and outer aromaticity (ring current), influences the conjugative pathway in the molecule and are expressed in the chemical shifts of the hydrogen atoms at the periphery of the molecule. Therefore, subsequently, a high resolution NMR study of these porphyrins, their conjugate acids and some of their metal complexes is carried out to know the changes in inner and outer aromaticity due to the interaction between the heteroatom [10a]. These results are entirely consistent with the X···Y interaction described. The emission spectra, optical absorption spectra, ^{1}H NMR and X-ray structure of **SSeTPP** and **Se2TPP** were studied and interpreted by theoretical analysis using the IEH (iterative extended Hückel) model [10b].

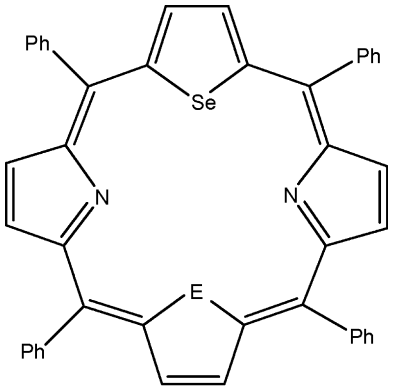

1a, E = S
1b, E = Se

2. Cyclophanes

Mitchell [11] in 1980 reported the first selenacyclophane, 2,11-diselena[3,3]metacyclophane (**2a**) as well as the cyclic trimer, 2,11,19-triselena[3,3,3]metacyclophane (**3a**) and their corresponding dimethyl (**2b**) and trimethyl derivatives (**3b**), respectively. These were prepared, in poor yield, from the coupling of xylylene bromide and Na_2Se. The low yield of the products is because of the reaction of highly air-sensitive intermediates diselenol or its dianion under alkaline condition with the dibromide to give a difficultly separable diselenide-polymer along with the desired coupling product.

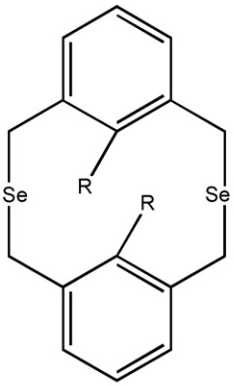

2a R = H,
2b r = CH_3

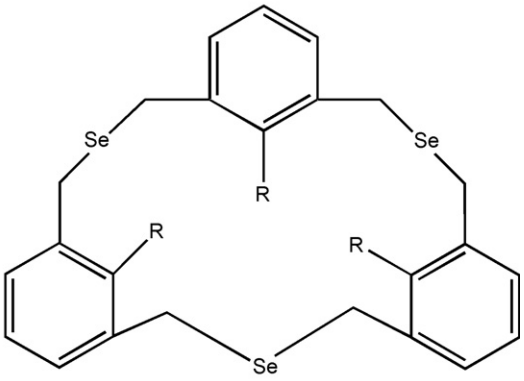

3a, R = H
3b, R = CH_3

Following this, Misumi and co-workers [12] proposed a method which provides much higher yields of the selenacyclophanes than *via* the sodium selenide coupling. Several cyclic diselenides (diselena[3,3]cyclophanes including **2a** (85% yield), alicyclic diselenides and diselenacrown ethers) were obtained *via* reductive coupling of bisselenocyanates and dihalide. Furthermore, this new method is convenient to prepare unsymmetrical as well as symmetrical diselenacyclophanes and it is easier to purify the products because of the formation of no tedious polymer. Later on the coordination chemistry of 2,11-diselena[3,3]orthocyclophane was studied with the (π-benzene)ruthenium(II) moiety. The cyclophane bonds as bidentate group 16 donors in [(η^6-C_6H_6)Ru(cyclophane)X]X (X = Cl or Br) [13].

In 1989, Muralidharan et al. [14a] reported the synthesis of 2,11-diselena[3,3] (2,6) pyridinophane (**PyPySe$_2$**). **PyPySe$_2$** exists predominantly in the *syn* conformation, which has undergone a flip of the pyridine rings and twist of the methylene bridges. The similar stability constants for Ni^{2+} and Cu^{2+} complexes with **PyPySe$_2$** indicate the equal adaptation of both metal ions in the heterophane cavity. The stability constant values also point to a typical host–guest interaction. The structure of [Ni**PyPySe$_2$**(H_2O)$_2$][ClO_4]$_2$·CH_3NO_2 (Fig. 1) shows a highly symmetrical heterophane in a *syn* conformation, in contrast to the Ni^{2+} complex of the thia analogue where the heterophane is distorted from the *syn* conformation. Interesting differences in the spectroscopic and conductivity properties of the Cu(II) complex are observed when the coordinated H_2O was replaced by Cl^-. The heterophane and its metal and charge-transfer complexes behave as semiconductors at room temperature with the Cu**PyPySe$_2$**Cl_2 complex exhibiting the best conductivity. This is the first report of the complexation and conductivity properties of the selenacyclophanes. Subsequently, several symmetrical and unsymmetrical bis-selenacyclophanes were prepared in excellent yields from the corresponding bis(selenocyanatomethyl) derivatives modifying Misumi's procedure [14b].

3. Selenium coronands

The first synthesis of macrocyclic polyethers was described by Pedersen many years ago. Crown ethers are able to form complexes with alkali and alkaline-earth metal cations, whereas thiacrown ethers prefer to coordinate with transition metals. Pinto et al. pioneered work on the synthesis of selenium coronands. The interest in selenium coronands arose because of (1) the accidental discovery of macrocyclic polyselenoethers from the reaction of sodium propane-1,3-bis(selenolate) in liquid ammonia and THF with dibromoethane and (2) to compare the properties of the selenium coronands with the lighter sulfur congeners which possesses conformations that differed significantly from those of their oxygen counterparts and yield metal complexes with unexpected electronic structures and redox properties. The synthesis of selenacrown ethers opened up the possibility of forming new complexes. Various metal complexes of selenacrown ethers have been investigated by a number of groups around the world (*vide infra*).

3.1. Synthesis of the ligands

The first example of a novel class of selenium coronands was reported by Pinto and co-workers [15a–e]. They described the synthesis, characterization and conformational analysis of the first ever selenium coronands **4**, **5**, 1,5-diselenacyclooctane (**8Se2**), 1,5,9,13-tetraselenacyclohexadecane (**16Se4**), **14Se4** and **24Se6** [15d] (Scheme 1).

1,3,7,9-Tetraselenocyclododecane (**4a**) exists in two distinct quadrangular conformations in the solid state where selenium atoms occupy alternate corner and side positions [15a]. In contrast, the preferred conformation of **4a** and its 5,5,11,11-tetramethyl analogue (**4b**) in solution is a [3333] quadrangle with the selenium atoms occupying only side positions [15b]. This is the first recorded dynamic NMR study of a selenium coronand.

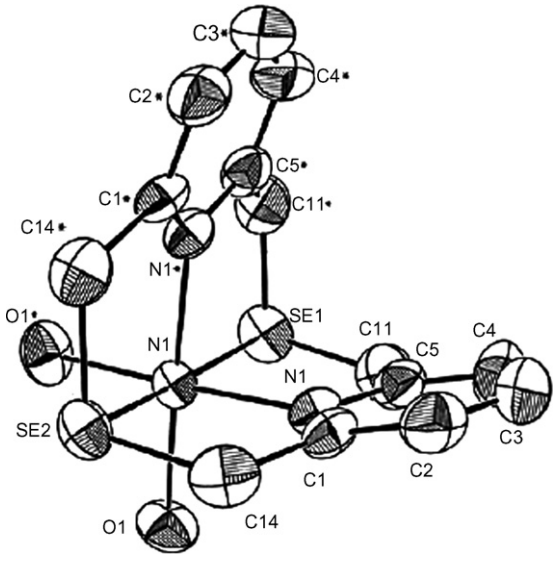

Fig. 1. ORTEP drawing of [Ni**PyPySe$_2$**(H_2O)$_2$]$^{2+}$. Reprinted with permission from [14a]. Copyright (1989) American Chemical Society.

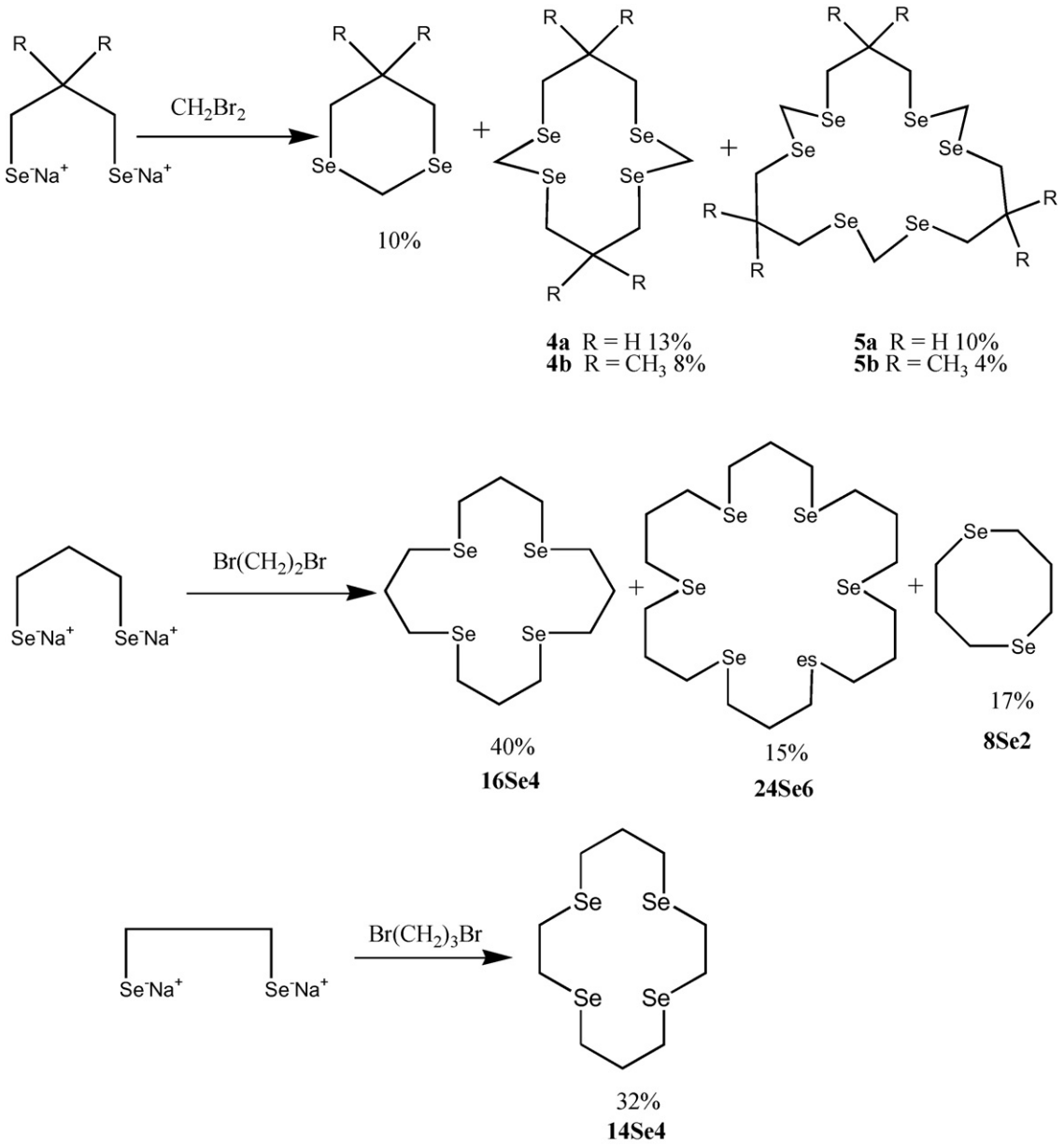

Scheme 1.

The structural model for **16Se4** (Fig. 2), though not definitive, contains two ordered and one disordered molecule which are all [3535] quadrangles with selenium atoms in alternate corner and side positions on the long sides [15d].

The structure of **24Se6** [15d] (Fig. 3) contains a single conformer possessing crystallographic inversion symmetry. While not in quadrangular shape, this molecule can be visualized as arising from the compression of a [4848] quadrangle.

The molecular structure of **14Se4** (Fig. 4) contains a single conformer lying on a crystallographic centre of inversion. The molecule is a [3434] quadrangle with selenium atoms at four corners. The corner-to-corner packing of molecules in this structure results in a significant Se···Se contact [15d].

The above method for the one-step synthesis of selenium coronands is ideally suited to the synthesis of macrocycles containing an even number of constituent selenium atoms. In 1995, the first examples of stepwise synthesis of two new selenium coronands, **12Se3** and **20Se5**, containing an odd number of selenium atoms

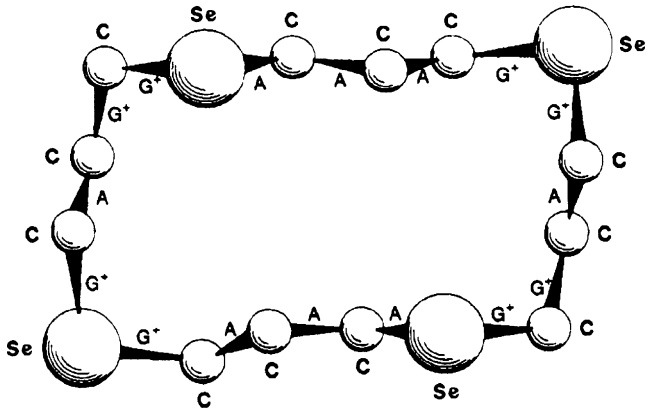

Fig. 2. Molecular structure of **16Se4**. Reprinted with permission from [15d]. Copyright (1989) American Chemical Society.

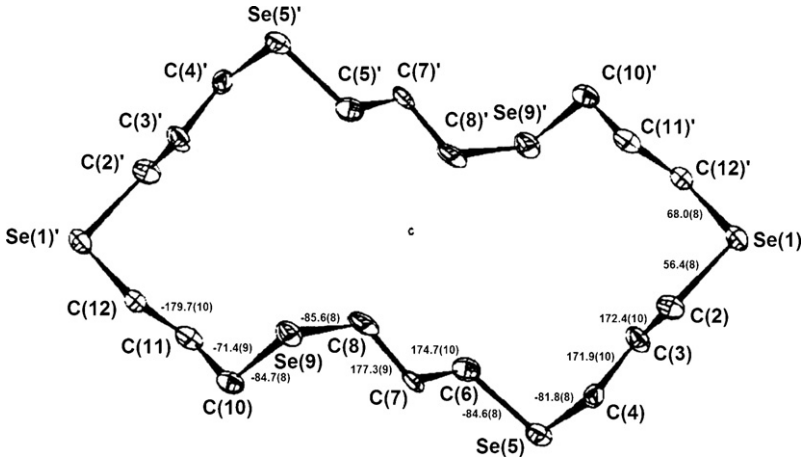

Fig. 3. Molecular structure of **24Se6**. Reprinted with permission from [15d]. Copyright (1989) American Chemical Society.

were reported by the same group (Scheme 2) [16] and provided new candidates for further study. The molecular structure of **12Se3** [17] adopted a conformation which maximizes the number of possible gauche C–Se–C–C bond torsion angles (Fig. 5). The molecule has no crystallographic symmetry but does have approximate local mirror (C_s or m) symmetry across a plane passing through Se(9) and C(3).

This methodology was modified subsequently to afford functionalized selenium coronands for incorporation into polymers or for the ready attachment of aliphatic or functionalized chains. The latter compounds are of interest for the development of transition metal ion-selective electrodes and membrane transport systems or for the generation of water soluble or micellar transition-metal ion transport systems. The hydroxyl-functionalized di and tetraselenoether macrocycles **8Se2(OH)**, **16Se4(OH)** and **16Se4(OH)$_2$** were synthesized using the appropriate hydroxyl-functionalized bis-selenocyanate precursor [18]. The strategy for the synthesis of the polymeric selenium coronands is to use these hydroxy functionalized selenium coronands subsequently to tether, to a second functional group (acrylate ester) to form a reactive monomer (Scheme 3). These are the first polymer bound selenium coronands which are electroactive. Their redox chemistry is rich, but complex, due to inter- and intra-molecular reactions that occur following oxidation.

A new selenium coronand 6,7,13,14-dibenzo-1,5,8,12-tetraselenacyclotetradecane (**dibenzo-14Se4**) was synthesized in a stepwise manner as shown in Scheme 4 [17]. The structure of **dibenzo-14Se4** presents a disordered superposition of two conformers. An interesting feature of this coronand is that the two arene rings are nearly coaxial (Fig. 6). Extension of this approach to the synthesis of analogues containing only two-carbon bridges was not successful due to the formation of labile ethylene episelenonium ions which decomposed by extrusion of ethylene.

A stepwise synthesis of **16Se2S2** [17] is performed (Scheme 5) in a manner analogous to that used for the thiamacrocycles [19]. The crystal structure of **16Se2S2** is similar but not isomorphous with, that of **16Se4**. There is disorder corresponding to the interchange of selenium and sulfur at the chalcogen atom sites in **16Se2S2** (Fig. 7), but it is not like the extensive orientational and/or conformational disorder shown in **16Se4** [15d].

A new symmetrical diseleno peri-bridged naphthalene, dinaphthol[1,8-b,c]-1,5-diselenocin, was reported by Fujihara et al. [20]. The facile electrochemical oxidation of dinaphthol[1,8-b,c]-1,5-diselenocin and its reaction with conc. H_2SO_4 to give the selenoxide confirm the existence of *peri* Se–Se interaction. New macrocyclic polyselenides containing naphthalene rings, **naptho-**

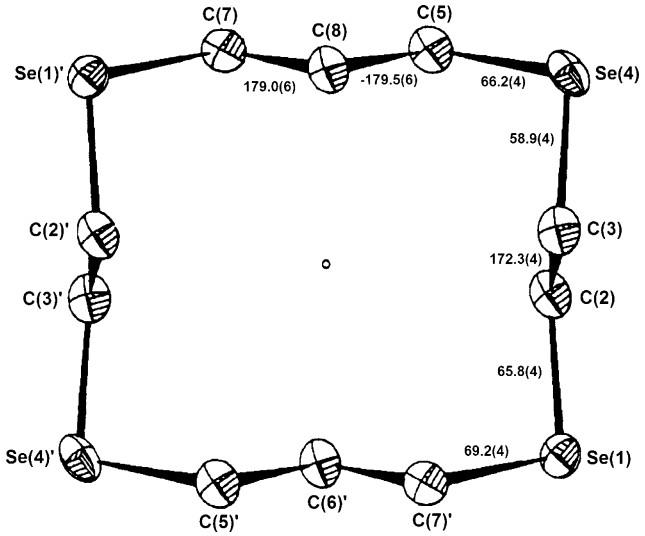

Fig. 4. Molecular structure of **14Se4**. Reprinted with permission from [15d]. Copyright (1989) American Chemical Society.

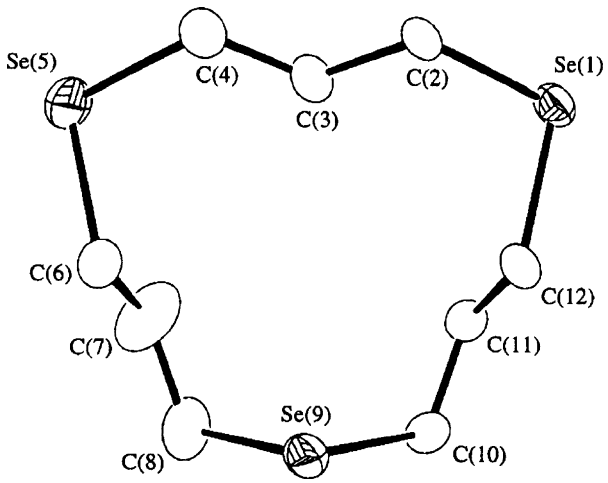

Fig. 5. Molecular structure of **12Se3**. Reprinted with permission from [17] and Prof. B. M. Pinto. Copyright (2000) American Chemical Society.

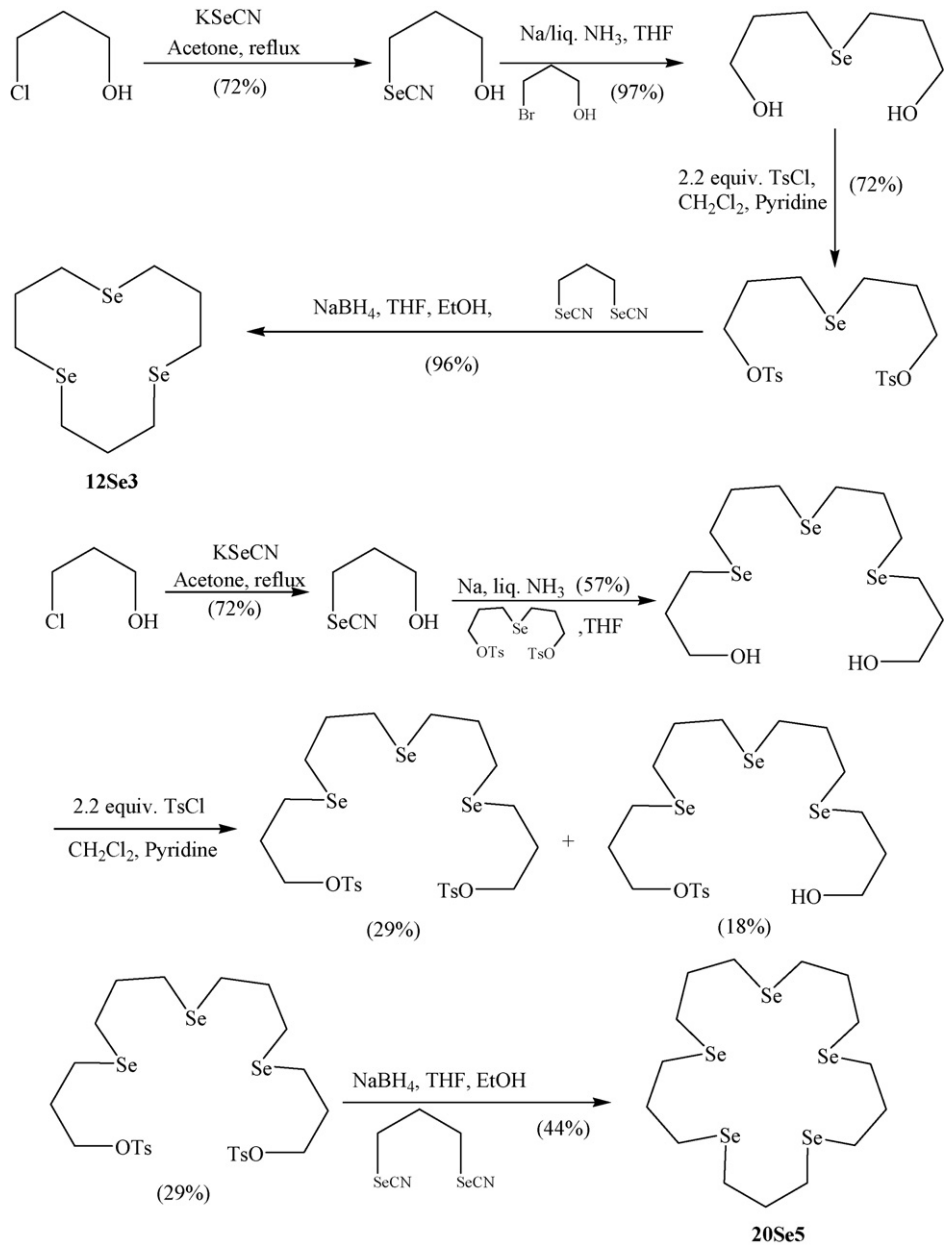

Scheme 2.

8Se2 (**17**), **naptho-12Se3** (**18**) and **dinaptho-16Se4** (**19**), were synthesized from the diselenide **15** as depicted in Scheme 6 [21]. The structure of the tetraselenide **19** indicates the transannular Se···Se contacts (Fig. 8) and intra-molecular π–π stacking of the naphthalene rings. The cyclic voltammograms of the selenides **17**–**19** show reversible oxidation peaks with remarkably low oxidation potentials. These facile oxidations of **17**–**19** are ascribed to the destabilization of macrocyclic polyselenides by transannular lone pair–lone pair repulsion and stabilization of the oxidized products by *peri* selenium participation, i.e. bond formation between the two selenium atoms. Hydrolysis of **naptho-8Se2** and **naptho-12Se3** in conc. H_2SO_4 affords the stable monoxides whereas the ring contracted products were obtained for **dinaptho-16Se4**.

Adams and co-workers [22,23] demonstrated a new procedure to synthesize polyselenoether macrocycles. The catalytic cyclo-oligomerization of 3,3-dimethylselenatane yields three new polyselenoether macrocycles **Me$_4$8Se2**, **Me$_6$12Se3** and **Me$_8$16Se4** (Scheme 7). This is a similar approach which the authors used to obtain a range of thioether macrocycles. In all cases, the gem-dimethyl groups of the macrocycles are directed towards the exterior of the rings (Fig. 9). Interestingly some methylene groups are directed towards the interior of the rings. The conformations of the rings and packing of the molecules are completely analogous to those of the reported sulfur homologues [24].

Booth et al. [25] reported an improved synthesis of 3H-1,4,5,7-tetrahydro-2,6-benzodiselenonine (**sebc**) *via* a [1+1] cyclization of $NCSe(CH_2)_3SeCN$ with *o*-$C_6H_4(CH_2Br)_2$. The analogous reaction with $Br(CH_2)_3Br$ however led to a mixture of **8Se2**, **16Se4**, **24Se6** and higher polymers [15d]. The structure of **sebc** shows Se atom lone pairs pointing out of the ring (Fig. 10).

Sebc and two other novel selenacrown ethers (**22**, **23**) were also prepared earlier by Kumagai and Akabori but was not completely characterized [26]. These selenacrown ethers were used as extractants for heavy and precious metal ions and are good extractants for copper(I), palladium (II), mercury(I) and methylmercury(II) in the presence of cobalt(II), nickel(II) and copper(I). The extractabilities

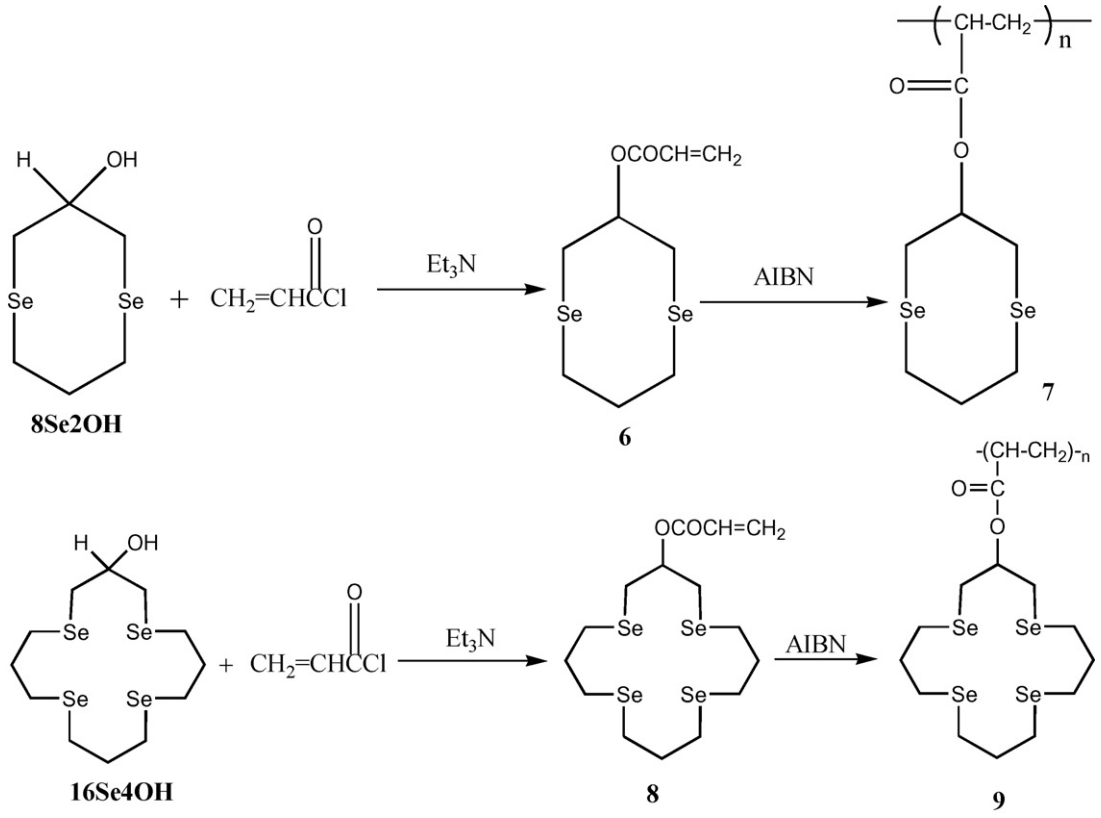

Scheme 3.

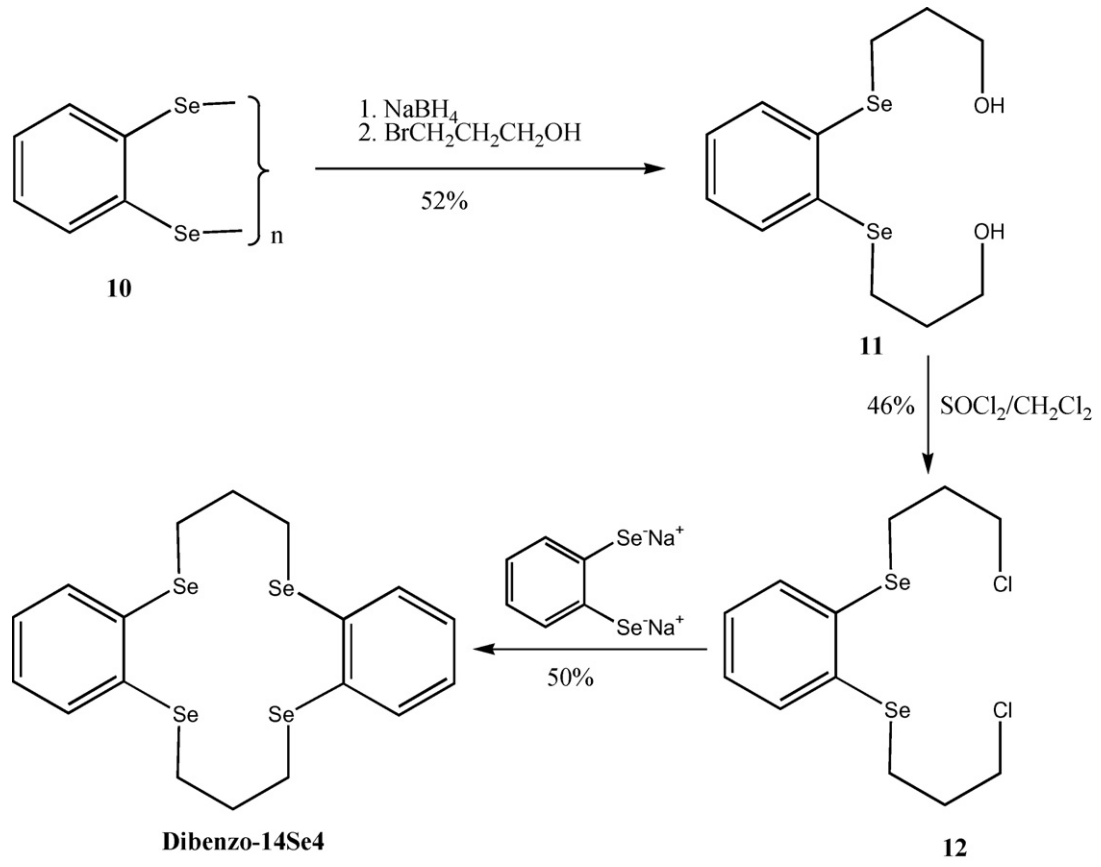

Scheme 4.

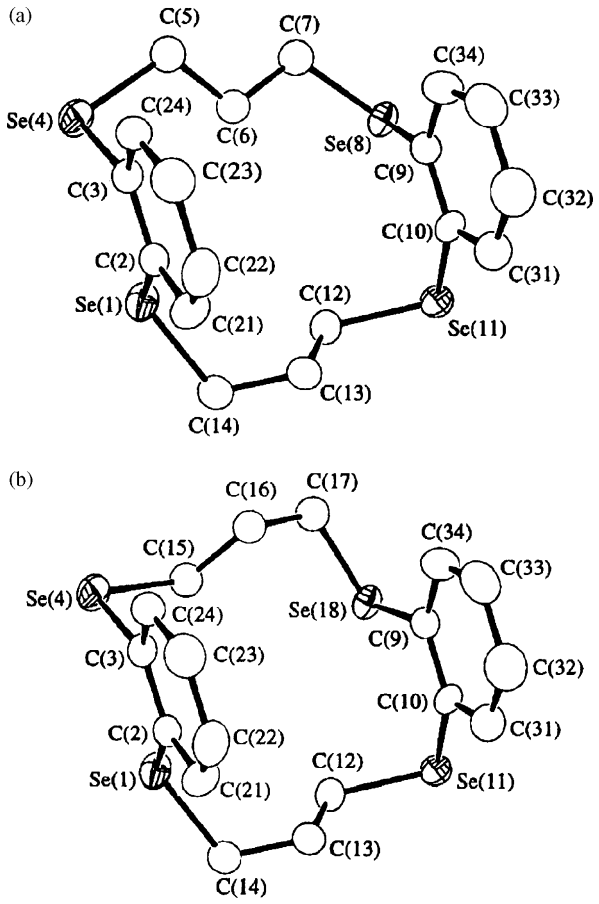

Fig. 6. Molecular structure of the major conformer (a) and minor conformer (b) of **dibenzo-14Se4**. Reprinted with permission from [17] and Prof. B. M. Pinto. Copyright (2000) American Chemical Society.

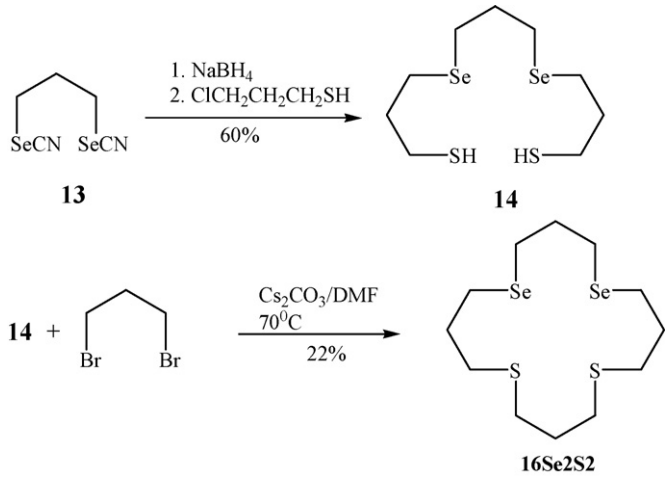

Scheme 5.

of these selenacrown ethers towards methylmercury(II) are higher than those of the structurally corresponding thiacrown ethers [26].

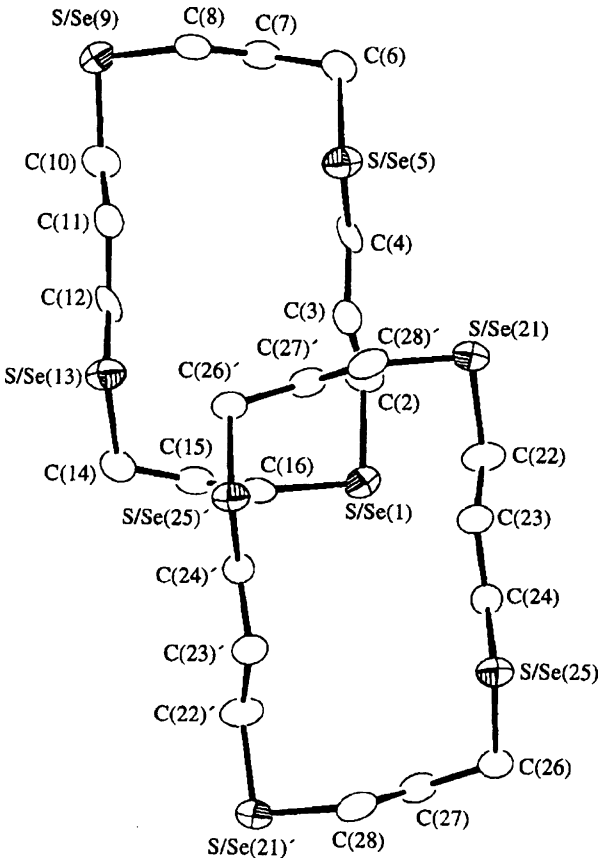

Fig. 7. The two crystallographically distinct molecules of **16Se2S2**. Reprinted with permission from [17] and Prof. B. M. Pinto. Copyright (2000) American Chemical Society.

3.2. Coordination chemistry with d-block elements

3.2.1. *8Se2*

The *cis*-disubstituted tetracarbonyl species of the early transition metal of the type [$M(CO)_4$**8Se2**] (M = Cr, Mo or W) were reported [27]. The structure of [$W(CO)_4$**8Se2**] shows the **8Se2** ligand occupying two mutually *cis* coordination sites with the CO ligands completing the distorted octahedral geometry. The W–CO distance *trans* to Se is significantly shorter than those *trans* to CO (Fig. 11). The ligand is in a chair–boat conformation.

The neutral *fac*-tricarbonyl species [$MX(CO)_3$**8Se2**] (M = Mn or Re and X = Cl, Br or I) are also known [27]. The CO stretching frequencies are comparable with those analogous structurally characterized *fac*-acyclic diselenoether complexes [28], hence indicating a *fac*-tricarbonyl arrangement for the **8Se2** compounds. The single peak in the ^{77}Se NMR indicates the presence of a single invertomer, unlike the presence of several invertomers in analogous acyclic diselenoether complexes. These species are isostructural, each displaying a distorted octahedral arrangement at the metal centre comprising three mutually *fac* CO ligands, a bidentate **8Se2**

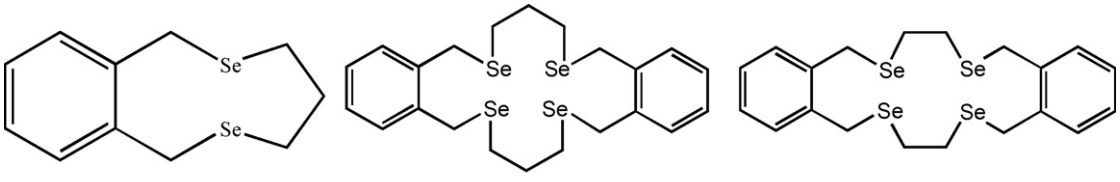

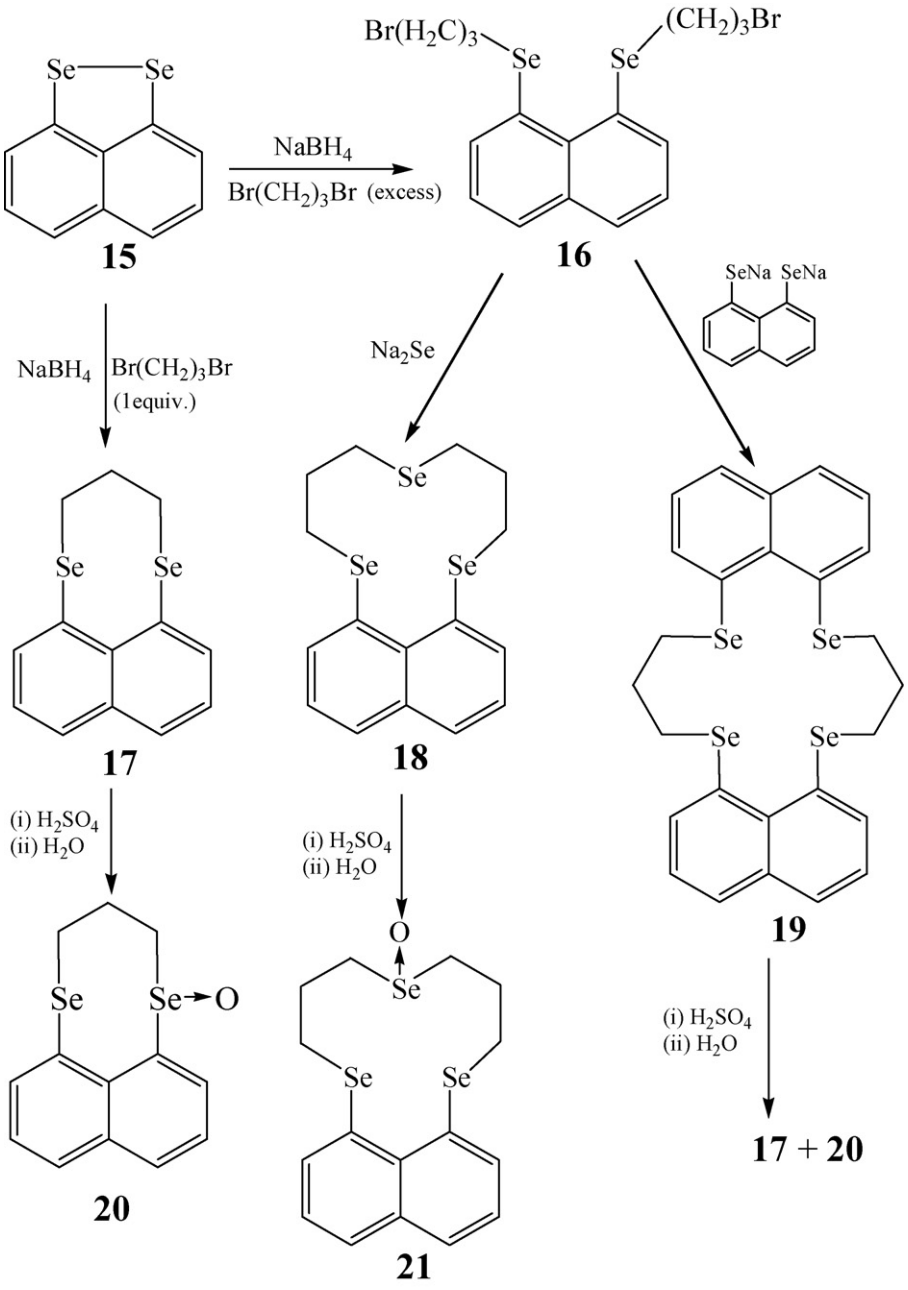

Scheme 6.

and a Br^- ligand (Fig. 12). The coordinated diselenoether adopts a chair–boat conformation.

The observation of two peaks at δ +244 and +197 in ^{77}Se-{^{1}H} NMR spectrum of [$RuCl_2$(**8Se2**)$_2$] confirms the *cis*-dichloro arrangement in solution [29]. Attempts to convert *cis*-[$RuCl_2$(**8Se2**)$_2$] into the *trans* isomer by the same route followed for *cis*-[$RuCl_2$**16Se4**] (*vide infra*) were unsuccessful. However, treatment of [$RuCl_2(py)_4$] with **8Se2** yields [$RuCl_2$(**8Se2**)$_2$] as a mixture of *cis* and *trans* isomers [δ (^{77}Se-{^{1}H}) 134] though the yield was poorer. [$RhCl_2$(**8Se2**)$_2$]BF_4 is also known [30].

The spectroscopic data of [M**8Se2**Cl_2] (M = Pd or Pt) are comparable with those of [M{$MeSe(CH_2)_3SeMe$}Cl_2] [31] which is concurrent with *cis*-planar Se_2Cl_2 donor sets [32]. The structure of [Pd**8Se2**Cl_2] (Fig. 13) shows coordination of both Se donors of the bidentate **8Se2** ligand and two *cis*-chloro ligands to the metal ion [32]. The coordinated **8Se2** ligand adopts the chair–boat conformation. Complexes of the type, bis(ligand) complexes, [M(**8Se2**)$_2$][PF_6]$_2$ (M = Pd, Pt) are known [32]. The high symmetry of the coordinated cyclic ligands excludes the occurrence of enantiomers for all four complexes, whereas the acyclic diselenoether complexes exist as both meso and DL enantiomers [31].

The planar dimethyl(selenoether)Pt^{II} complex [$PtMe_2$**8Se2**] was obtained by treatment of [$PtMe_2(SMe_2)_2$] with **8Se2** and was thoroughly characterized by spectroscopic methods and microanalysis [33]. Only one form of the complex is evident due to the cyclic structure of the **8Se2** ligand which eliminates the possibility of the stereoisomers. A stable distorted octahedral complex [$PtMe_3$I**8Se2**] forms in good yield and has been characterized similarly. This represents the first exam-

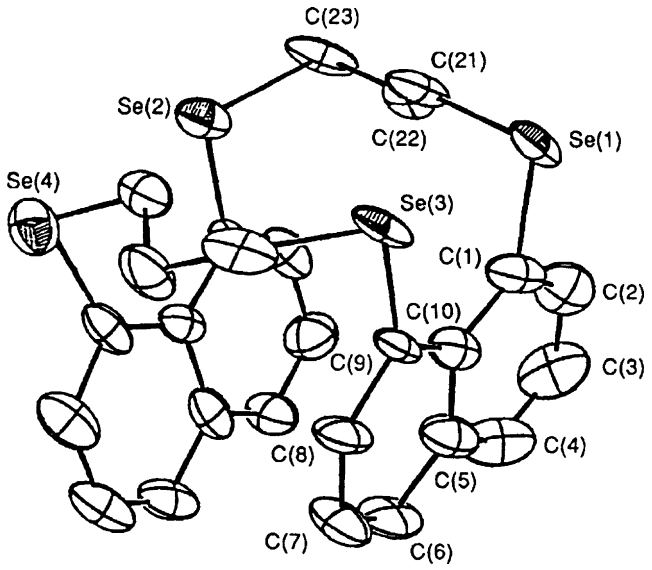

Fig. 8. The X-ray crystal structure of **dinaptho-16Se4** (**19**). Taken from Ref. [21a]. Reproduced by permission of The Royal Society of Chemistry.

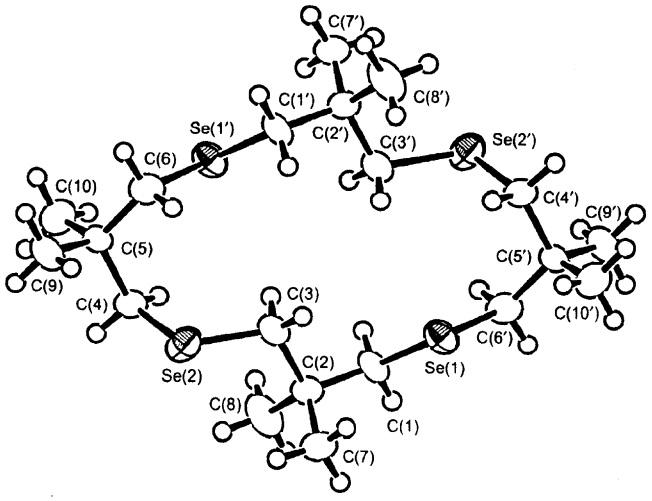

Fig. 9. ORTEP diagram of 3,3,7,7,11,11,15,15-octamethyl-1,5,9,13 tetraselenacyclohexadecane. Taken from Ref. [22]. Reproduced by permission of The Royal Society of Chemistry.

ple of alkyl Pt^{IV} complex with cyclic selenoether coordination [33].

Reid and co-workers [25] also reported complexes of type [M(**8Se2**)$_2$]Y (M = Cu, Y = PF_6; M = Ag, Y = BF_4) and [$(AuCl)_2$**8Se2**]. The structure of the Ag(I) complex shows a distorted tetrahedral Ag(I) monomer with two bidentate **8Se2** ligands (Fig. 14). The discrete molecular structure of this complex is different from the polymeric structure of the Ag(I) complex of acyclic diselenoether, i.e. $[Ag_n\{PhSe(CH_2)_3SePh\}_{2n}]^{n+}$. The **8Se2** ligands adopt a boat–boat conformation which is in contrast to the chair–boat conformation for all other structurally characterized complexes of **8Se2**.

8Se2 adopts a boat–boat conformation (crystal structure) when it binds to Ag(I) in a bis(bidentate) manner. However, a chair–boat conformation is observed when it binds to the metal ions {Pd(II), W(0), Mn(I)} in a bidentate manner. Also, by changing the ligand from acyclic to cyclic there is a substantial change in the solid state structure of Ag(I) complex. In most cases, the M–Se distances are comparable with the acyclic analogue.

3.2.2. *16Se4*

3.2.2.1. Cr, Mo and W. The blue, moisture sensitive Cr(III) complex [CrX_2**16Se4**]PF_6 was reported [34]. Attempts to prepare similar complexes from the ligand **8Se2** failed reflecting the weaker coordinating power of the diselenoether compared to **16Se4**. The low 10Dq and large B value of the complex show a weak binding of the soft selenium ligands to the hard Cr^{III} as might be expected from a hard-metal–soft-ligand complex. The longer bond length $d(Cr^{III}–Se)$, obtained from chromium *K*-edge EXAFS studies, compared to the M–Se bond lengths of other complexes (Table 1) supports a weak Cr–Se bonding despite the smaller radius of Cr(III). The syntheses of the seven-coordinate M(II) species [{$MX_2(CO)_3$}$_2$**16Se4**] (M = Mo or W and X = Br or I) were described [27]. Because of the poor solubility of these complexes in chlorocarbons and decomposition in coordinating solvents, complete characterization was not successful. Comparison of the IR data of the dinuclear complexes with analogous seven-coordinate

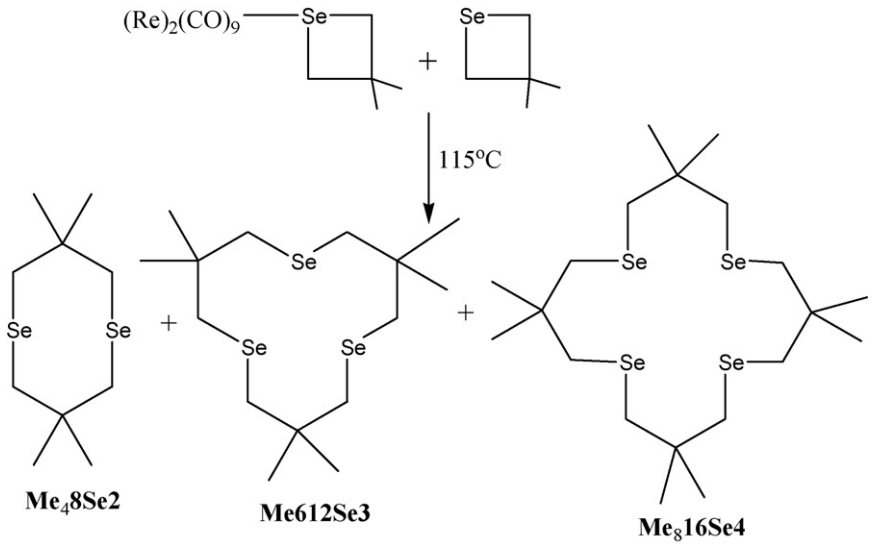

Scheme 7.

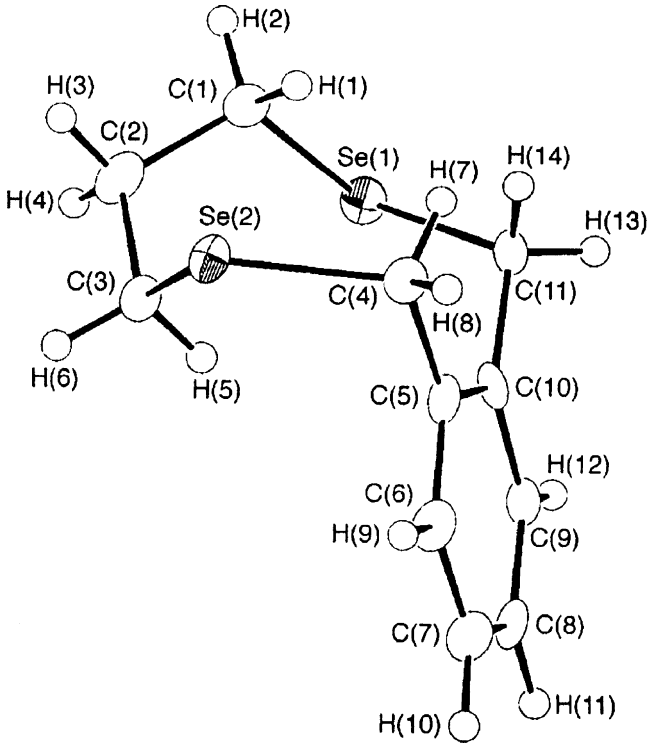

Fig. 10. Molecular structure of **sebc**. Taken from Ref. [25]. Reproduced by permission of The Royal Society of Chemistry.

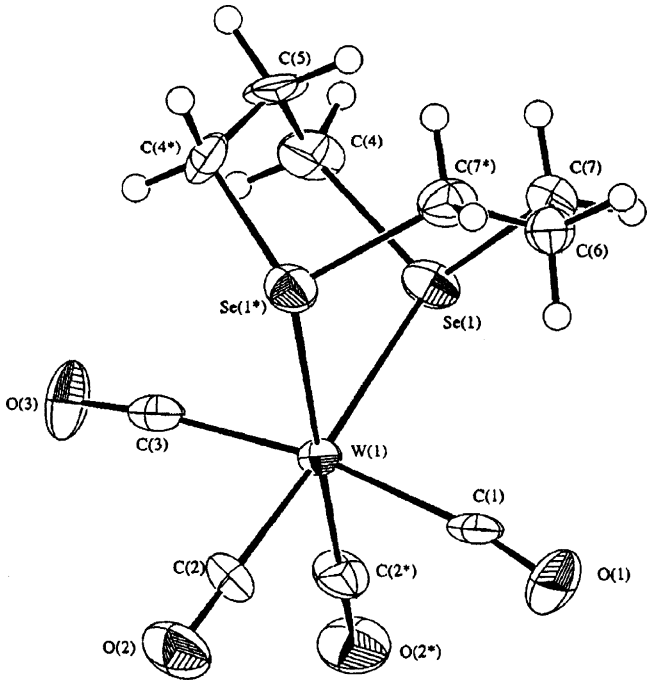

Fig. 11. View of the structure of $[W(CO)_4(\mathbf{8Se2})]$. Taken from Ref. [27]. Reproduced by permission of The Royal Society of Chemistry.

thioether macrocyclic derivative suggested a probable seven-coordinate structure with bridging **16Se4**, which can be formulated as $[Mo_2X_4(CO)_6(\mu\text{-}\mathbf{16Se4}\text{-Se,Se′,Se″,Se‴})]$. In contrast, the W(II) complex of **16Se4** is mononuclear with two-coordinated Se donors leaving the remaining two Se atoms uncoordinated.

3.2.2.2. Mn and Re. **16Se4** acts as a bidentate ligand in both the dinuclear, $[\{MnCl(CO)_3\}_2\mathbf{16Se4}]$, and in the mononuclear complex, $[ReCl(CO)_3\mathbf{16Se4}]$, leaving two free Se donors in later. The bright orange cationic manganese(I) species *fac*-$[Mn(CO)_3(\eta^3\text{-}\mathbf{16Se4})]CF_3SO_3$ was also reported [27].

3.2.2.3. Ru and Os. A series of *cis* and *trans* $[Ru(II)X_2\mathbf{16Se4}]$ (X = Cl, Br or I) have been reported [29]. The *cis* arrangement of the two halogen atoms in the complex $[RuX_2\mathbf{16Se4}]$ was verified by ^{77}Se-{H} NMR spectroscopy. The rapid formation of *cis* isomer of Ru(II) compound is in contrast to the observation of *trans* dichloro arrangement of Rh(III) in $[RhCl_2\mathbf{16Se4}]^+$ [35], though the ionic radii of Ru^{II} and Rh^{III} are very similar. The structure of the complex confirms that the Ru^{II} ion is coordinated in a distorted octahedral arrangement to two mutually *cis* chlorine atoms and four Se donors of a folded **16Se4** molecule. *d*(Ru–Se) *trans* to Se are marginally longer than *d*(Ru–Se) *trans* to Cl, indicating the greater *trans* influence of Se over Cl (Fig. 15) [29]. The effect observed in this selenoether species is smaller than that seen in the thioether species [36].

Unlike $[RuX_2\mathbf{8Se2}]$, the *trans* isomers of $[RuX_2\mathbf{16Se4}]$ (X = Cl or Br) could be prepared by refluxing the corresponding *cis* complexes in nitromethane. Because of the poor solubility of $[RuI_2\mathbf{16Se4}]$ in common organic solvents, complete characterization of the complex could not be done. The *trans* arrangement was confirmed by ^{77}Se NMR spectroscopy which shows a single resonance at δ +155. Attempts to obtain suitable crystals for an X-ray analysis were unsuccessful.

Also, the *trans*-$[RuCl(PPh_3)\mathbf{16Se4}]PF_6$ could be generated from the reaction of $[RuCl_2(PPh_3)_3]$ and **16Se4**. Multinuclear NMR (^{31}P and ^{77}Se) spectra support the *trans*-arrangement of Cl and PPh_3 [29]. The structure of this complex shows the Ru^{II} coordinated in an endocyclic manner to the tetradentate selenoether ligand, with mutually *trans* Cl and PPh_3 ligands completing the distorted octa-

Table 1
M–Se and M–S bond distances (Å) of **16Se4** complexes and macrocyclic polythiaethers

Complexes of **16Se4**	M–Se	Complexes of thia-macrocycles	M–S
$[CrCl_2(\mathbf{16Se4})]^+$	2.566(5)		
trans-$[CoBr_2(\mathbf{16Se4})]^+$	2.393(1), 2.402(1)		
trans-$[RhCl_2(\mathbf{16Se4})]^+$	2.456(1), 2.461(1)	*trans*-$[RhCl_2(\mathbf{16S4})]^+$	2.348(3)
trans-$[IrBr_2(\mathbf{16Se4})]^+$	2.470(3), 2.461(3), 2.462(3)		
cis-$[RuCl_2(\mathbf{16Se4})]$	2.465(1), 2.440(2), 2.453(1), 2.396(1)	*cis*-$[RuCl_2(\mathbf{14S4})]$	2.262(1), 2.333(1)
trans-$[RuCl(PPh_3)(\mathbf{16Se4})]$	2.488(3), 2.465(3), 2.497(3)		
$[Pd(\mathbf{16Se4})](PF_6)_2\cdot 2MeCN$	2.435(2), 2.428(1)	$[Pd(\mathbf{16S4})]^{2+}$	2.303(10), 2.304(10)
$[Pd(\mathbf{16Se4})](BF_4)_2$	2.423(1)		
$[Pd(\mathbf{16Se4}](BF_4Cl)$	2.4560(7), 2.4395(7), 2.4583(7), 2.4430(7)		
$[Pt(\mathbf{16Se4})]^{2+}$	2.420(3), 2.417(3)		
$[PtCl_2(\mathbf{16Se4})]^{2+}$	2.501596), 2.4957(7)		
$[Cu(\mathbf{16Se4})]^{2+}$	2.4592(9), 2.4553(9)	$[Cu(\mathbf{16S4})]^{2+}$	2.3314(13), 2.3874(17)
$[Cu(\mathbf{16Se4})]+$	2.42–2.52	Cu^{I} complex of **15S5**, **16S6**, **18S6**, **14S4**	2.243(5)–2.342(3)

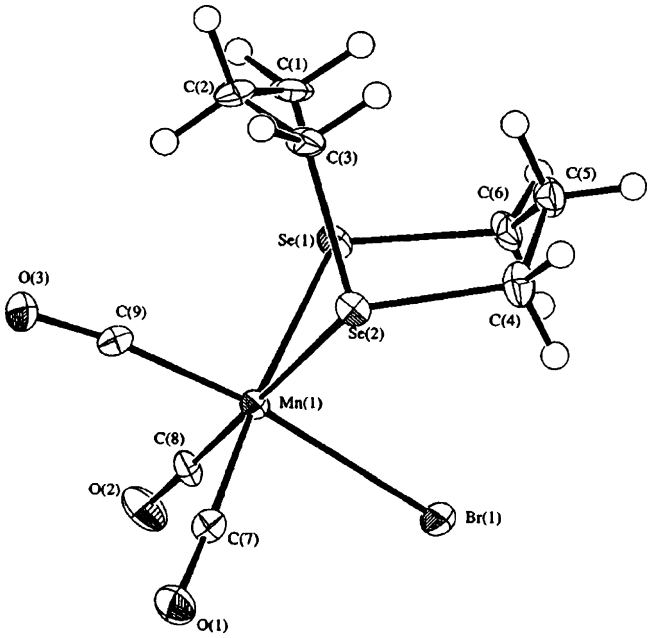

Fig. 12. Crystal structure of [$MnBr(CO)_3$(**8Se2**)]. Taken from Ref. [27]. Reproduced by permission of The Royal Society of Chemistry.

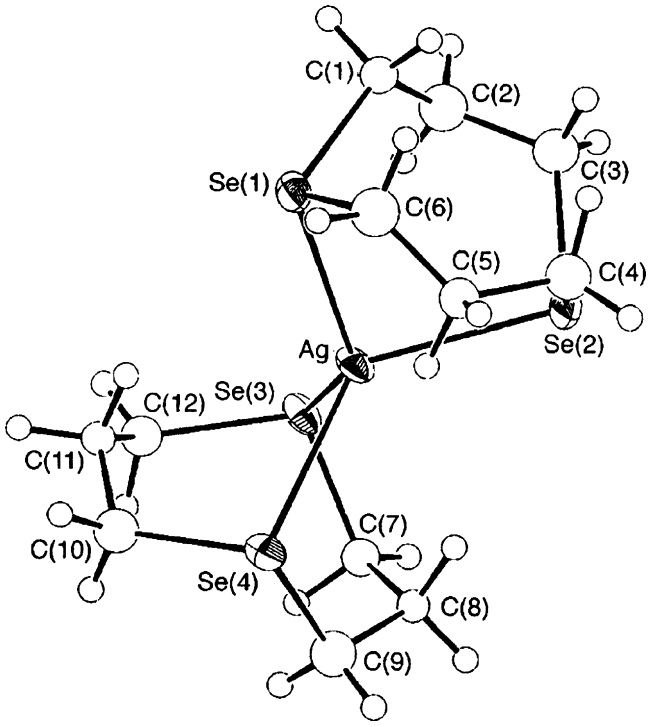

Fig. 14. Molecular structure of [Ag(**8Se2**)$_2$]BF_4. Taken from Ref. [25]. Reproduced by permission of The Royal Society of Chemistry.

hedral geometry (Fig. 16). Due to the steric influence of the bulky PPh_3, all the methylene groups are directed to the opposite side of the RuSe4 plane from the PPh_3 ligand, which in turns leads to a rare *all up* arrangement for the Se-based lone pairs of the ligand.

A *trans* chlorophosphine arrangement at the octahedral Os^{II}, as seen for the ruthenium analogue, was confirmed from the ^{77}Se-$\{^1H\}$ NMR spectrum of [$OsCl(PPh_3)$**16Se4**]PF_6 [29]. Electrochemical studies on metal(II) compounds showed that all the dichloro, dibromo and chlorophosphine complexes exhibits a reversible M^{II}–M^{III} couple. The chemical oxidation of *trans*-[$RuBr_2$**16Se4**] to the corresponding ruthenium(III) species was achieved by treating the complex with Br_2–CCl_4 giving a green solid of *trans*-[$RuBr_2$**16Se4**]Br.

3.2.2.4. Co, Rh and Ir. Reid and co-workers [30,35] reported the preparation and characterization of the homologous species [MX_2**16Se4**]$^+$ (M = Co, X = Cl, Br or I; M = Rh or Ir, X = Cl or Br).

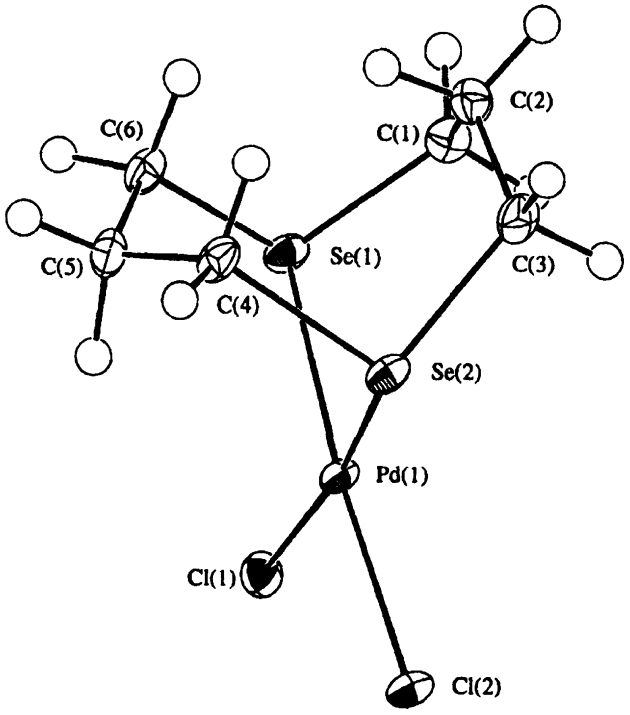

Fig. 13. Crystal structure of [Pd(**8Se2**)]Cl_2. Reprinted from Ref. [32]. Copyright (1995), with permission from Elsevier.

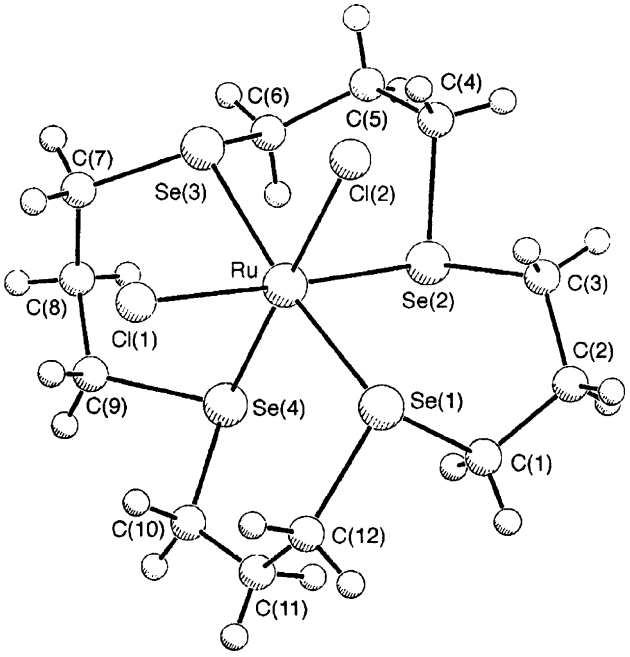

Fig. 15. Crystal structure of *cis*-[$RuCl_2$(**16Se4**)]. Taken from Ref. [29]. Reproduced by permission of The Royal Society of Chemistry.

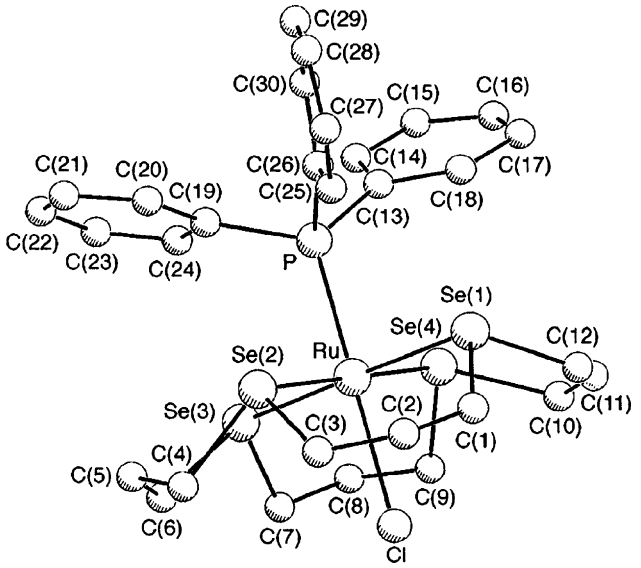

Fig. 16. Crystal structure of *trans*-[RuCl(PPh_3)(**16Se4**)]$^+$. Taken from Ref. [29]. Reproduced by permission of The Royal Society of Chemistry.

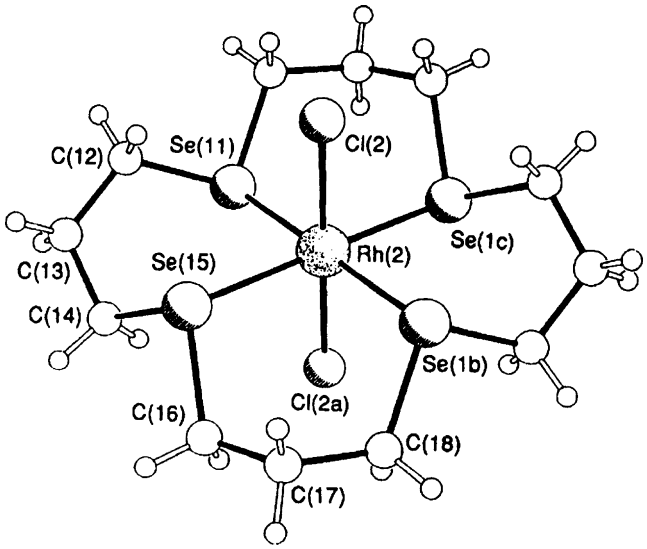

Fig. 18. Crystal structure of one molecule of *trans*-[$RhC1_2$(**16Se4**)]$^+$. Taken from Ref. [35]. Reproduced by permission of The Royal Society of Chemistry.

The UV/vis, ^{59}Co and ^{77}Se NMR spectroscopy data of [CoX_2**16Se4**] (X = Cl, Br) show the presence of only the *trans* species whereas a mixture of *cis* and *trans* forms is present when X = I. The ^{77}Se NMR studies show the presence of *cis* and *trans* isomers for Rh(III) and Ir(III) complexes in dmf solution whereas only *trans* in $MeNO_2$ which reflects the different solubilities of the *cis* and *trans* forms in the two solvents. The structure of the centrosymmetric cations [MX_2**16Se4**]$^+$ (M = Co, Rh or Ir) show a *trans*-dihalide arrangement with the macrocyclic Se donors occupying the equatorial coordination sites and the non-bonded selenium lone pairs adopting up, up, down down configuration (Figs. 17 and 18) [30]. The M(III) ions occupy the macrocyclic cavity and have distorted octahedral geometry coordinating through all Se donor atoms and two *trans*-halide ligands. The stereochemistry is similar to that seen for [$RhCl_2$**16S4**]$^+$ which also exhibits a *trans*-dichloro geometry with the thioether crown occupying the equatorial plane. Attempts to prepare the cobalt(III) species of **8Se2**, [CoX_2(**8Se2**)]$^+$, *via* an analogous route were unsuccessful reflecting the enhanced stability imparted by the macrocycle **16Se4**.

3.2.2.5. Ni, Pd and Pt. The assignments of *trans* octahedral geometries to the paramagnetic complexes [NiX_2**16Se4**], from NiX_2 (X = Cl, Br or I) with **16Se4**, follows from their paramagnetism (μ ca. 3 μ_B) and UV/vis spectra [37]. The poor solubility of [NiX_2**16Se4**] in most solvents precluded growth of crystals suitable for an X-ray study. So, nickel *K*-edge (extended X-ray absorption fine structure) was used to obtain structural data [37].

Reaction of MCl_2 (M = Pd, Pt) with **16Se4** and $TlPF_6$ afforded [M**16Se4**]$(PF_6)_2$ [M = Pd, Pt] as yellow and colorless solids [38]. Both the species are isomorphous with a square planar arrangement of the four selenoether donors around the central metal ion in an endocyclic arrangement (Fig. 19). The macrocycle adopts an up, up, down, down (*c*,*t*,*c*,*t*) configuration in each case. The metal ion lies precisely in the Se4 coordination plane. A similar structure has been observed for the thioether macrocyclic complex [Pd**16S4**]$(PF_6)_2$ suggesting a similar cavity size. Two non-coordinating MeCN solvent molecules are associated with each M^{2+} cation. The overall stereochemistry of [M**16Se4**]$^{2+}$ is similar to the acyclic bis(bidentate) Pt^{II} complex [32]. Variable temperature ^{77}Se and ^{195}Pt NMR studies show the presence of invertomers for these complexes in solution [38] contrast to the retention of the solid-state configuration of all the other complexes of **16Se4** in solution.

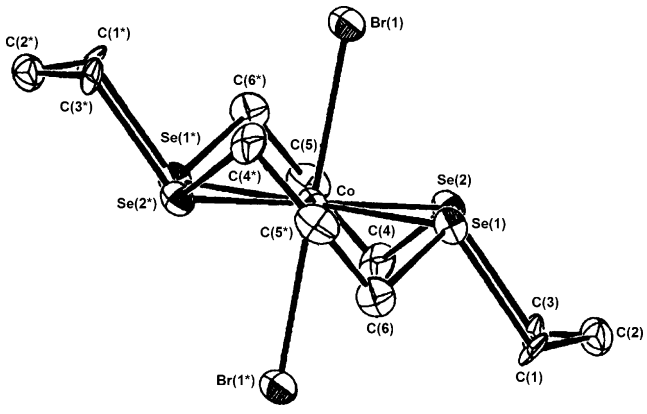

Fig. 17. Crystal structure of the *trans*-[$CoBr_2$**16Se4**]$^+$ cation. Taken from Ref. [30]. Reproduced by permission of The Royal Society of Chemistry.

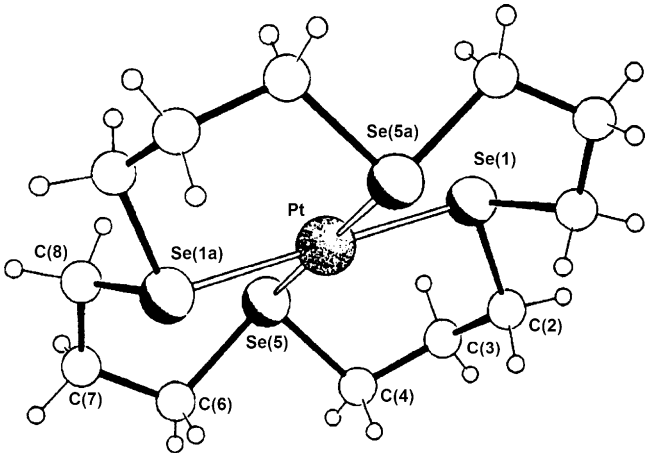

Fig. 19. Crystal structure of [Pt(**16Se4**)]$^{2+}$. Reprinted with permission from Ref. [38]. Copyright (1995) American Chemical Society.

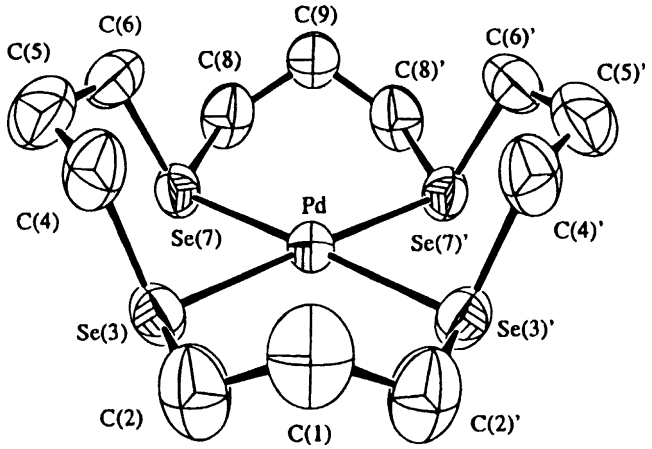

Fig. 20. Structure of the [Pd(**16Se4**)](BF$_4$)$_2$. Reprinted with permission from Ref. [39]. Copyright (1996) American Chemical Society.

In the following year Pinto and co-workers [39] reported the Pd(II) complexes of **16Se4** having different counterions with a different ligand configuration. In both [Pd(**16Se4**)][BF$_4$]$_2$ (**24**) (Fig. 20) and [Pd(**16Se4**)]ClBF$_4$ (**25**) complexes Pd is centrally bound by the four Se atoms in a square planar arrangement. In both cases the configuration of the complex cation was *c*,*c*,*c*.

In principle, **16Se4** can form diastereomeric coronand complexes of four different configurations. Based on the relative orientations with respect to the coordination plane of the non-bonding pairs of electrons on adjacent selenium atoms, these diasteromers can be characterized as *c*,*c*,*c*; *c*,*t*,*c*; *t*,*t*,*t*; *c*,*c*,*t* (Fig. 21). The *c*,*c*,*c* and *c*,*t*,*c* configurations are the most commonly observed configurations in metal complexes of the analogous thia macrocycle **16S4** and related coronands.

In all the complexes of **16Se4** reported untill 1995, where the structures contains a pseudotetragonally coordinated metal complex, the **16Se4** ligand was in *c*,*t*,*c* configuration. The complexes **24** and **25** represent the first observation of **16Se4** complexes having the *c*,*c*,*c* configuration (the non-bonding electron pairs of all the Se atoms are directed toward one side of the coordination plane of the coronand) [39].

The complex cation [Pd(**16Se4**)]$^{2+}$ which was observed as *c*,*t*,*c* diastereomer [38] occurs as its *c*,*c*,*c* diasteromer in crystals of its tetrafluoroborate and chloro, tetrafluoroborate salts. This is because, the complex cation in **24** and **25** contain smaller BF_4^-, and thus more polarizing anions and no solvent of crystallization whereas the Pd^{2+} complex reported by Reid and co-workers [38] contains larger PF_6^- anions and two solvent molecules of crystallization. Examples of *t*,*t*,*t* and *c*,*c*,*t* configurations are rare. The *t*,*t*,*t* isomer is observed in [Hg(**16S4**)][ClO$_4$]$_2$, suggesting that larger metal ions might prefer this configuration. Molecular orbital calculations [40] of the energy required to transform **16S4** from its free conformation to some of the conformations required for square planar complexation indicate that the conformations may be preferred in the order *c*,*t*,*c* > *c*,*c*,*c* > *t*,*t*,*t*. No calculation was reported for *c*,*c*,*t*. The multinuclear, variable temperature and two-dimensional NMR spectroscopic results show that aqueous solutions of [Pd(**16Se4**)][BF$_4$]$_2$, at room temperature, contain the *c*,*t*,*c* and *c*,*c*,*c* forms as predominant species in the ratio 1.6:1. At elevated temperatures, ^{1}H NMR spectroscopy reveals the configurational interconversion.

The first example of platinum(IV) complexes [Pt**16Se4**X$_2$][PF$_6$]$_2$ (X = Cl, Br) was obtained by the halogen oxidation of [Pt**16Se4**][PF$_6$]$_2$ [41]. The structure of the complex confirmed the Se$_4$X$_2$ donor set in these octahedral species, and illustrate the ability of the soft selenoether macrocycle to stabilize the relatively hard platinum(IV) centre. In [PtCl$_2$**16Se4**)][PF$_6$]$_2$ the Pt atom has a *trans*-dichloro arrangement with the four Se donor atoms coordinated equatorially. The ligand is in an up, up, down, down configuration [41]. Observation of single ^{77}Se{^{1}H} and ^{195}Pt{^{1}H} resonances indicates the presence of only one invertomer similar to the other octrahedral complexes and thus denies the presence of several invertomers as shown by the Pt(II) precursor [38] in solution.

The reaction chemistry of alkyl-(chalcogenoether)transition-metal species are rare. The first planar dimethyl(selenoether)Pt^{II} complex [PtMe$_2$**16Se4**] was obtained by treatment of [PtMe$_2$(SMe$_2$)$_2$] with **16Se4** [33]. Due to the poor solubility of this compound only ^{1}H NMR spectroscopic data were obtained for this compound, although the formulation was supported by microanalysis and positive ion electrospray MS measurements. This Pt(II) complex is rather unstable and decomposes even when stored under N_2.

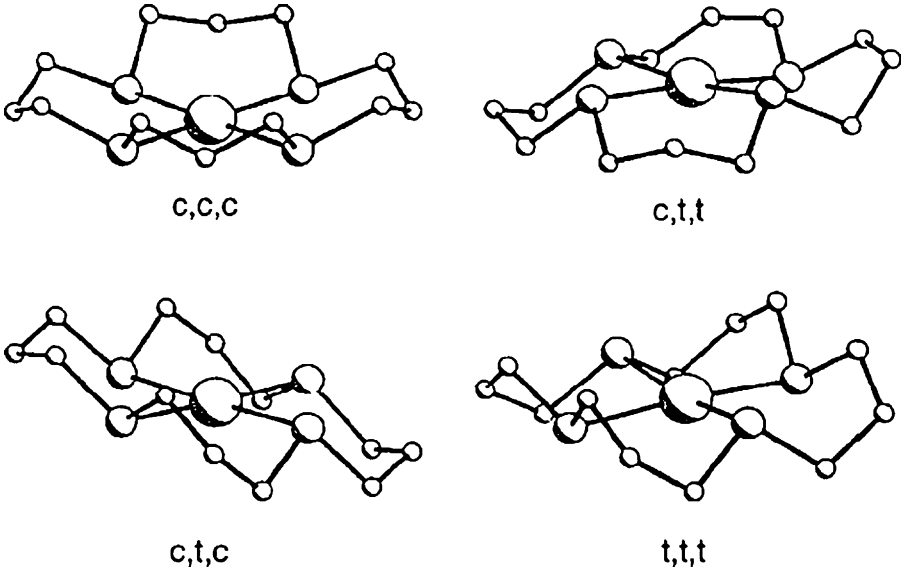

Fig. 21. Four possible configurations of **16Se4** in [Pd(**16Se4**)][BF$_4$]$_2$. Reprinted with permission from Ref. [39]. Copyright (1996) American Chemical Society.

The distorted octahedral (trimethyl)Pt^{IV} complex, [$PtMe_3$I**16Se4**], is the first example of alkyl Pt^{IV} complex with macrocyclic selenoether coordination [33]. Treatment of [$PtMe_3$I(κ^2-**16Se4**)] with $TlPF_6$ resulted in clean abstraction of the iodo ligand giving [$PtMe_3$(κ^3-(**16Se4**))]PF_6 as a white solid. This is a rare and first example of a cationic (alkyl)Pt^{IV} complex with selenoether coordination. The Pt^{IV} complex is more stable than the Pt(II) species possibly due to the very strong ligand field imparted by the Me ligands in the Pt^{IV} species. This compound is coordinatively saturated and hence provides limited possibility for metal-assisted Se–C bond fission.

3.2.2.6. Cu, Ag and Au. In 1990 Pinto and co-workers [42] reported the first complex of a selenium coronand **16Se4**, namely (1,5,9,13-tetraselenacyclohexadecane)copper(II) trifluoromethanesulfonate, [Cu(**16Se4**)][SO_3CF_3]$_2$. The Cu(II) complex is structurally similar to that of thia ether complex [Cu(16S4)][ClO_4]$_2$ [43]. The complex possesses a tetragonally distorted octahedral geometry at Cu with *trans*-axial triflate donors (Fig. 22). The stereochemistry of the coronand is *c,t,c* [42].

The complex undergoes an unprecedented electron-transfer reaction in coordinating organic solvents to give [Cu(**16Se4**)][SO_3CF_3] (a polymeric Cu(I) adduct) as well as the intermediate radical cation [**16Se4**]$^{+\bullet}$ and the stable dication [**16Se4**]$^{2+}$. The structure of the **16Se4** dication is significantly

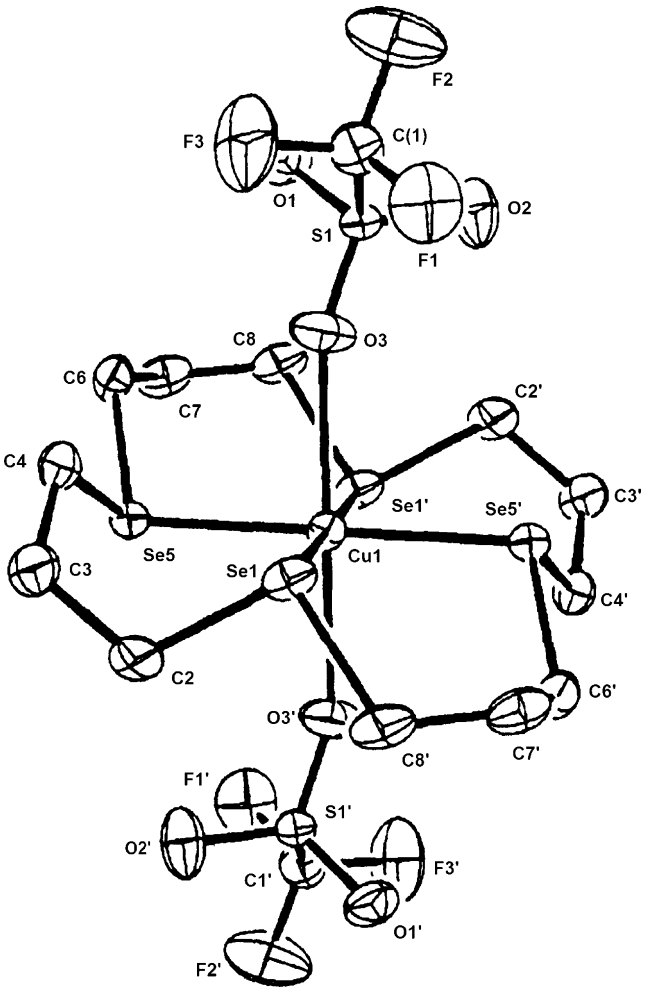

Fig. 22. Molecular structure of [Cu**16Se4**][CF_3SO_3]$_2$. Reprinted with permission from Ref. [42]. Copyright (1990) American Chemical Society.

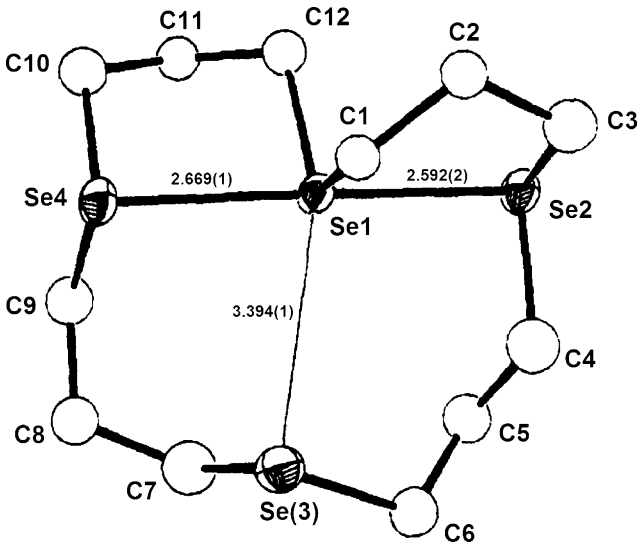

Fig. 23. Molecular structure of the dication from [**16Se4**]$^{2+}$([SO_3CF_3]$^-$)$_2$. Reprinted with permission from Ref. [42]. Copyright (1990) American Chemical Society.

different from **16Se4**. In the [**16Se4**]$^{2+}$ dication, three selenium atoms are nearly collinear so that the positive charges are on the two outside selenium atoms for best separation (Fig. 23). There is a weak secondary interaction between the fourth selenium atom and the central selenium atom so that the positive charges are dispersed among the four selenium atoms. The bonds to the central Se atom (Se(1)) are arranged in a pseudo-trigonal-bipyramidal geometry typical of tetracoordinate Se(IV). The longer Se···O and Se···F distances suggests dipolar electrostatic attraction between cation and anion. This was the first report of a selenium coronand dication resulting from an electron-transfer reaction of a metal–selenium coronand complex. The intermediates, **16Se4**$^{+\bullet}$ and **16Se4**$^{2+}$, in the reaction were characterized by UV–visible spectroscopy and electrochemical studies [44]. The information from UV–visible spectroscopy, cyclic voltammetry, spectroelectrochemistry and coulometry show that **16Se4** is first oxidized to **16Se4**$^{+\bullet}$ then to **16Se4**$^{2+}$. Kinetic studies on the reaction between the complex and **16Se4** show a first order kinetics in each of these species, second order overall. The reaction stereochemistry is 2Cu(**16Se4**)$^{2+}$ + **16Se4** → 2Cu(**16Se4**)$^{+}$ + **16Se4**$^{2+}$ [44].

Reaction of copper(I) trifluoromethane sulfonate with **16Se4** yields the adduct of Cu(SO_3CF_3) with **16Se4** [45]. The Cu(I) is not encapsulated by **16Se4** as in the cyclic polythiaether complexes of Cu^I [46] and Cu(II) complex of **16Se4**. In the adduct, each Cu^+ ion is pseudo-tetrahedrally coordinated by Se atoms from four different **16Se4** rings. There are almost no significant contacts between the anion $SO_3CF_3^-$ and the complex cation [45]. The reason for the formation of the unique type of Cu(I) complex, was attributed to the special lattice stability associated with the choice of anion and to the low energy conformation of **16Se4** ring. The Cu–Se bond lengths are slightly longer than Cu–S bonds in Cu^I complexes of cyclic polythiaethers.

Reaction of $AgBF_4$ with **16Se4** afforded the silver(I) complex as a white solid [25]. The poor solubility of this complex in organic solvents, leads to the presumption of a polymeric arrangement for the complex similar to the copper(I) analogue in the solid state.

3.2.2.7. Hg. $Hg(CN)_2$ reacts with **16Se4** to give an adduct. The Hg atom has a tetragonally distorted octahedral ligand environment (Fig. 24). The molecules packing is such that the four Se atoms from four different rings most closely approach Hg in a plane approximately perpendicular to the molecular axis of $Hg(CN)_2$ [45].

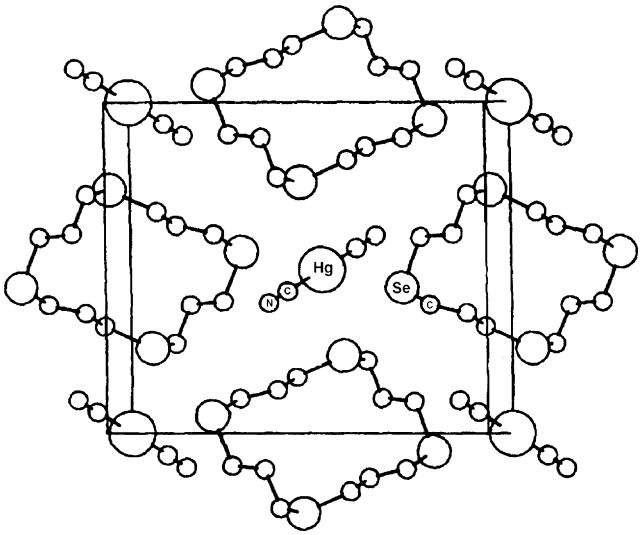

Fig. 24. Crystal structure of $Hg(CN)_2$**16Se4**. Reprinted with permission from Ref. [45]. Copyright (1991) Elsevier.

To summarize, the following are the most noticeable points for the complexes of **16Se4**:

(1) The ligand has potential to bind to various metal atoms across the periodic table.
(2) All the complexes retain its solution state structure in solid state except Pd(II) and Pt(II) complexes for which a number of invertomers are present in the solution.
(3) All the octahedral complexes [Cu(II), Rh(III), Pt(IV), Co(III), Ir(III) and Ru(II)] display a *c*,*t*,*c* configuration of the coronand except the Ru(II) complex which shows *c*,*c*,*c* arrangement of the ligand when it binds to a bulky PPh_3 group.
(4) Of particular interest is the square planar Pd(II) complexes which show two ligand configurations. The complex cation displays the more common *c*,*t*,*c* geometry with the larger PF_6^- counter ions and two solvent molecules of crystallization and the *c*,*c*,*c* stereochemistry when it contains smaller and thus more polarizing anions (BF_4^-/Cl^-) and no solvent of crystallization.
(5) All the complexes have similar configurations to their thia-analogs and coordinate in an endocyclic manner except Cu(I) and Hg(II) which form an adduct with **16Se4**.
(6) The longer *d*(M–Se) bonds over M–S bonds (Table 1) reflect the larger size of selenium over sulfur.

3.2.3. *24Se6*

Pinto and co-workers [39] reported the first binuclear complex $([PdCl)_2$(**24Se6**)$][BF_4]_2 \cdot 2CH_2Cl_2$ where **24Se6** chelates two individual palladium atoms in a tridentate fashion, while a chlorine atom occupies the fourth coordination site in each case forming $[(PdCl)_2$(**24Se6**)$]^{2+}$ cation (Fig. 25). The environments of both Pd were approximately square planar. There are no intra-molecular interactions between the palladium atoms or between a palladium atom and the chlorine atom bound to the other palladium atom. The crystal structure of $[(PdCl)_2$(**24Se6**)$]^{2+}$ presents 1–15 potential diastereomers of an interesting binuclear complex. This report displays very interesting chemistry as a consequence of the binuclear nature of **24Se6** and the possibilities for direct or ligand mediated metal–metal interactions.

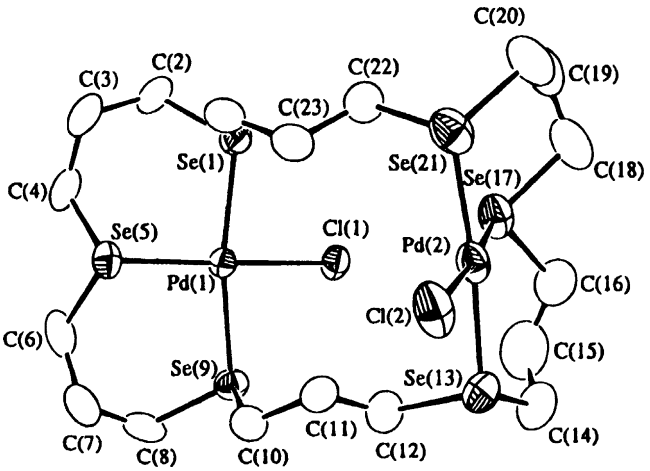

Fig. 25. Molecular structure of $[(PdCl)_2$(**24Se6**)$]^{2+}$. Reprinted with permission from Ref. [39]. Copyright (1996) American Chemical Society.

3.2.4. *Sebc*

The reaction of **sebc** with metal (II) species (M = Mo or W) gives seven-coordinated $[MX_2(CO_3)L]$ (M = Mo, X = Br or I; M = W, X = I) [27]. These compounds are poorly soluble in chlorocarbons and hydrocarbons and decompose rapidly in coordinating solvents which precludes NMR spectroscopic investigations on these species.

Reactions of MCl_2 (M = Pd or Pt) with **sebc** afforded the neutral species $[MCl_2$(**sebc**)] as orange (Pd) or yellow (Pt) solids [25]. The structure of mononuclear $[PdCl_2$(**sebc**)] has the expected *cis*-dichloro arrangement with one chelating **sebc** ligand completing the distorted square planar geometry (Fig. 26) [25]. In this species the six-membered chelate ring is in a chair conformation in contrast to the boat conformation in Cu(I) and Ag(I) complex (*vide infra*). The compounds $[MCl_2$(**sebc**)] show a low frequency shift of ^{77}Se NMR peaks relative to free **sebc** in contrast to their corresponding $[MCl_2$**8Se2**], which show high frequency shifts relative to free **8Se2**.

The structure of $[Cu($**sebc**$)_2]BF_4$ shows a discrete copper(I) monomer with two chelating **sebc** ligands generating a distorted-

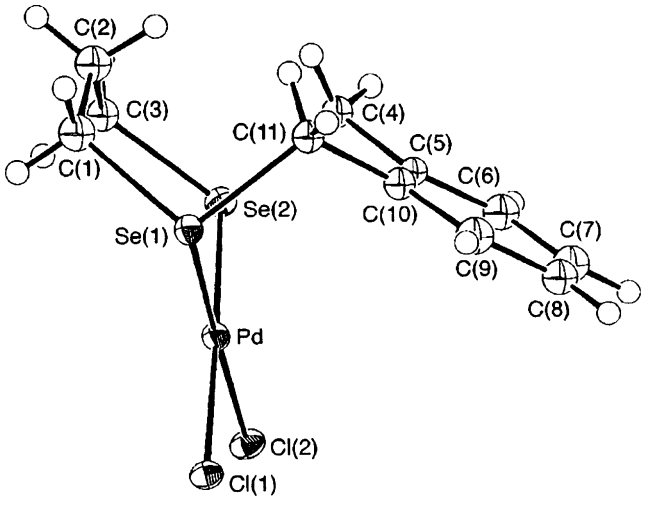

Fig. 26. The structure of *cis*-$[PdCl_2$(**sebc**)]. Taken from Ref. [25]. Reproduced by permission of The Royal Society of Chemistry.

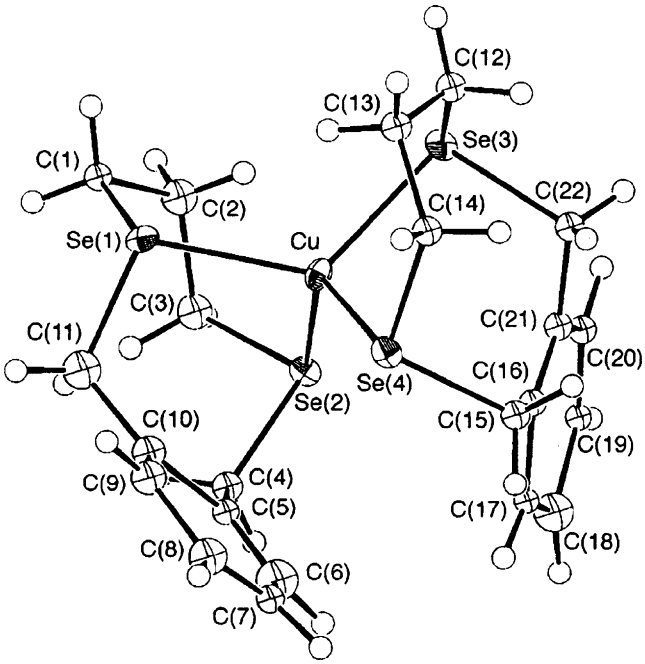

Fig. 27. The structure of $[Cu(\mathbf{sebc})_2]^+$. Taken from Ref. [25]. Reproduced by permission of The Royal Society of Chemistry.

tetrahedral stereochemistry (Fig. 27) [25]. The two six-membered chelate rings in the $[Cu(\mathbf{sebc})_2]^+$ cation adopt a boat arrangement. The structure of the corresponding silver(I) complex $[Ag(\mathbf{sebc})_2]BF_4$ shows a similar arrangement. The increasing M–Se distances (M = Pd, Cu and Ag) are in accord with the increasing radius of M(I). [$(AuCl)_2$**sebc**] (tht = tetrahydothiophene) is also reported.

3.2.5. Coordination chemistry of other coronands

Brown crystals of $[Cu(\mathbf{16Se2S2})][SO_3CF_3]_2$ (**26**) were obtained from **16Se2S2** and $Cu(SO_3CF_3)_2$ [17]. The structure is similar to $[Cu(\mathbf{16Se4})][SO_3CF_3]_2$ [42] with Se and S atoms disordered in a 50:50 ratio. The complex **26** shows the typical tetragonally distorted octahedral coordination environment of Cu(II) and displays a *c,t,c* configuration of the coronand (Fig. 28).

The spontaneous reduction of $[Cu(\mathbf{16Se2S2})][SO_3CF_3]_2$ to $[Cu(\mathbf{16Se2S2})][SO_3CF_3]$ (**27**) was observed during recrystallization of the Cu(II) complex in organic solvents. In this complex, the metal adopts a tetrahedral geometry with *t,t,t,* ligand stereochemistry (Fig. 29), and with disorder of the S and Se atoms.

The molecular structure of the complex shows that the configuration of the $[Cu(\mathbf{16Se4(OH)_2})][SO_3CF_3]_2$ (**28**) with regard to the stereochemistry at the selenium atoms is *c,t,c*. The hydroxyl substituents of the coronand ligand have a mutual *cis* relationship. This combination of stereochemical features allows only one hydroxyl group to chelate to the copper centre, imposing a boat conformation on the corresponding Se–Cu–Se–C–C ring. The coordination environment of the copper ion can also be described as approximately tetragonally distorted octahedral, with a hydroxyl oxygen atom and an SO_3CF_3 oxygen atom each occupying one of the pseudoaxial positions. The non-coordinated hydroxyl group forms a hydrogen bond to an oxygen atom of the non-coordinated $SO_3CF_3^-$ ion. Recrystallization of the Cu(II) complex of **16Se4(OH)** yields a mixture of the Cu(II) complex as brown crystals and the

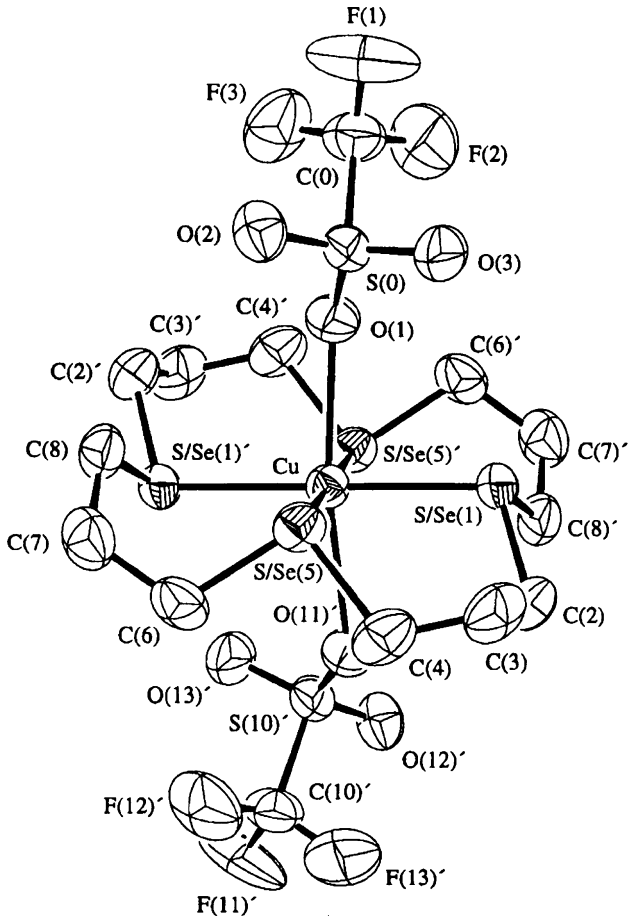

Fig. 28. Crystal structure of $[Cu(\mathbf{16S2Se2})]^{2+}$, taken from Ref. [17]. Reprinted with permission from Ref. [17] and Prof. B. M. Pinto. Copyright (2000) American Chemical Society.

Cu(I) complex $[Cu(\mathbf{16Se4(OH)})][SO_3CF_3]$ (**29**) as white crystals. The structure of the Cu(I) species reveals a distorted tetrahedral Se4 donor set at Cu(I) with no hydroxyl coordination. The configuration in which the coronand complexes Cu is denoted as *t,t,t* (Fig. 30).

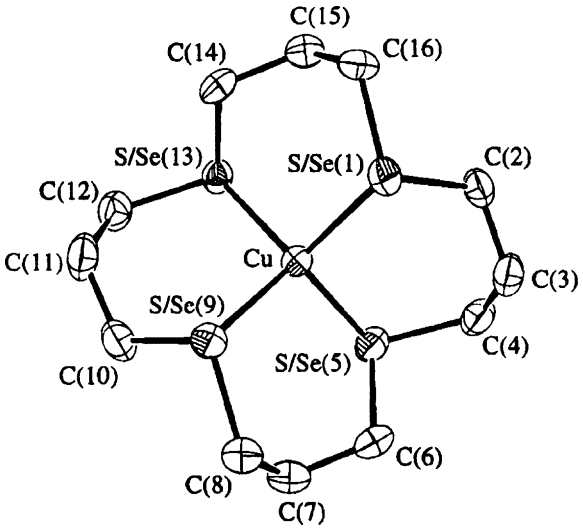

Fig. 29. Predominant cationic structure of **27**. Reprinted with permission from Ref. [17] and Prof. B. M. Pinto. Copyright (2000) American Chemical Society.

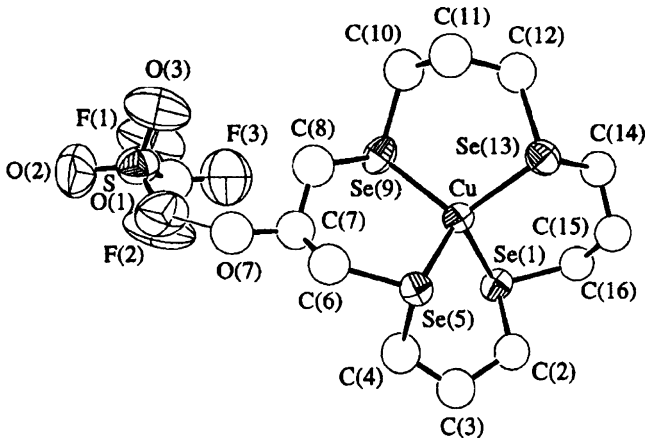

Fig. 30. Predominant ion-pair combination of **29**. Reprinted with permission from Ref. [17] and Prof. B. M. Pinto. Copyright (2000) American Chemical Society.

A similar attempt to prepare a Cu(II) complex of **Dibenzo-14Se4** from **Dibenzo-14Se4** and $Cu(SO_3CF_3)_2$ was not successful. The $[Cu(\mathbf{8Se2(OH)})_2][SO_3CF_3]_2$ (**30**) complex has an approximately tetragonally distorted octahedral geometry with the hydroxyl oxygen atoms occupying the more weakly bound axial positions. The hydroxyl groups form hydrogen bonds to neighbouring $SO_3CF_3^-$ anions (Fig. 31) [17].

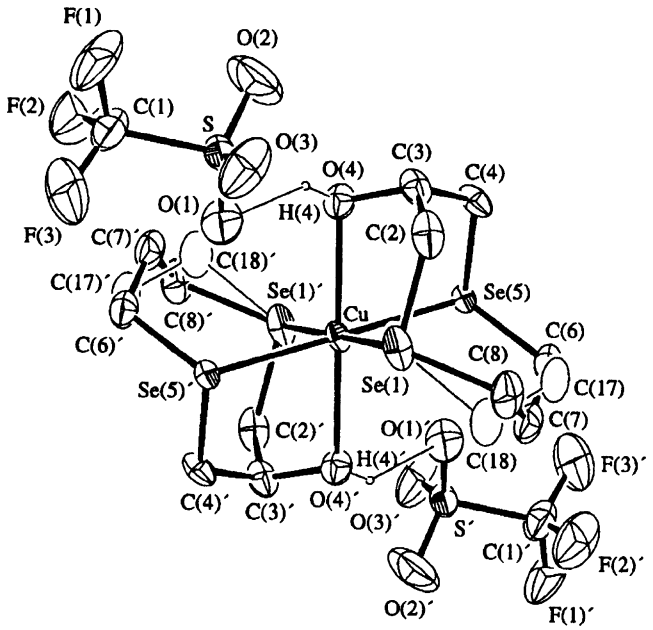

Fig. 31. Crystal structure of $[Cu(\mathbf{8Se2(OH)})_2][SO_3CF_3]_2$, taken from Ref. [17]. Reprinted with permission from Ref. [17] and Prof. B. M. Pinto. Copyright (2000) American Chemical Society.

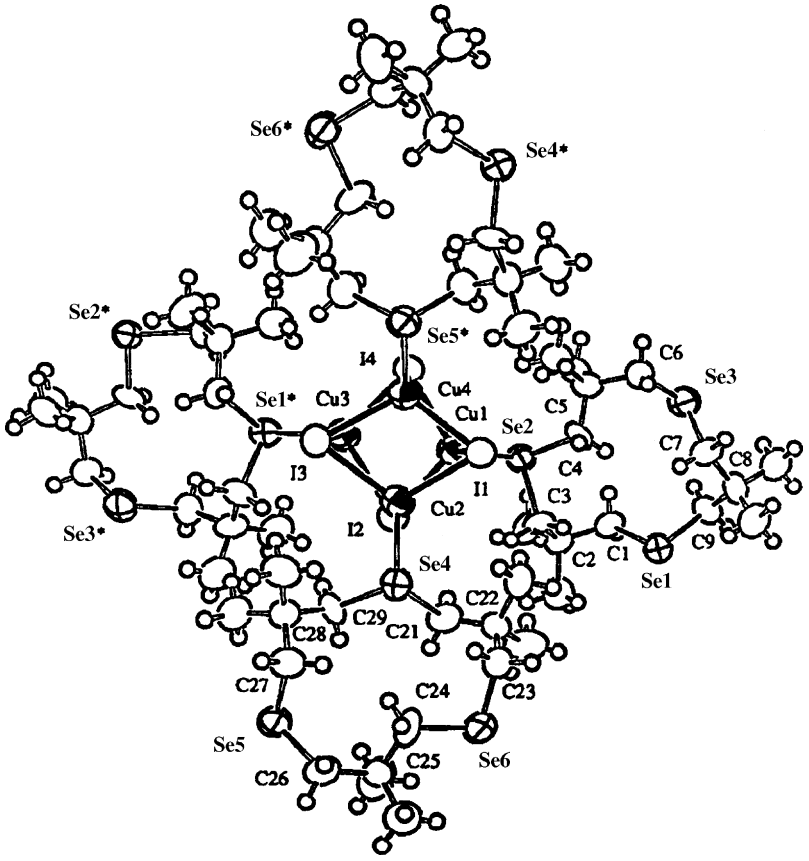

Fig. 32. Crystal structure of $Cu_4I_4(\mu\text{-}\eta^2\text{-}\mathbf{Me_6 12Se3})_2$. Reprinted with permission from Ref. [23]. Copyright (1997) American Chemical Society.

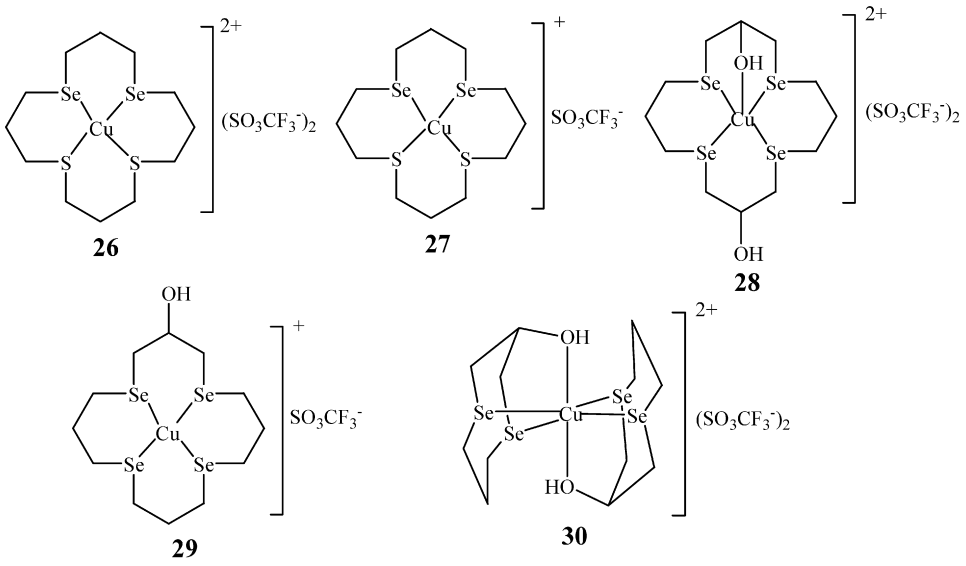

The reaction of **Me$_6$12Se3** with $Re_2(CO)_9(NCMe)$ and CuI afforded $Re_2(CO_9)$(**Me$_6$12Se3**) and a polymeric Cu_4I_4(μ-η^2-**Me$_6$12Se3**)$_2$, respectively [23]. The structure of Cu_4I_4(μ-η^2-**Me$_6$12Se3**)$_2$ (Fig. 32) shows a three-dimensional network of cubane-like Cu_4I_4 units linked by four bridging triselena crowns. Each Cu(I) ion links to one η^1 selenoether and the **Me$_6$12Se3** units use one more Se atom to bridge to an adjacent Cu(I), leaving the third Se atom uncoordinated.

3.3. Coordination chemistry with p-block elements

When compared to transition metal chemistry, main group coordination chemistry has in general received less attention, possibly due to the fact that the compounds often lack some of the features usually required for their characterization *via* conventional spectroscopic methods. Reid and co-workers [47–54] studied the coordination chemistry of macrocyclic selenoether ligands with p-block ions of group 15 (As, Sb, Bi). These ions readily form complexes with macrocyclic selenoether ligands to give a diverse range of unusual, and often polymeric, structural motifs based on a combination of primary M–X (X = Cl, Br or I) interactions and a series of secondary M···Se, and in some cases M···X interactions [47–54]. The presence and stereochemical significance of the M-based lone pair adds further diversity. Subtle changes in the nature of the group 16 donor ligand (donor atom type, interdonor linkage, cyclic *vs.* acyclic, etc.) lead to very marked differences in the structures which the complexes adopt.

3.3.1. *24Se6*

The first example of macrocyclic selenoether complex of a nonmetallic element [$(AsCl_3)_4$(**24Se6**)], was reported by Reid and co-workers [47] in 2001. The structure shows a very unusual arrangement of four $AsCl_3$ units per hexaselenoether macrocycle. Two $AsCl_3$ units coordinate *exo* to the ring *via* a single Se atom and the other two form a weakly associated dinuclear μ^2-chloro-bridged unit *endo* to the ring, with each of the As atoms coordinated to two *cis*-Se atoms from **24Se6**. Thus all the six Se atoms of the macrocycle bind to the As centres. The observation of both *exo* and *endo* coordination in a discrete macrocyclic complex and the inclusion of a dinuclear M_2X_6 fragment within the ring is very rare and novel. The coordination number and geometry of the As centres situated inside and outside the ring are different. The distorted octahedral environment at each As centre inside the ring is from the two *cis* Se atoms from the ring and four chlorine atoms (Fig. 33). The stereochemical activity of the lone pair on the As centres (*endo* to the ring) is not obvious since there is no significant deviation from the values expected for an octahedron. The distorted sawhorse geometry of As (*exo* to the ring) is from the coordination of three terminal Cl atoms, one Se atom from the ring and the stereochemical active lone pair of electrons. The only other crystallographically characterized complex of **24Se6** [$(PdCl)_2$**24Se6**]$^{2+}$, was reported by Pinto and co-workers [39]. A 2:1 complex, [$(AsBr_3)_2$(**24Se6**)] is also reported [48].

The reaction of BiX_3 [X = Br or Cl] with **24Se6** gave yellow-orange [BiX_3(**24Se6**)]. However, because of poor solubility complete characterization was not possible [49].

3.3.2. *16Se4*

Reaction of MX_3 (X = Cl, Br or I and M = As [48], Sb [50,51] or Bi [49]) with **16Se4** afforded solid complexes of 2:1 M:**16Se4** stoichiometry. Owing to the poor solubilities of the compounds in non-coordinating solvents and ready displacement of the selenoether ligand in the coordinating solvent, their characterization was restricted to analytical data, IR spectroscopy (in few cases) and single crystal X-ray diffraction studies. Both the As(III) Br and Cl complexes show very similar three-dimensional sheet polymeric structures with five-coordinate As(III) coordinated to three terminal Cl's/Br's and two *cis*-Se donor atoms from *exo* coordination to

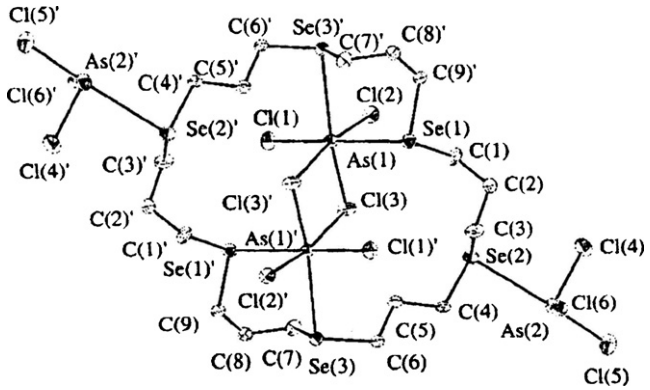

Fig. 33. ORTEP drawing of [$(AsCl_3)_4$(**24Se6**)]. Taken from Ref. [47] with permission from the American Chemical Society.

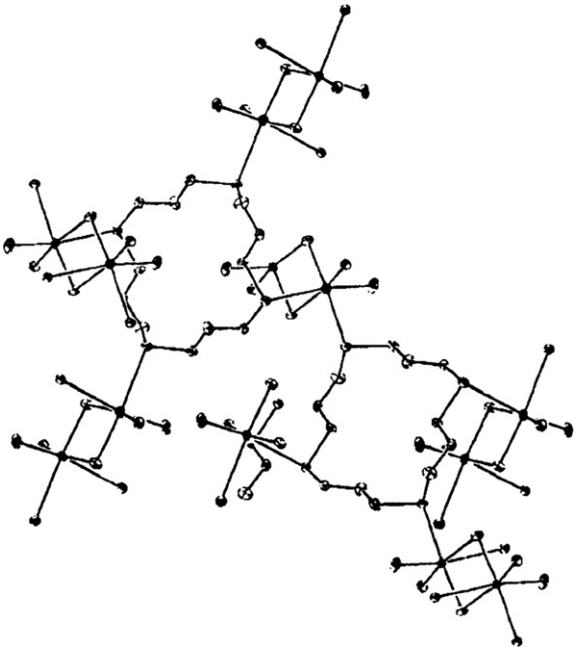

Fig. 34. View of part of the two-dimensional sheet structure of [$(AsCl_3)_2$(**16Se4**)]. Taken from Ref. [48] with permission from the American Chemical Society.

two different macrocyclic rings (Fig. 34) [48]. This five-coordinate geometry approximates to an 'octahedron' with one vacant vertex which was assumed to be occupied by the As-based lone pair.

The structure of [$(SbBr_3)_2$**16Se4**] shows **16Se4** molecules coordinated in an exocyclic configuration to four Sb centres each of which bridge to another selenacrown [50]. The geometry at Sb can be described as five coordinate *via* primary interactions to three *fac* terminal Br and secondary interactions to two *cis* Se atoms from different macrocycles to give a distorted square pyramidal coordination environment. The main feature of this compound is the retention of the pyramidal $SbBr_3$ unit observed in the parent antimony trihalide and the occurrence of weak secondary Sb–Se interactions on the opposite face which leads to the Se atoms occupying mutually *cis* coordination sites. [$BiBr_3$(**16Se4**)] adopts a one-dimensional ladder arrangement which is derived from almost planar Bi_2Br_6 units, with each Bi linked to the next Bi_2Br_6 units by bridging **16Se4** ligands (Fig. 35) [49]. The coordination is *via* one Se-donor atom to each Bi, i.e. μ-bridging **16Se4**. The macrocycles are bonded *via* mutually *trans* selenium donors and adopt an exocyclic conformation. Each Bi is coordinated *via* a *trans*-Se_2Br_4 donor set. The other two mutually *trans* selenium atoms within each **16Se4** unit remain non-coordinating. These structural arrangements are in contrast to those identified for the Sb(III) and As(III) analogues which are structurally very similar and show coordination through two mutually *cis* Se atoms from different macrocycles. In these three complexes **16Se4** ligands adopt exocyclic arrangement like in $[Cu_n(\mathbf{16Se4})_n]^{n+}$ [45].

Reaction of **16Se4** with SnX_4 affords the 1:1 adducts [SnX_4**16Se4**] (X = Cl or Br). The ^{77}Se and ^{119}Sn NMR data are consistent with a 1:1 adduct involving a distorted octahedral Cl_4Se_2 donor set at tin [52].

3.3.3. *8Se2*

The reaction of MX_3 [X = Cl, Br or I and M = As [48] or Sb [51] or Bi [49]] with **8Se2** afforded complexes having empirical formula MX_3(**8Se2**). Due to poor solubilities of the complexes, presumably associated with their polymeric nature, it was difficult to obtain useful NMR data. The [$AsCl_3$**8Se2**] adopts an infinite one-

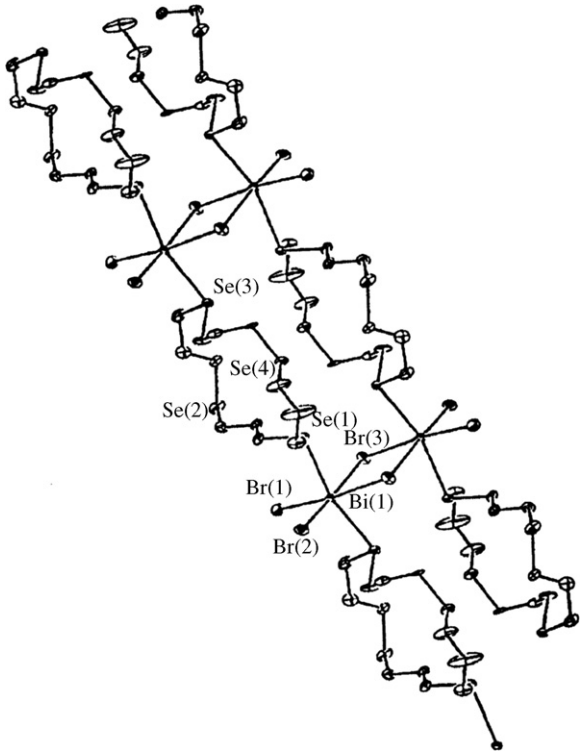

Fig. 35. View of the structure of a portion of the infinite one-dimensional ladder adopted by [$BiBr_3$(**16Se4**)]. Taken from Ref. [49]. Reproduced by permission of The Royal Society of Chemistry.

dimensional ladder structure containing near-planar As_2Cl_6 units linked by bridging **8Se2** molecules which occupy mutually *trans* coordination sites (Fig. 36). The angles subtended at As(III) are close to those expected for a regular octahedron [53].

The structure of [$BiCl_3$**8Se2**] shows an infinite one-dimensional ladder structure derived from almost planar Bi_2Cl_6 linked by four bridging **8Se2** [49]. The Se-donor atoms adopt mutually *trans* coordination sites on each Bi ion. The [$SbCl_3$**8Se2**] complex crystallizes as [$Sb_2Cl_6(\eta^1$-**8Se2**] dimers involving edge-bridged square pyramids with anti-**8Se2** ligands (Fig. 37). Additional long range Sb···Se interactions involving the remaining Se atoms link the dimers into an infinite ladder structure [53]. This is grossly similar to the structure observed for the As(III) and Bi(III) analogue.

The availability of the X-ray crystal structural data of these three homologous selenoether complexes allows a direct comparison of the structures. The Sb complex is very distorted giving 5 + 1-

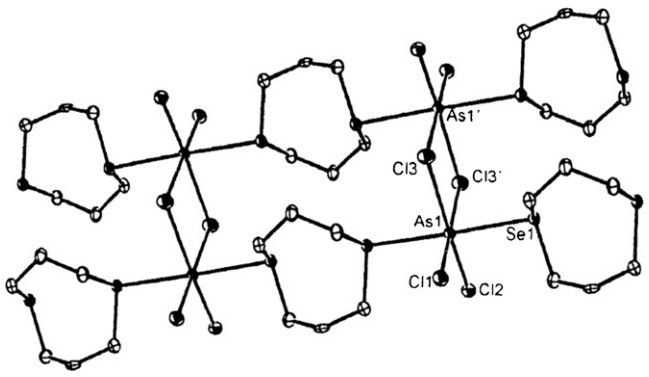

Fig. 36. View of a portion of the ladder structure of [$AsCl_3$(**8Se2**)]. Taken from Ref. [53]. Reproduced by permission of The Royal Society of Chemistry.

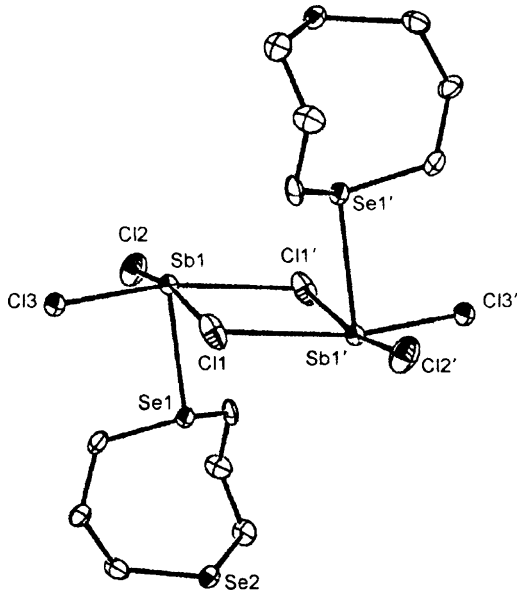

Fig. 37. View of the dimer unit in [$SbCl_3$**8Se2**]. Taken from Ref. [53]. Reproduced by permission of The Royal Society of Chemistry.

coordination whereas the As and Bi complexes are both much more regular six-coordinate geometries. The structural differences may be due to the differences in the degrees of stereochemical directionality of the M-based lone pair in these compounds. The regular geometry and elongation of all of the As–Cl and As–Se bond distances by approximately equal amounts for the As(III) complex suggests the stereochemical inactivity of the lone pair. Arsenic is too small to accommodate pseudo seven-coordination (either seven ligands or six ligands plus a lone pair). The regular six-coordination at Bi with no significant distortion of the bond lengths and angles for [$BiCl_3$**8Se2**] indicates the stereochemical inactivity and the possibility of Bi-based lone pair occupying the 6s orbital. The distortion in the bond lengths and angles around Sb in [$SbCl_3$**8Se2**] suggests the Sb-based lone pair being stereochemically directional and localized in the plane.

Reaction of $SnCl_4$ with **8Se2** affords the orange [$SnCl_4$**8Se2**] in good yield [52]. The ^{77}Se NMR data on [$SnCl_4$**8Se2**] is consistent with a chelating diselenoether.

4. Unsaturated crown ethers

Unsaturated thiacrown ethers having *cis* carbon–carbon double bonds are considered to be more conformationally restricted than the corresponding saturated systems and are highly selective for a number of metals [55]. Therefore, the unsaturated selenacrown ethers are also expected to exhibit different selectivities towards metals due to differences in the electronegetivities of the chalcogen atoms, the conformation, and the size of the cavities. Kamigata and co-workers [56,57] first synthesized unsaturated selenacrown ethers **15-US-5**, **18-US-6**, **21-US-7**, **24-US-8** and **27-US-9** [x – US – y: US, unsaturated selenacrown ether; x, x-membered ring; y, number of selenium atom] together with 1,4-diselenin (Scheme 8). The 9- and 12-membered unsaturated selelacrown ethers are not obtained in the above reaction due to the unfavorable configuration during the ring closure reaction [57]. From the *ab intio* molecular orbital calculations, the relative energies of the 9- and 12-membered compounds are higher than those of the other selenacrown ethers (geometries were optimized using Hartee–Fock (HF) method with the LANL2DZ basis set). The crystal structures of **15-US-5** to **24-US-8** show that all carbon–carbon double bonds exhibit *cis* geometry and all the selenium atoms lay almost on their respective planes and are oriented toward the cavities (Fig. 38). The molecular structures become elliptically slender with increasing ring size whereas the structures of the corresponding unsaturated thiacrown ethers become rounder with increasing size [55a]. The cyclic voltammograms indicate that the large unsaturated selenacrown ethers are oxidized more easily than the small ones. The unsaturated selenacrown ethers are thermally less stable than their corresponding sulfur analogues due to the weak carbon–selenium bonds compared to the carbon–sulfur bond [57].

The reaction of US (unsaturated selenacrown ethers) with silver ions yields the novel silver complexes Ag^I(**15-US-5**)(CF_3COO) (**31**), Ag^I_5(**18-US-6**)$_3$(CF_3COO)$_5$ **(32)**, Ag_5(**21-US-7**)$_7$(CF_3COO)$_7$ **(33)**, Ag(**24-US-8**)$_2$(CF_3COO) **(34)**, Ag_2(**24-US-8**)$_3$(CF_3COO)$_2$ **(35)**, Ag_3(**24-US-8**)$_3$(CF_3COO)$_3$ **(36)**, Ag(**15-US-5**)NO_3 **(37)** and Ag(**21-US-7**)BF_4 **(38)**. In **31** one silver atom is present in the macrocycle

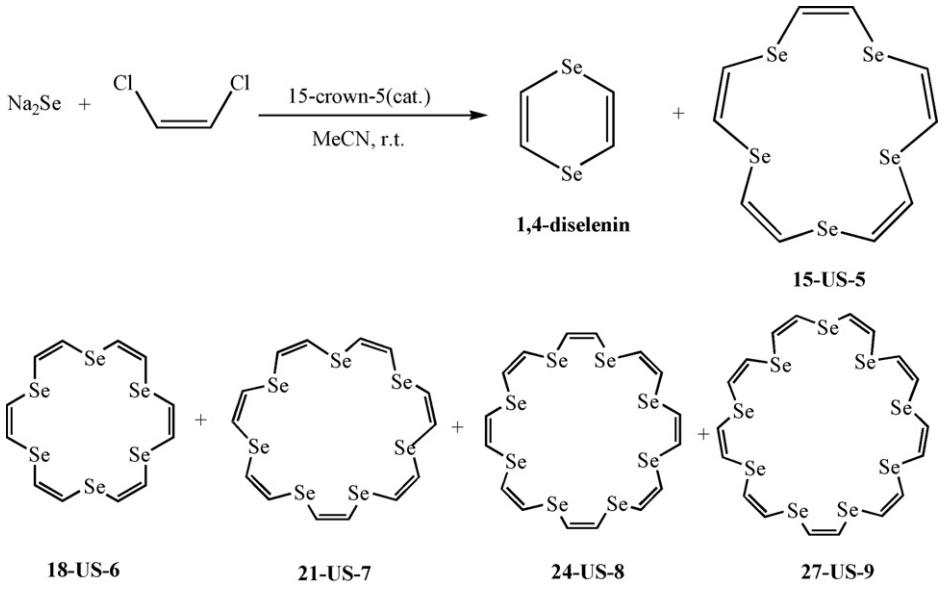

Scheme 8.

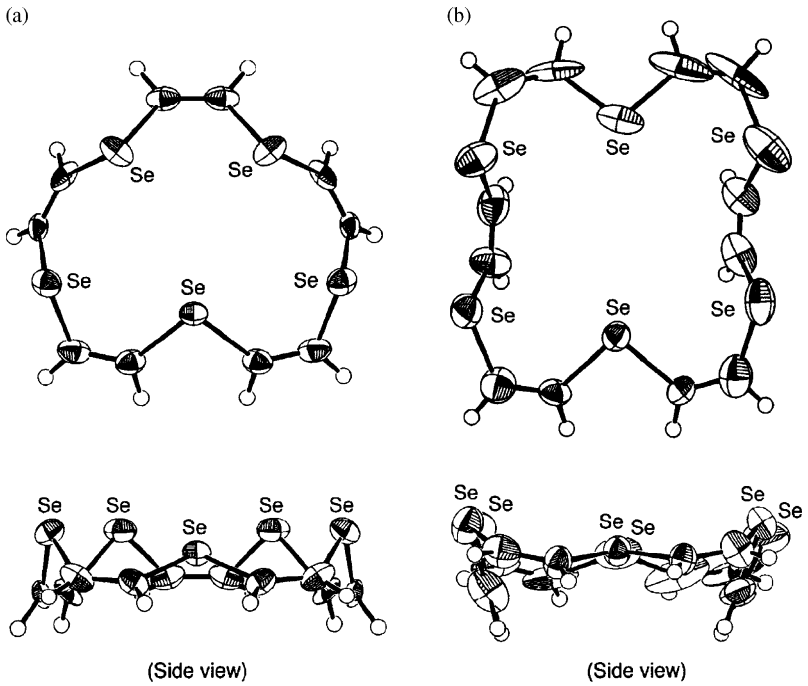

Fig. 38. ORTEP drawings of (a) **15-US-5** and (b) **18-US-6**. Reprinted with permission from Ref. [56]. Copyright (2003) American Chemical Society.

cavity. Thus, the geometry around the silver atom has a distorted five-coordinate square pyramidal arrangement coordinating by three selenium atoms, one oxygen atom from the trifluoroacetate group and weakly coordinating by another selenium atom. The structure of **37** is similar to **31**. In **32**, Ag^{I}_{5}(**18-US-6**)$_3$($CF_3COO)_5$, out of three crown subunits, one **18-US-6** includes one silver atom and the other two macrocycles include two silver atoms, respectively (Fig. 39). The structure of **35** shows the presence of two silver atoms in the cavity of one **24-US-8** unit. The two trifluoroacetate groups are located at the opposite sides of the ring

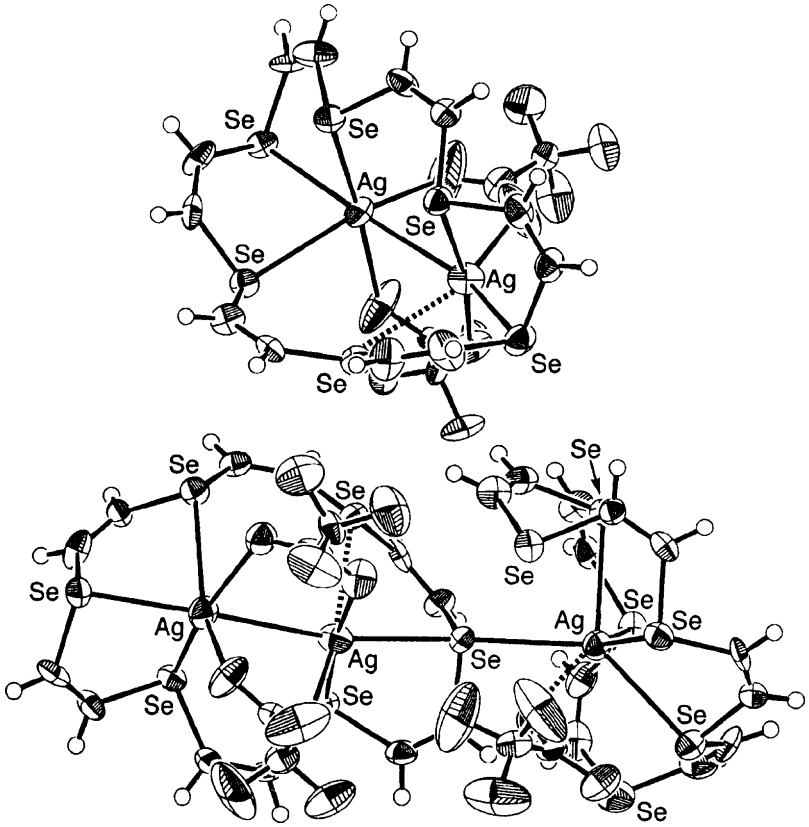

Fig. 39. ORTEP drawing of $Ag^{1}{}_{5}$(**18-US-6**)$_3$($CF_3COO)_5$. Reprinted with permission from Ref. [56]. Copyright (2003) American Chemical Society.

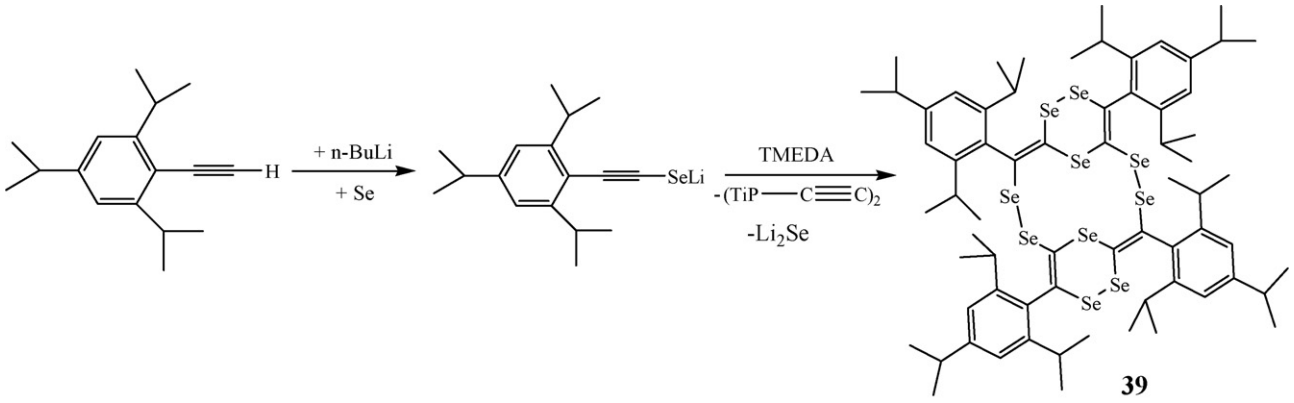

Scheme 9.

plane, and two oxygen atoms of each trifloroacetate group coordinate to different silver atoms. The silver ion inclusion behavior of the unsaturated selenacrown ethers were examined in solution. The US selectively forms 1/1 complexes at low concentration in solution.

The reaction of 2,4,6-triisopropylphenylethynyllithium with gray selenium affords the sterically crowded lithium 2,4,6-triisopropylphenylalkynylselenolate which is unstable in solution and undergoes self-addition to yield an unusual selenium-rich macrocycle (**39**) (Scheme 9) [58]. This conversion seemed to be greatly accelerated by coordinating reagents such as tetramethylethylenediamine. The structure of the macroheterocycle showed a central 12-membered ring fused together with two outer six-member rings (Fig. 40). The rigid tricyclic backbone of the rings consists only of selenium and quaternary alkenylidene units. Because of the position of the alkenylidene units, the flexibility of this selenium-rich macrocycle is very limited.

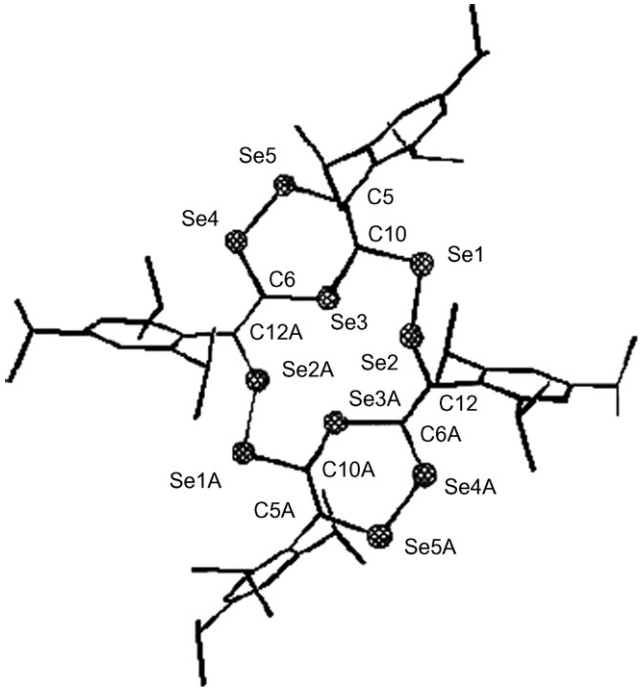

Fig. 40. Crystal structure of **39**. Reprinted with permission from [58]. Copyright (2003) American Chemical Society.

5. Mixed donor N, P and O/Se macrocycles

The mixed donor macrocycles have attracted considerable interest due to their highly selective nature for the complexation of ions. Incorporation of the larger Se atom should result in a change in size of the cage cavity and hence allow for some interesting coordination behavior. Furthermore, owing to the low electronegativity of selenium, selenium-containing macrocycles exhibit excellent ligands for transition metals and this have been extensively studied. Thus, macrocycles incorporating hard donor atoms such as P, N or O and soft selenium atoms into the ring system may act as potential heterodinucleating macrocyclic ligands. These macrocyclic ligand will feature 'hard' and 'soft' binding sites in close proximity and hence have the potential to coordinate to both 'hard' and 'soft' guest ions or molecules. The co-complexation of a hard cation and a transition-metal cation in the same macrocycle will change the redox properties of the transition-metal cation. Such complexes may be used for bimetallic catalysis, activation and formation of supramolecular systems [59].

5.1. Se/O macrocycles

Organoselenium compounds containing Se–Se bonds are of particular interest because they are useful reagents for selective organic synthesis. They are also suggested to be intermediates in a biologically important process involving glutathione peroxidase, a selenium-containing enzyme. Incorporation of this bond into crown ether type host molecules might provide a unique opportunity for a new molecular device, which would undergo selective membrane transport of specific metal ions under light irradiation or act as a catalyst in a photochemically induced redox cycle, if appropriate metal ions are present inside the cavity [60]. The syntheses of the first macrocycles containing a Se–Se bond (**40**, **41**) were reported by Tomoda and Iwaoka [60] by the inter- and intra-molecularcyclization of the selenium-containing precursors (Scheme 10). The most interesting feature of the molecular structure of **40** and **41** is the unusual proximity between Se and O atoms. These apparently short interatomic distances may suggest the existence of strong attractive interactions between these atoms. Almost linear alignment of these four atoms, O(12')–Se(1)–Se(2)–O(51) in **40** [Se(6)–Se(5)–O(16) in **41**] clearly show that these interactions are due to the hypervalent property of the selenium atoms. The combined effects, the hypervalent interactions and the π-electron conjugation between the benzene ring and the carbonyl group, contribute to the conformational stability of the macrocyclic system.

Three different tetraselena crown ethers (**42**) were obtained from dipotassium benzene-1,2-diselenolate [o-$C_6H_4(SeK_2)$] and

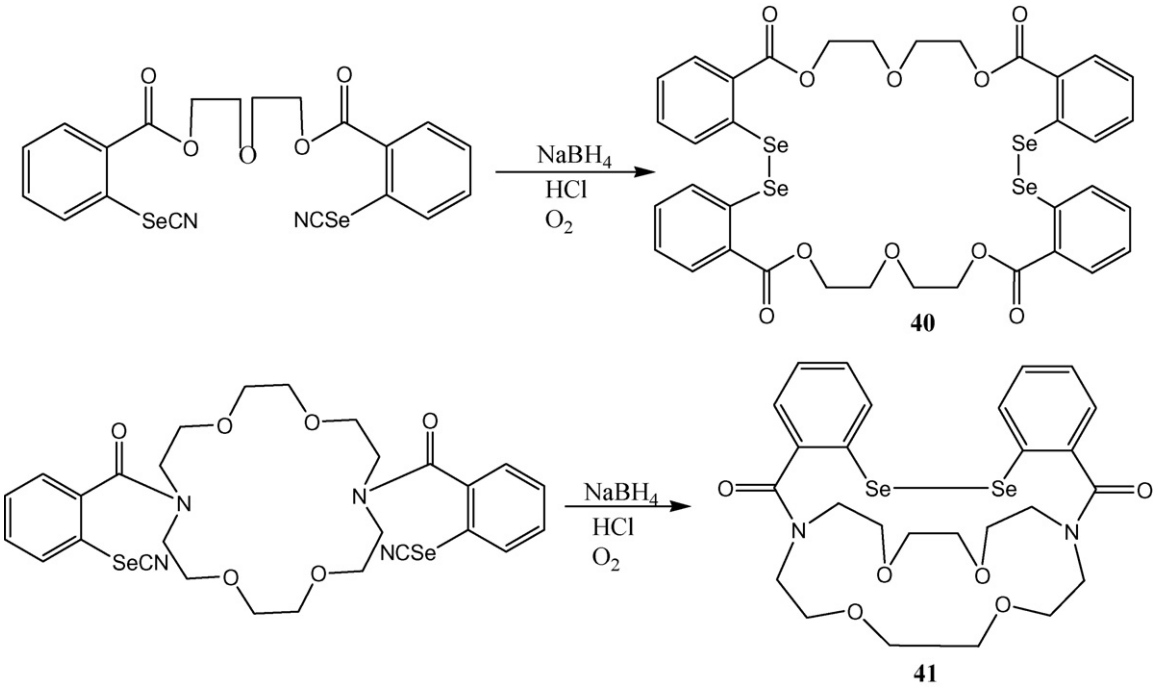

Scheme 10.

dihalogeno selenoethers o-$C_6H_4\{SeCH_2(CH_2OCH_2)_nCH_2X\}_2$ (X = Cl, n = 1–3 or X = Br, n = 3, 4) [61]. The yield could be increased by using the 'cesium effect' according to Scheme 11. The structural parameters and the conformation in the solid state of one of the tetraselenacrown ethers (**42**, n = 2) were determined by X-ray diffraction (Fig. 41). The 'cesium effect' has also been applied to the synthesis of unsymmetrical crown ether substituted on one benzene ring only. The syntheses of these selenacrown ethers (**42**) from polybenzene-1,2-diselenol were published prior to this work by Xu and co-workers [62], but with poor spectroscopic characterization. These selena-crown ethers bind two mole equivalents of HgI_2 to form dinuclear complexes of general formula [$(HgI_2)_2$(**42**)]. The structure of **43** indicates that only the Se donors of the macrocycle coordinate to the approximately tetrahedral Hg^{II} centres, with iodide donors occupying the remaining two coordination sites at each metal centre.

The ligand **dic-Se** [63] was synthesized modifying the procedure reported for (2-pyridylmethyleneamino)benzo-15-crown-5(**dic**) [64] and the photophysics and electrochemistry of the complex [$Cu(PPh_3)_2$(**dic-Se**)]BF_4 have been reported [63]. The encapsulation

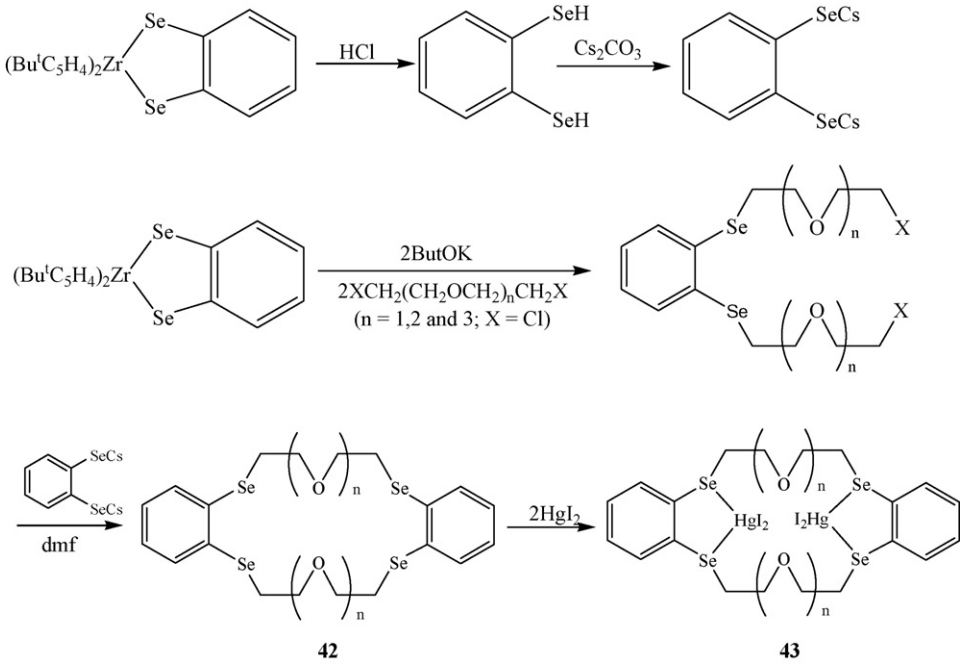

Scheme 11.

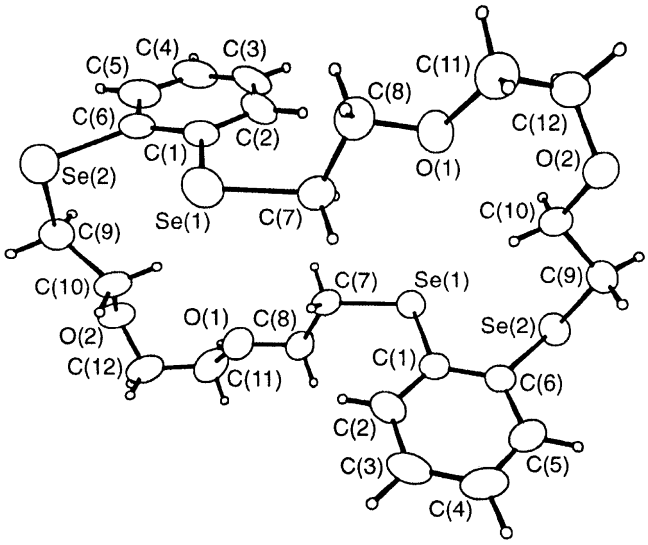

Fig. 41. The ORTEP plot for compound **42** ($n = 2$). Taken from Ref. [61]. Reproduced by permission of The Royal Society of Chemistry.

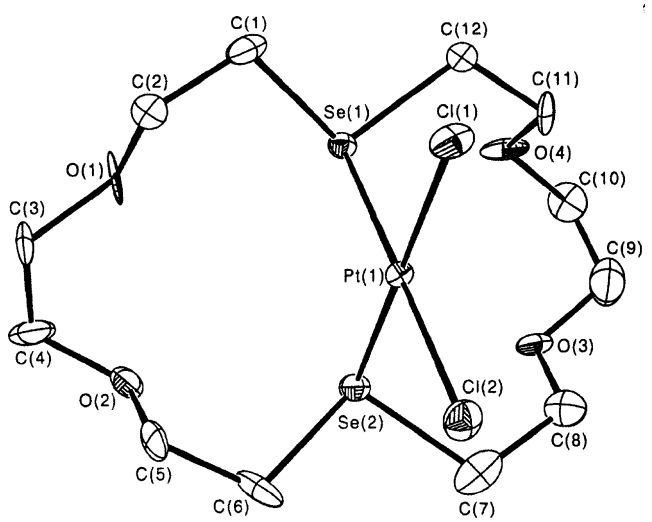

Fig. 43. Crystal structure of [$PtCl_2${18O4Se2}]. Taken from Ref. [69]. Reproduced by permission of The Royal Society of Chemistry.

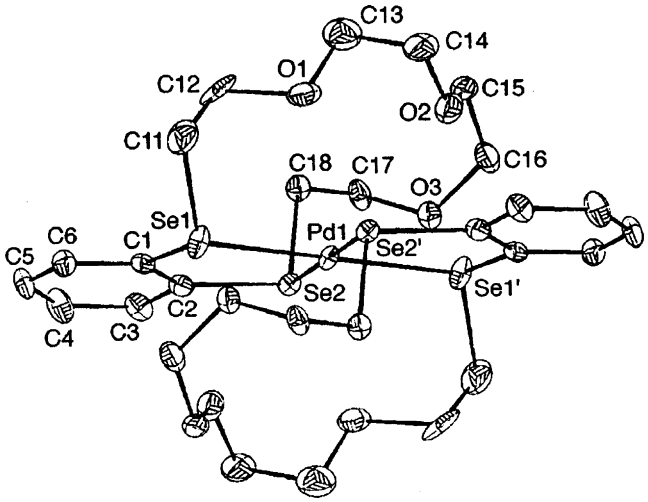

Fig. 42. Crystal structure of [Pd(**benzo-15Se2O3**)$_2$]$^{2+}$, taken from Ref. [66]. Reproduced by permission of The Royal Society of Chemistry.

of soft metal ions by the cavity of the complex is investigated by electronic absorption and emission spectroscopy. [$Cu(PPh_3)_2$(**dic-Se**)]BF_4 prefers to bind transition metal ions such as Zn^{2+} and Cd^{2+} unlike [$Cu(PPh_3)_2$(**dic**)]BF_4 which preferentially binds alkali and alkaline-earth metal ions such as Na^+, K^+ and Ba^{2+}. The observed differences in ion binding property may be ascribed to the introduction of the softer Se donor atom in **dic-Se**, which would give a higher affinity for softer metal ions. Thus, in the present system, the hard–soft acid–base factor appeared to be dominant rather than size-match selectivity (considering the fact that Cd^{2+} and Na^+ have same ionic diameter) for governing the ion binding properties [63].

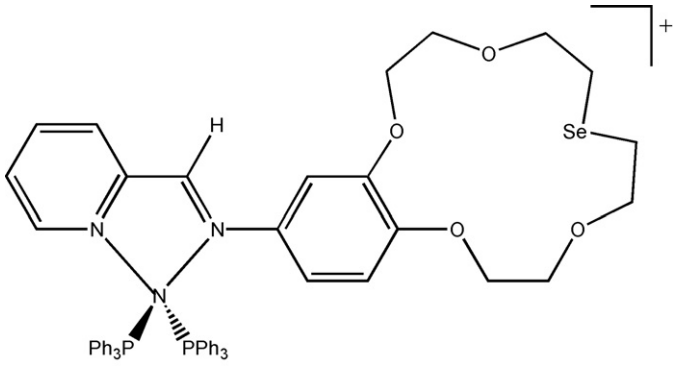

[$Cu(PPh_3)_2$(dic-Se)]$^+$

Meunier and co-workers [65] prepared **benzo-15Se2O3** by a route similar to the preparation of **42**. The neutral species [$PdCl_2$(**benzo-15Se2O3**)] was synthesized from the reaction of **benzo-15Se2O3** and Li_2PdCl_4 in which the palladium is probably bonded to an Se_2Cl_2 set (Scheme 12) [66]. The structure of the novel selenocationic palladium complex [Pd(**benzo-15Se2O3**)$_2$]Y_2 [Y = NO_3, PF_6] shows a square planar arrangement of the four sele-

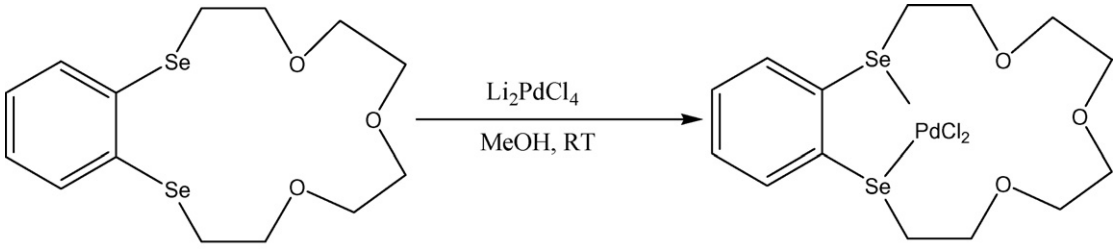

Benzo-15Se2O3 **[Pd(benzo-15Se2O3)Cl_2]**

Scheme 12.

nium atom donors from two selenamacrocyclic ligands around the central metal ion (Fig. 42).

Metal-ion complexation by mono- and di-selena macrocyclic ligands containing additional donor atoms has also been reported [67]. Also a series of selenacrown-4 derivatives were synthesized and their cation binding abilities with aqueous alkali (Li^+, Na^+, K^+) and some heavy (Ag^+, Tl^+) metal picrates are evaluated [68].

The yield of the new macrocycle **18O4Se2** could be increased by conducting the experiment in ethanol instead of liquid ammonia [69]. The nine-membered ring compound 1-selena-4,7-dioxacyclononane (**9O2Se**) is obtained as by product which was also observed as an unexpected ring contraction product of the reaction of $BrCH_2CH_2OCH_2CH_2OCH_2CH_2Br$, $NCSeCH_2CH_2SeCN$ and $NaBH_4$ [12b]. The complex [$PtCl_2$**18O4Se2**] (Fig. 43) has *cis* square planar geometry (Se_2Cl_2) with no interaction between the Pt centre and the ether oxygens.

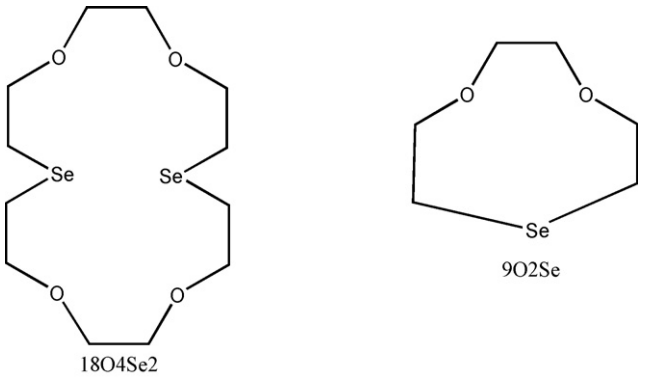

Two novel selenium functionalized calix[4]crowns **45a** and **b** were reported by Zeng et al. (Scheme 13) [70]. Double bridged bis-calix[4](tetraseleno)crown ether **46** is obtained as a byproduct in 4% yield in the preparation of **45b**; however this yield can be increased by the slow addition of the disodium salt of 1,3-propanediselenol to the solution of **44b**. Calix[4]crown ether **45a** adopts the cone conformation (Fig. 44). It forms a dimer structure *via* self-inclusion of the two cavities. Interestingly, this dimeric structure further assembled into a two-dimensional aggregate *via* inter-molecular Se···Se interactions in the solid state (Fig. 45). They are good ionophores for silver ion-selective electrodes. The polymer membranes containing ionophores **45a** and **45b** give excellent potentiometric selectivity coefficients for Ag^+. This is due to its strong coordination to Se-donor atoms *via* soft–soft interaction against those ions with high hydration energies and transition metal ions with +2 charges for their weak interaction with selenium donors of the ionophores.

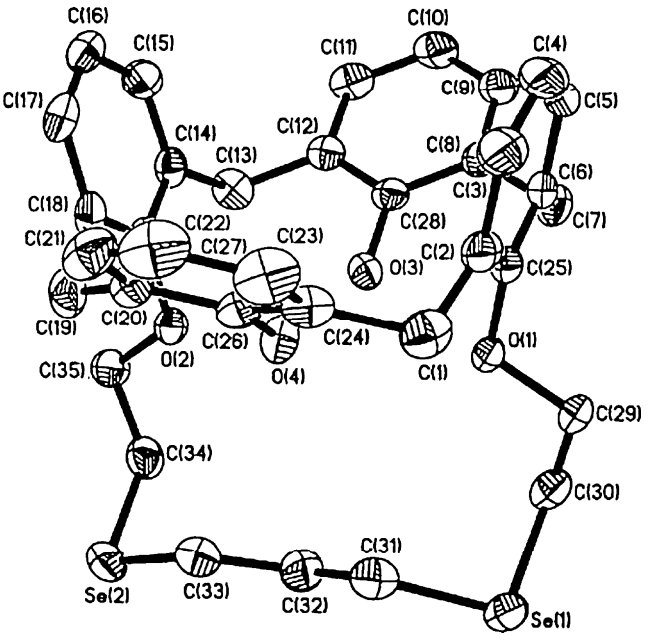

Fig. 44. X-ray crystallography of calix[4]crown ether **45a**. Reprinted from Ref. [70]. Copyright (2001), with permission from Elsevier.

Two new selenacrown ethers, i.e. 7,11-diseleno-2,3,15,16,-dibenzo-1,4,14,20,23-hexaoxacyclopentacosane (**47**) (Scheme 14) and *N*,*N*'-dimethyl-1,11-diaza-4,8,14,18,-tetraselenacycloicosane (**48a**, Scheme 15) were synthesized in a stepwise manner [71]. The complex stability constants and the thermodynamic parameters for complexation of C60 with these crown ethers were determined by UV–vis spectrometry, showing the highest K_s value for **48a**. Thermodynamically, the complexation of C60 with **48a** and **47** is absolutely enthalpy-driven, while the complex stability is governed by the entropy term.

5.2. S/N macrocycles

A new type of selena-aza-crown ether-6-(4-nitrobenzyl)-1,4,7,10-selenatriazacyclododecane, its Pt(II) complex and the catalytic activity of this complex for the hydrosilylation of olefins by triethoxysilane is investigated [72a]. Also, a series of selena-aza-crown ethers were reported [72b]. The new seleno-azacrown ether, *N*,*N*'-ditosyl-1,11-diaza-4,8,14,18-tetraselena cycloicosane **48b** was synthesized according to Scheme 15 [73]. The reaction of seleno-azacrown ether with copper(II) perchlorate and platinum(IV) tetrachloride gives the corresponding Cu(I) and Pt(IV) complexes, respectively. The formation of Cu(I) and Pt(II) complexes despite the use of Cu(II) and Pt(IV) in the initial stage of the reaction may be due to the electron-transfer process from Se atoms to the coordinated metal centres. The structure of the Cu(I) complex shows the coordination of copper though four selenium atoms to complete a distorted-tetrahedral geometry with no π–π interactions between the adjacent complex units. A ring contracted complex, from 20-member to a 10-member ring, is obtained by switching the central copper ion to a platinum ion. The platinum centre is coordinated by two selenium atoms and two chlorine atoms to complete a square planar geometry with no interaction between platinum and nitrogen. The packing structure of the Pt(II) complex shows several type of interactions among the complex monomers.

5.2.1. Schiff base macrocycles

A novel series of selenamacrocycles **50** were synthesized by Singh and co-workers [74–76] from the metal free [2+2] condensation of bis(*o*-formylphenyl) selenide (**49**) and a series of diamines as depicted in Scheme 16. This is the first time selenium has been incorporated into a macrocyclic Schiff base. Secondary intra-molecular Se···N coordination plays an important role in the formation of the macrocycle by reducing the unfavorable lone pair–lone pair interaction between the nitrogen atoms and this interaction acts as a template in the formation of the ring.

The structures of all macrocycles show secondary Se···N interactions, the strongest being in the 22-membered macrocycle **50a** (Table 2). Macrocycle **50b** has the longest transannular Se···Se distance. The solid state geometry of the molecules indicates the presence of only one attractive interaction per selenium atom, i.e. it corresponds to the structure of 10-Se-3 selenurane. The replacement of an ethylene bridge with a cyclohexane bridge leads to a significant change in the cavity size (Table 2). One representative crystal structure of **50c** is shown in Fig. 46.

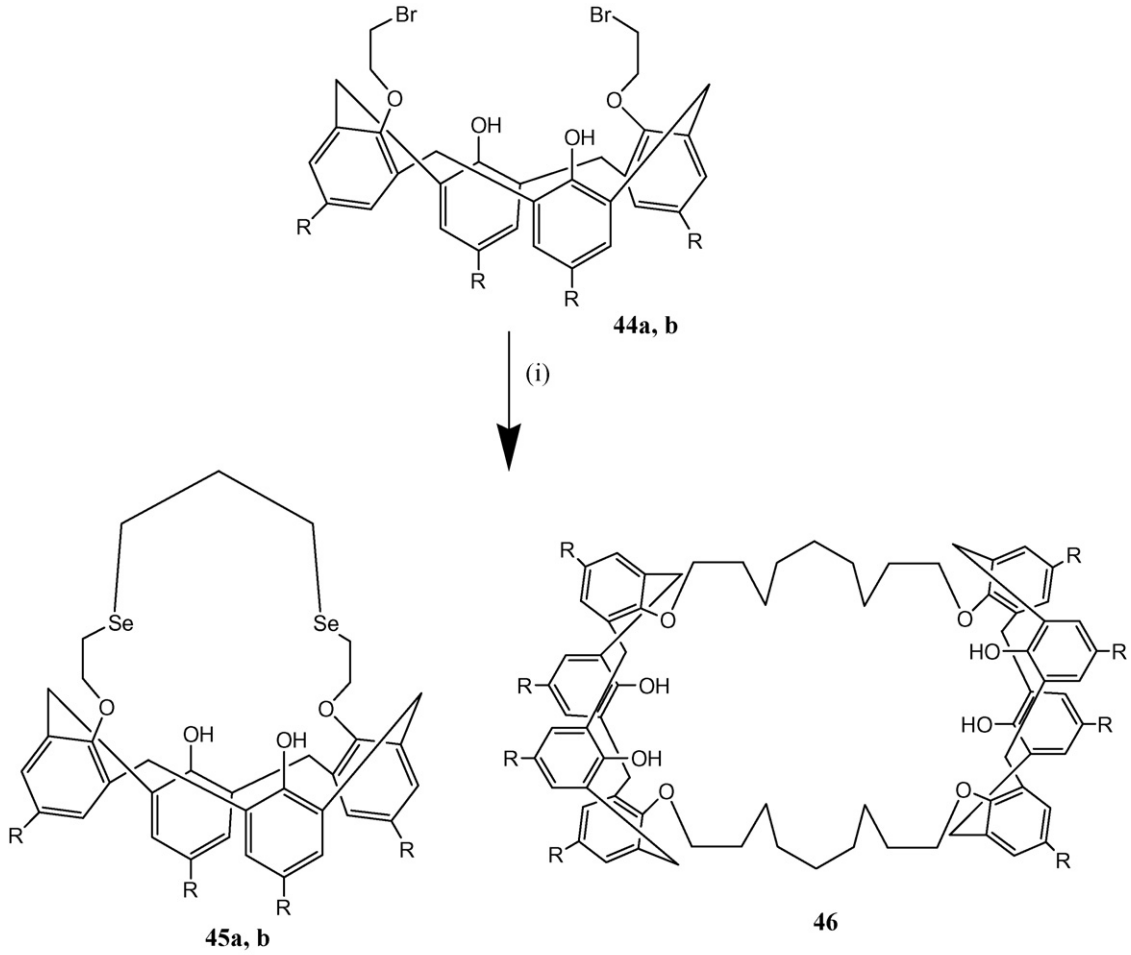

Scheme 13. (i) Disodium salts of 1,3-propanediselanol, ethanol/THF refluxed for 6 h.

The reaction of **50a** or **50b** with $[PdCl_2(COD)]$ (COD = 1,5-cyclooctadiene) affords the complexes **51** and **52**, respectively, as yellow solids (Scheme 17) [74]. The microanalytical and spectroscopic data show the hydrolysis of two CH = N of the macrocycle **50a** to –CHO groups and is supported by the solid state structure of **51**. The hydrolysis of selenaaza macrocycle may be due to excessive strain on the ring which forces the metal to adopt a planar geometry. However, a similar reaction of the Pd^{II} precursor with the 22-membered tellurium analog gives the cationic complex $[Pd(L)]^{2+}$ [L [77] = macrocycle derived from bis(*o*-formylphenyl)

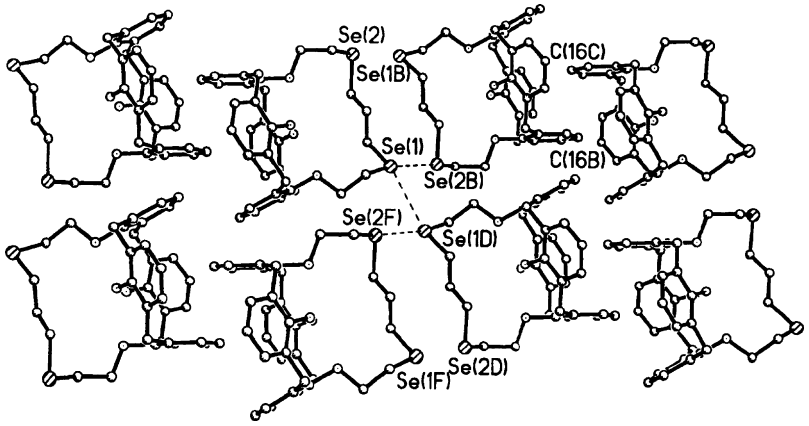

Fig. 45. Infinite sheet aggregate of calix[4]crown ether **45a** *via* self-inclusion of the hydrophobic cavities and inter-molecular selenium···selenium contacts. Reprinted from Ref. [70]. Copyright (2001), with permission from Elsevier.

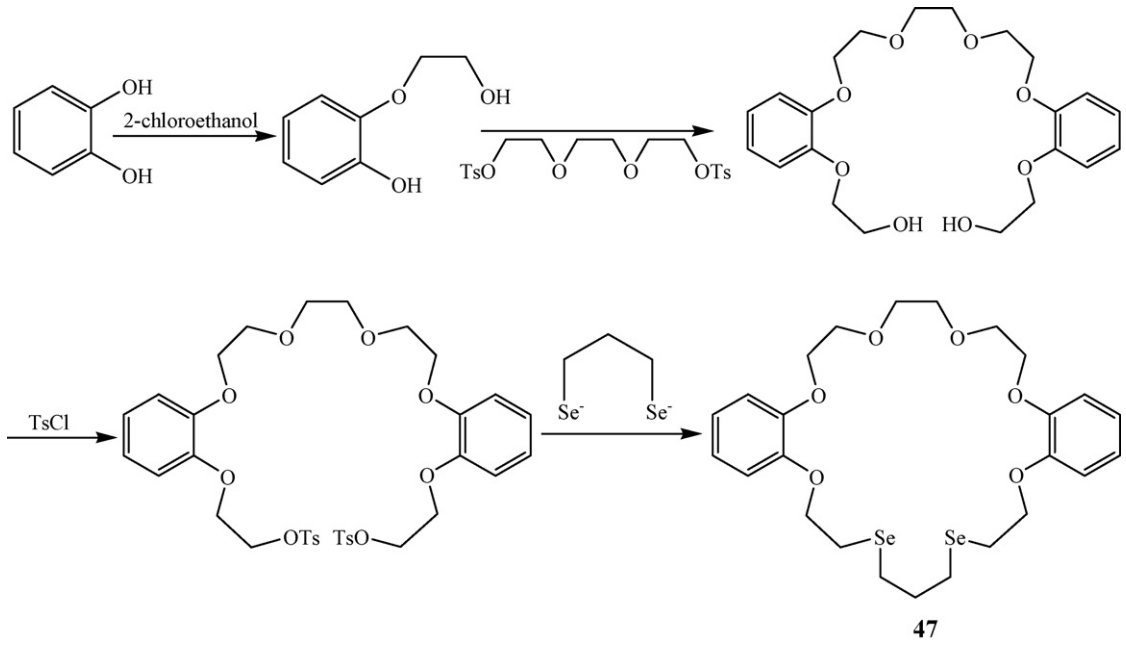

Scheme 14.

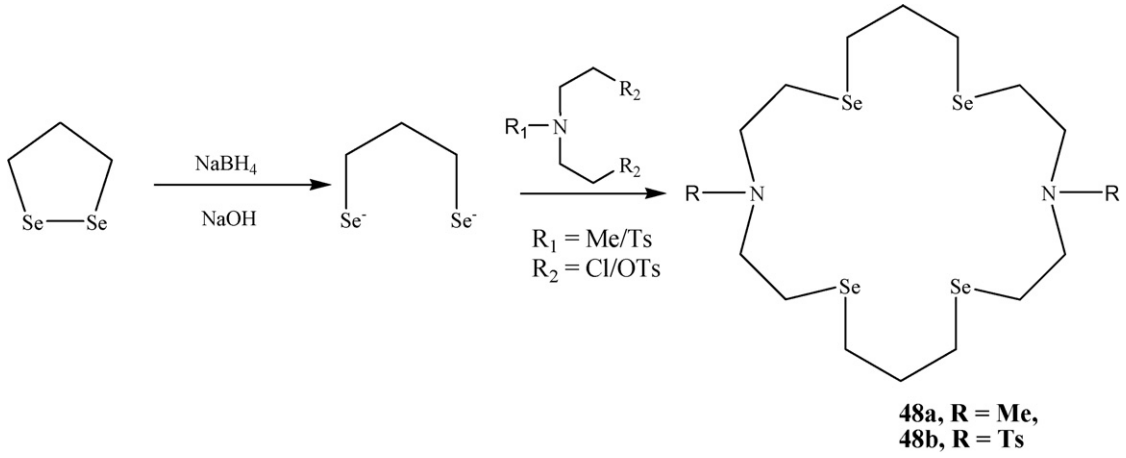

Scheme 15.

Table 2
Non-bonding distances (Å) of Schiff base selena-aza macrocycles

Compound no.	Bond	Distance
50a	Se(1)···N(1A)	2.723
	Se(2)···N(1C)	2.729
	Se···Se	3.808
50b	Se···N(1B)	2.773
	Se···Se	7.229
50c	Se···N(1BA)	2.814
	Se···Se	4.177
50d	Se1···N1A	2.816
	Se2···N2A	2.782
	Se···Se	5.881
55	Se···N(1A)	3.01
	Se···Se	4.75

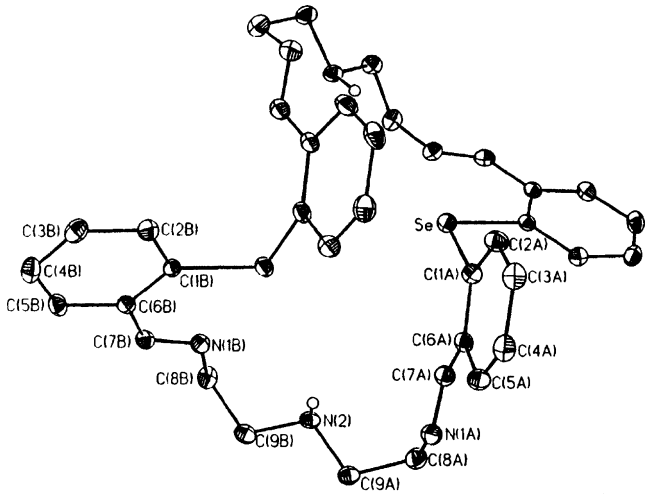

Fig. 46. Crystal structure of **50c**. Reprinted from Ref. [75]. Copyright (2001), with permission from Elsevier.

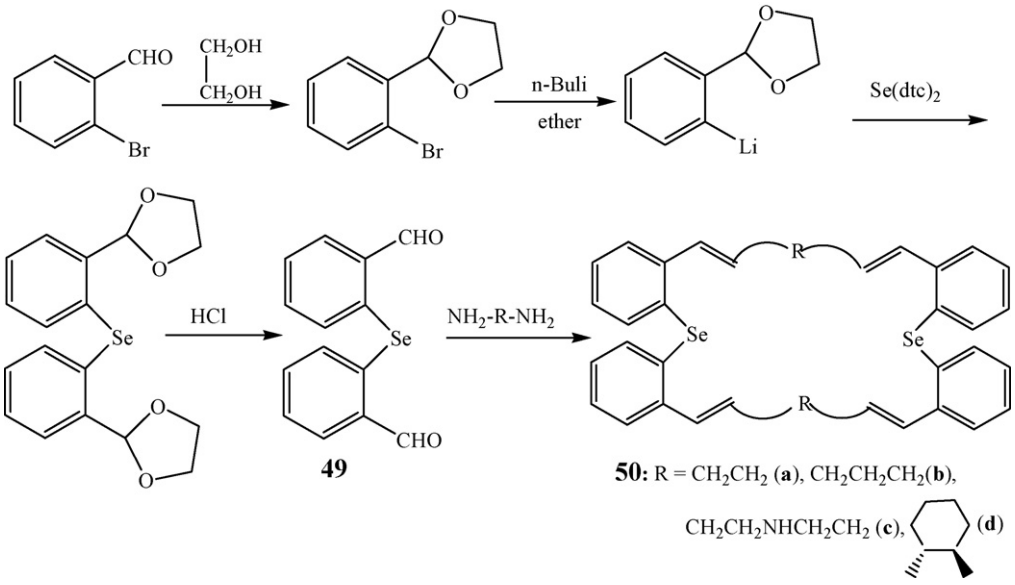

Scheme 16.

telluride and 1,2-diaminoethane] without any hydrolysis [78]. This may be due to the larger hole size of the tellurium analog (Te···Te 4.979 Å). The geometry around Pd(II) metal ion is square planar through N_2Se_2 coordination. There is a weak coordination between the Se and O atom (2.855 Å) (Fig. 47). The formulation and structure of **52** as [Pd(**50b**)]$(PF_6)_2$ was confirmed from the microanalytical and spectroscopic data. The large ring size of **50b** (24 membered and Se···Se distance 7.229 Å) probably mitigates against coordination of the selenium atoms to Pd^{II}.

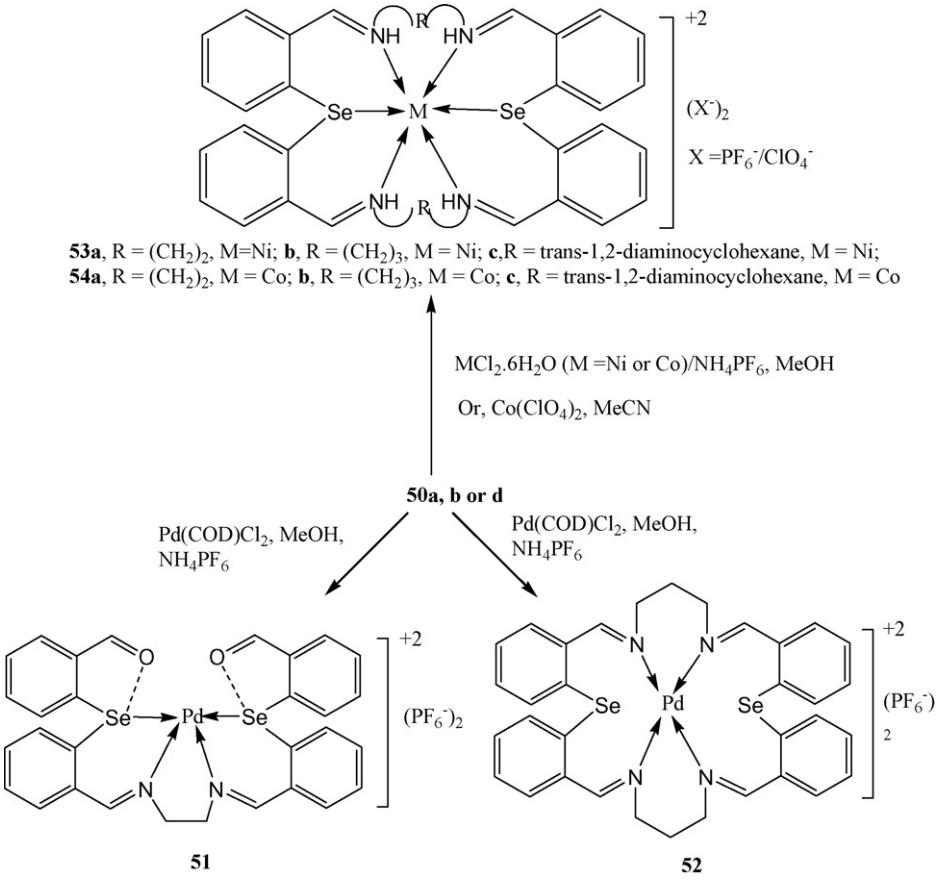

Scheme 17.

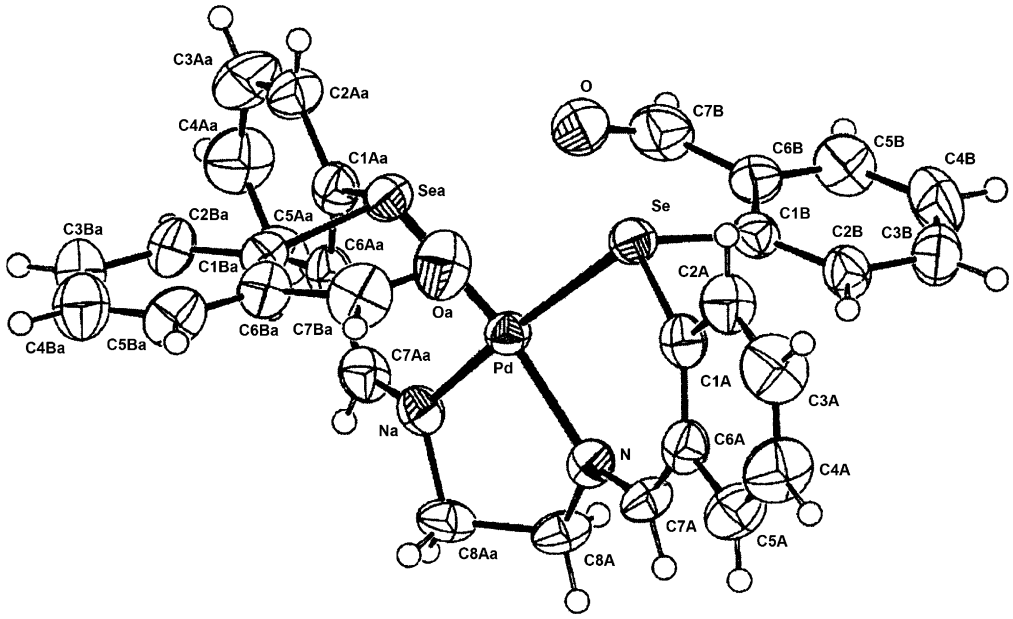

Fig. 47. Crystal structure of **51**. Taken from Ref. [74]. Copyright Wiley-VCH Verlag GmbH & Co. KGaA. Reproduced with permission.

The reaction of $MX_2 \cdot 6H_2O$ [M = Ni(II), X = Cl or Co(II), X = Cl/ClO_4] with **50a**, **50b** or **50d** affords the paramagnetic complexes **53a**–**53c** and **54a**–**54c** (Scheme 17). The Ni(II) ion in **53a**–**53c** [74,76] (Fig. 48) occupies the macrocyclic cavity and is bonded to all four nitrogen and two selenium donors to complete the distorted octahedral geometry. In all cases, the two selenium atoms are mutually *cis* to each other. **54b** is isostructural to the analogous Ni(II) complex **53b** [76]. Surprisingly, Co^{II} complexes **54a** and **54c** are low-spin whereas **54b** is high spin.

These Schiff base macrocycles are prone to transmetallation and hydrolysis on treatment with metal salts, which leads to cleavage of macrocycle (*vide supra*). So, to study the ligation behavior of the reduced form of the Schiff base macrocycles, reduction of all the macrocycles (**50a**–**50d**) was undertaken to generate the tetraamino derivatives [76,79] which are superior in chemical stability and flexibility to their Schiff base parents. Also the reduced form of macrocycles have only sp^3 hybridized donor atoms and can accommodate a larger range of shapes and sizes than the parent Schiff base macrocycles that have sp^2 hybridized donor atoms. In the reduced forms, the macrocycles have weaker E···N interactions as indicated by their multinuclear NMR spectra and single crystal X-ray structures (*vide infra*). The molecular structure of **55** (Fig. 49) shows that, of two possible nitrogen atoms available for interaction, only one interacts with the Se atom. The longer Se···N and Se···Se distances (Table 2) show, respectively, the weaker interaction and the larger cavity size than its parent Schiff base **50a**. Their complexation towards various transition metal ions are studied [80–82].

The structure of the Ni(II) complex **56** [80] is similar to **53a**. The two Se atoms are *cis* to each other in the distorted octahedral geometry as they are in the parent Schiff base complex **53a**. The formation of the desired 1:1 complexes **57** and **58**, from the

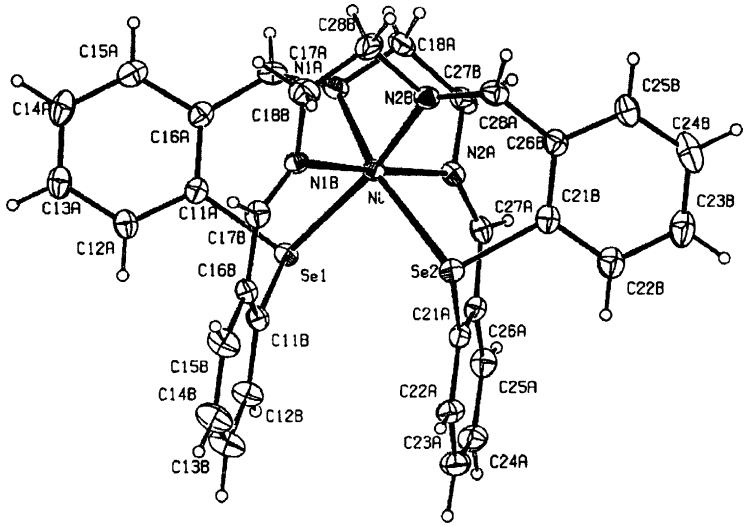

Fig. 48. ORTEP diagram of **53a**. Taken from Ref. [74]. Copyright Wiley-VCH Verlag GmbH & Co. KGaA. Reproduced with permission.

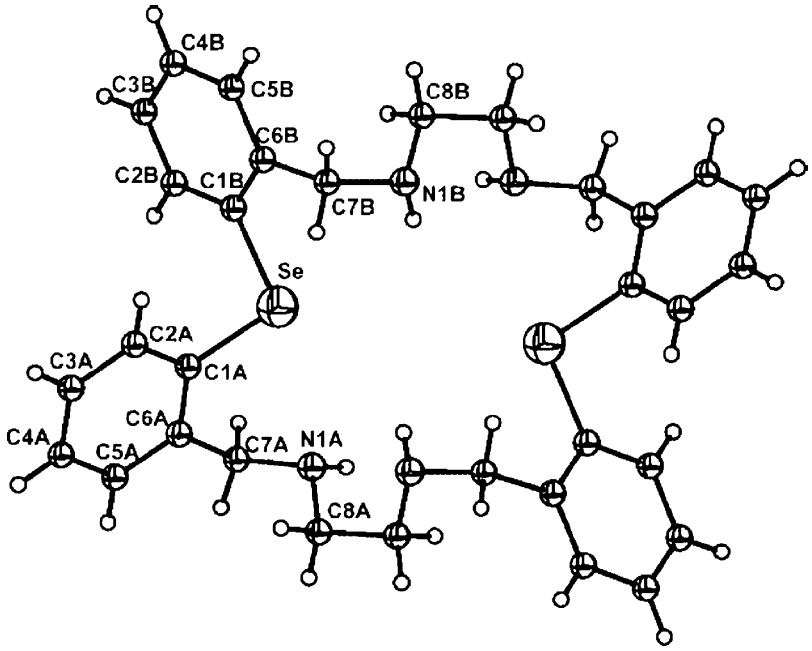

Fig. 49. ORTEP diagram of **55**. Taken from Ref. [80]. Copyright Wiley-VCH Verlag GmbH & Co. KGaA. Reproduced with permission.

reaction of Pd(II) precursors with **55** [80], is in contrast to the formation of hydrolyzed product **51** [74]. This may be due to the larger hole size of **55** compare to **50a** [74] (see Table 2). The downfield shift of the peaks of **57** and **58** in ^{77}Se NMR spectra (869 and 787 ppm, respectively) relative to that of free ligand (δ = 329 ppm) indicates the possibility of selenium coordination to the metal in solution which is not observed in the solid state structure (*vide infra*). The variable-temperature ^{1}H NMR spectroscopy study on **57** shows that, the metal effectively hops between the six donor sites of the macrocycle. However, a single peak in the ^{77}Se NMR spectrum rules out N3Se coordination. Both complexes are isostructural. The cation Pd^{2+} adopts a square planar geometry with coordination of the four nitrogen atoms in the solid state (Fig. 50). This is in contrast to isolation of Pd(II) complexes of mixed donor Se/Te macrocycles containing O or P where soft donor centres Se/Te coordinate to Pd(II) [52,66,69,70,83]. This anomalous behavior is due to the conformational requirement of the ligand around the central Pd^{II} atom for coordination with donor atoms, as well as the chelate ring effect [80].

A similar reaction of $PtCl_2$ and **55** gave brick red crystals of **59** [80,81]. The structure of **59** clearly suggests the formation of an unexpected 23-membered metallamacrocyclic complex with C–Pt–Se linkage (Fig. 51). The geometry around Pt^{IV} is octahedral. The Pt–N bond *trans* to Pt–Se is longer than the other two Pt–N bonds because of the strong *trans* influence of –SePh. The behavior of the macrocycle to form the cationic Pt^{IV} complex by oxidative addition of the C–Se bond to the Pt^{II} centre is in contrast to those of the reported stable Pt^{II} and Pt^{IV} complexes with homodonor and mixed donor cyclic selenoether ligands [32,38,39,41,52,66,69,70,83]. The facile oxidative addition in this

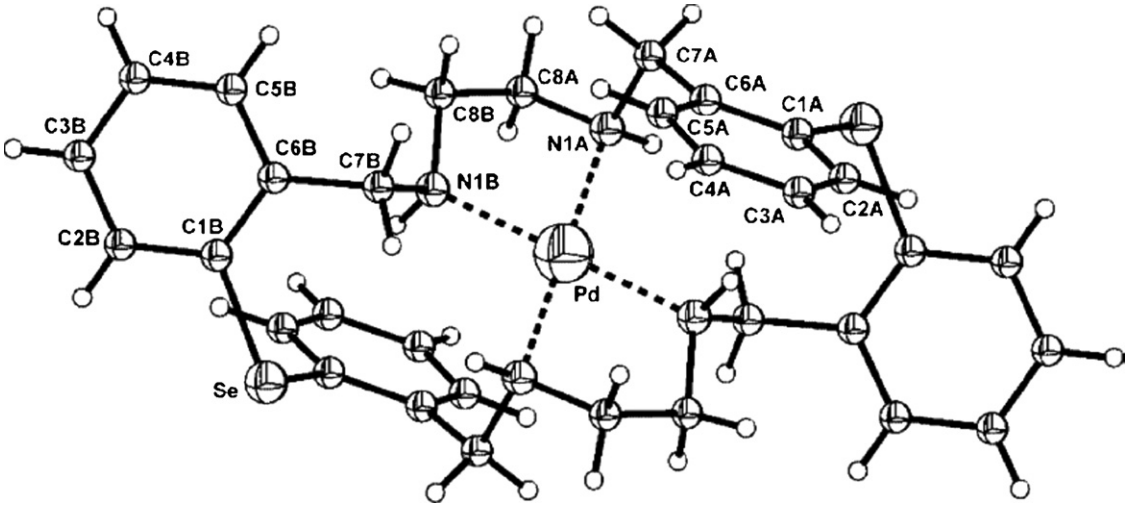

Fig. 50. ORTEP diagram of **58**. Taken from Ref. [80]. Copyright Wiley-VCH Verlag GmbH & Co. KGaA. Reproduced with permission.

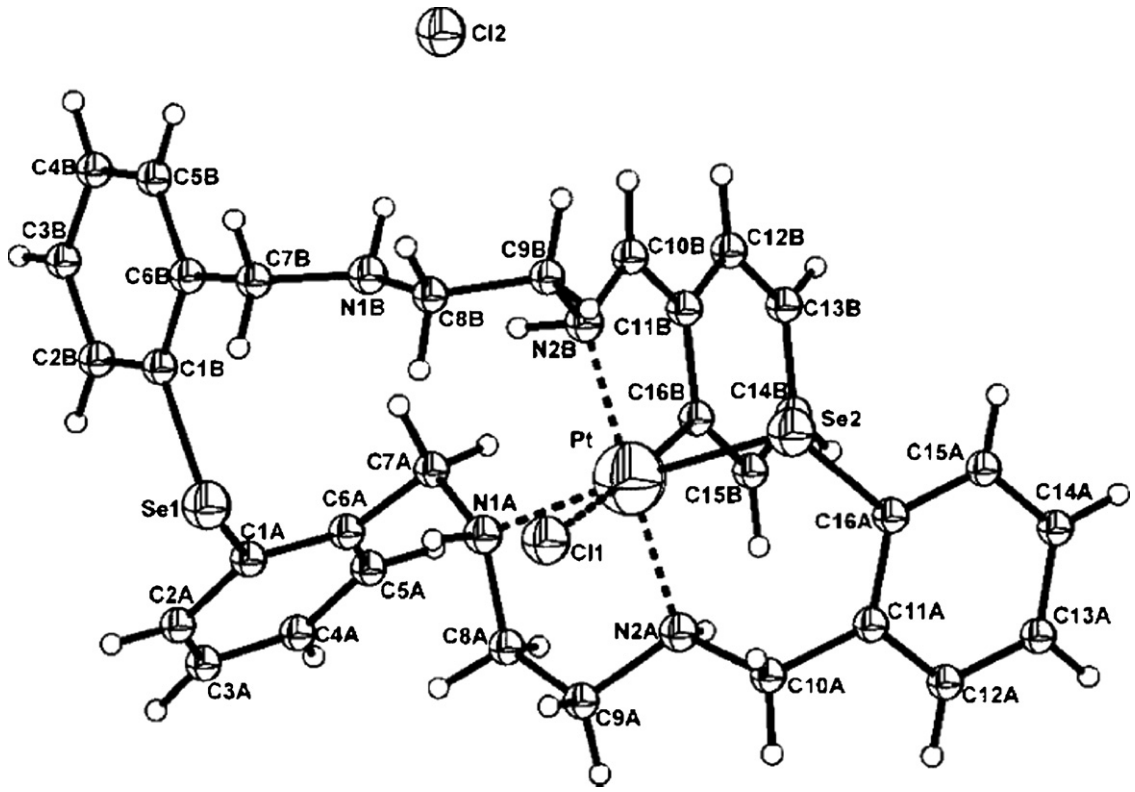

Fig. 51. ORTEP diagram of **59**. Taken from Ref. [80]. Copyright Wiley-VCH Verlag GmbH & Co. KGaA. Reproduced with permission.

case may be facilitated by the more polar nature of C–Se bond that results from the N → Se intra-molecular interaction present in the parent macrocycle (*vide supra*). Though the oxidative addition of halogens and alkyl halides to the Pt^{II} centre are common [84], there is only one more example of oxidative addition of C–Se bond to Pt^{II} [85]. Another novel feature of the metallamacrocycle **59** is the stability of the cationic Pt(IV) species with a selenolate linkage in the macrocyclic ring.

The 1:1 complex **60** was obtained from a similar reaction of $Cu(CH_3CN)_4ClO_4/PF_6^-$ with ligand **55** [80]. The magnetic moment (1.79 BM) and the electron spin resonance spectrum confirm the square planar geometry of the complex **60**. The ^{77}Se NMR spectrum of the related Hg(II) complex **61** exhibits a single signal at $\delta = 315$ ppm (for the free ligand **55**, 329 ppm) indicating the absence of any interaction between Se and Hg^{II} [80] (Scheme 18).

Reaction of the ligand **62** (reduced form of ligand **50c**) with Pd(II) precursors afforded the complexes **63** and **64** in a 1:1 and 1:2 (ligand/metal) ratio, respectively (Scheme 19) [80]. Due to the poor solubility of the complex **64**, complete characterization was not possible. The structure of **63** shows the square planar geometry of the cation through coordination of four nitrogen atoms out of the possible N_6Se_2 coordination sites [80]. In $[Hg_2(PF_6)_2\{C_{36}H_{46}N_6Se_2\}]$ (**65**), a mercurous cation is trapped inside the cavity of the macrocycle [82]. This is the first and rare example of a structurally characterized Hg(I) cation complex of a monocycle where Hg_2^{2+} is trapped inside the cavity of the monocycle (Fig. 52) [82]. The negligible difference in the peak positions of the complex compared to the free ligand in ^{77}Se NMR disproves any coordination of the Se atoms to Hg_2^{2+} in the solution states.

The geometry around the Hg(I) is antiprismatic with Hg_2^{2+} coordinating to six nitrogen atoms (in accordance with the ^{77}Se NMR) forming four five-membered rings, and there is no interaction between the mercurous ion and the selenium donor atoms despite the expected soft–soft interaction between them. This is attributed to the formation of stable five-membered chelate rings rather than the formation of six-membered chelate rings which would result on coordination by Se.

The ^{77}Se NMR of the dinuclear lead complex $[Pb_2(PF_6)_2(OCOCH_3)_2\{C_{36}H_{46}N_6Se_2\}]$ (**66**) [82] also shows that the complex retains its solid state configuration in solution with no interaction between Se and Pb. The corresponding Pb(II) complexation with the azathia macrocycle shows Pb(II) coordination by both S and N atoms [86]. The geometry around each Pb(II) is a distorted octahedron due to a stereochemically active lone pair on Pb^{2+}. The two metal atoms and the bridging oxygen atoms form a central four-membered Pb_2O_2 ring. Each acetate ion in the molecular unit acts as chelating ligand toward one metal atom and is bridging between the two metals through one of its oxygen atoms (Fig. 53). This is the first example of a binuclear lead complex of a monocycle where the two lead atoms as well the chelating acetate anions are wrapped by the macrocycle cavity.

The polyamine macrocycles can act as receptors for cations, neutral molecules as well as anions. These polyamine macrocycles are capable of undergoing polyprotonation in solution forming positively charged polyammonium cations, which can bind selectively a variety of inorganic, organic and biologically important anions by electrostatic forces and hydrogen bonding. A series of macrocyclic adducts (**67a**–**67i**, **68a**–**68h**) with different counter anions such as halides, SO_4^{2-}, ClO_4^-, PO_4^{3-}, CF_3COO^- and NO_3^- were synthesized as white solids by treating the ligands **55** and **62** with the corresponding acids [87]. The ^{77}Se NMR spectra of the anion adducts of the selenaaza macrocycles reveal that in case of the sulfate adduct **67e** there is a considerable upfield shift (difference ~241 ppm) of peak position compared to the free ligand, whereas in case of other adducts there is only a marginal shift of the peak position. This

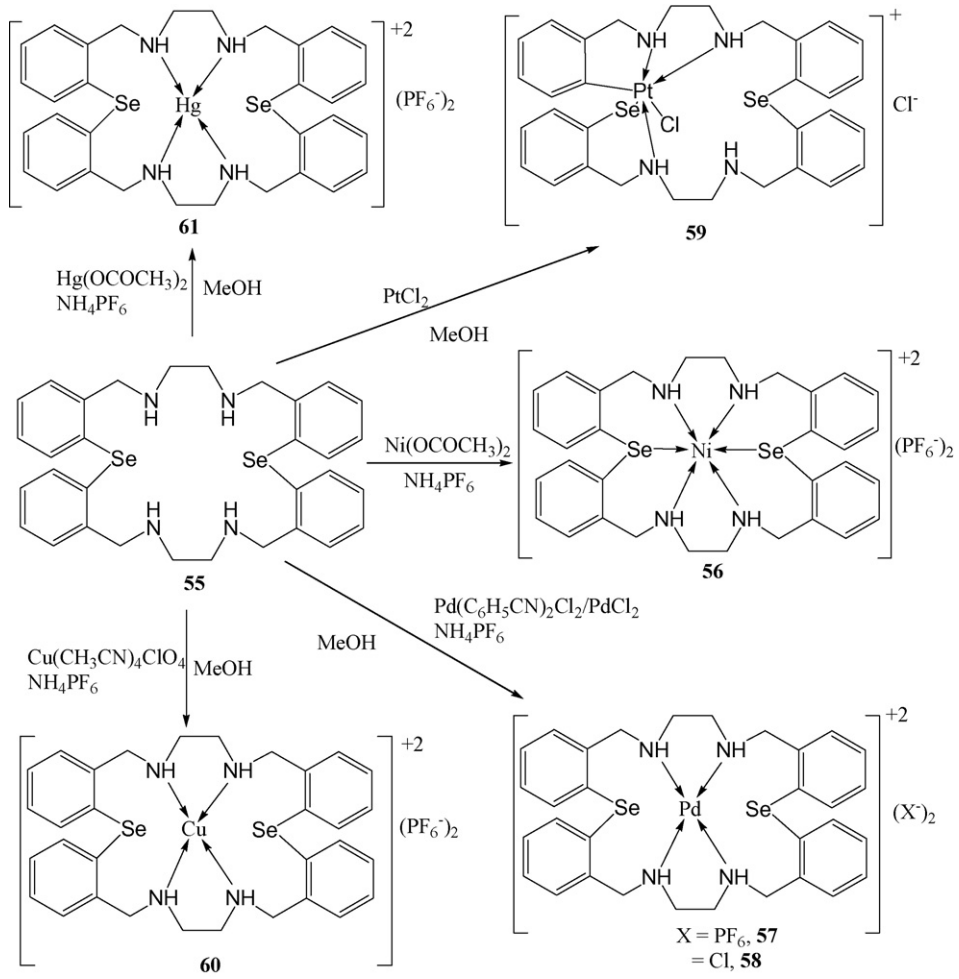

Scheme 18.

upfield shift in case of **67e** can be explained in terms of the short contacts between the sulfate ion and the macrocycle in the solid as well as in the solution state. The ^{77}Se chemical shift and the binding constant measured by the NMR titration method indicate that the macrocycle **55** has the highest binding affinity towards the sulfate ion of all the anions studied.

Crystal structures show that the macrocycles **55** and **62** form extensive hydrogen bonding adducts with the anions, which lie above and below the macrocycle framework. The TFA adduct of **55** afforded the diprotonated form of the macrocycle, whereas all other adducts show the macrocycles to be fully protonated. The packing diagram of **68e** shows extensive hydrogen bonding as well

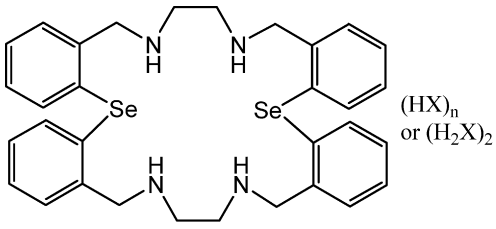

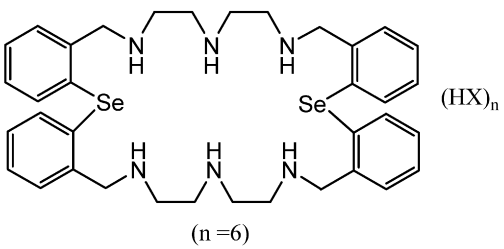

67a X = F^-; n = 4
67b X = Cl^-; n = 4
67c X = Br^-; n = 4
67d X = I^-; n = 4
67e X = SO_4^{-2}; n = 2
67f X = ClO_4^-; n = 4
67g X = $H_2PO_4^-$; n = 4
67h X = CF_3COO^-; n = 2
67i X = NO_3^-; n = 4

68a X = F^-
68b X = Cl^-
68c X = I^-
68d X = HSO_4^-
68e X = ClO_4^-
68f X = $H_2PO_4^-$
68g X = CF_3COO^-
68h X = NO_3^-

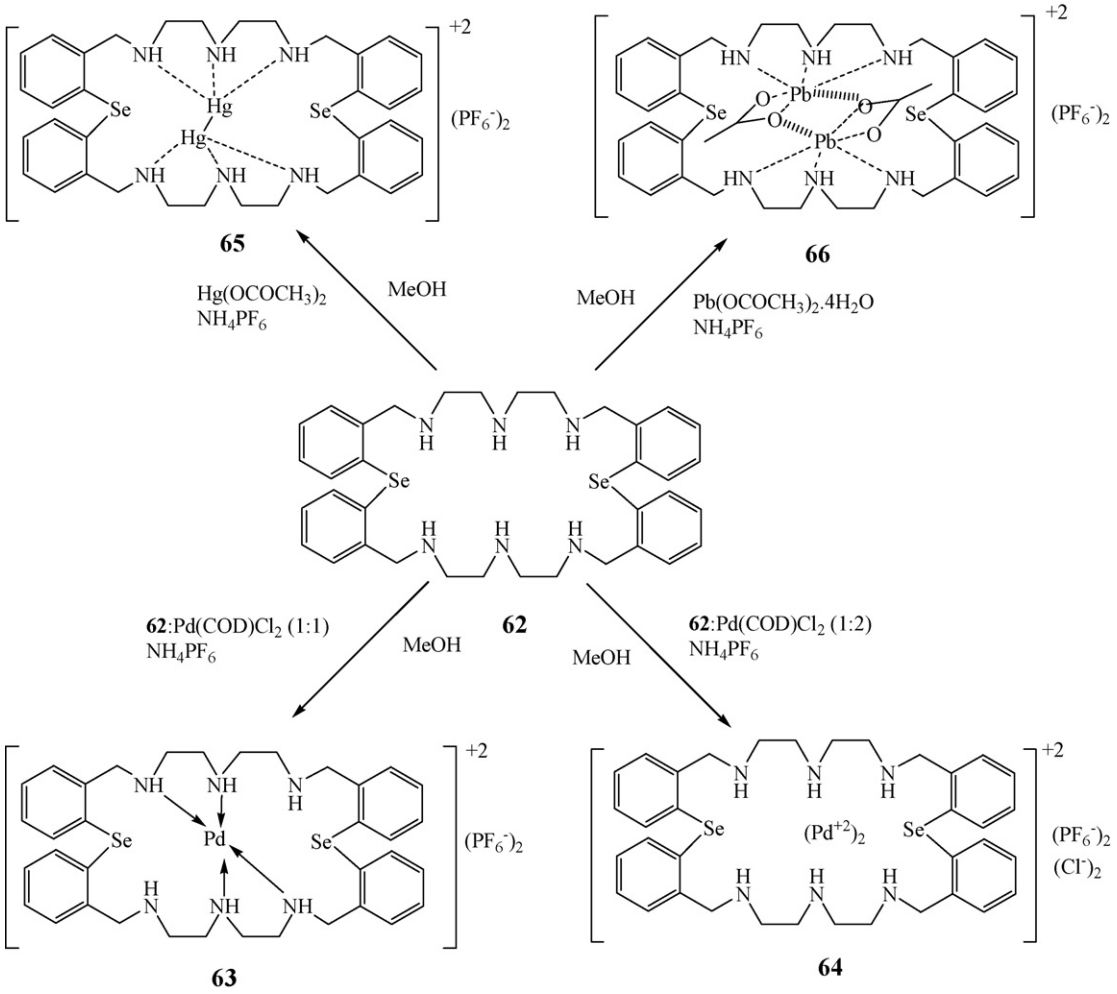

Scheme 19.

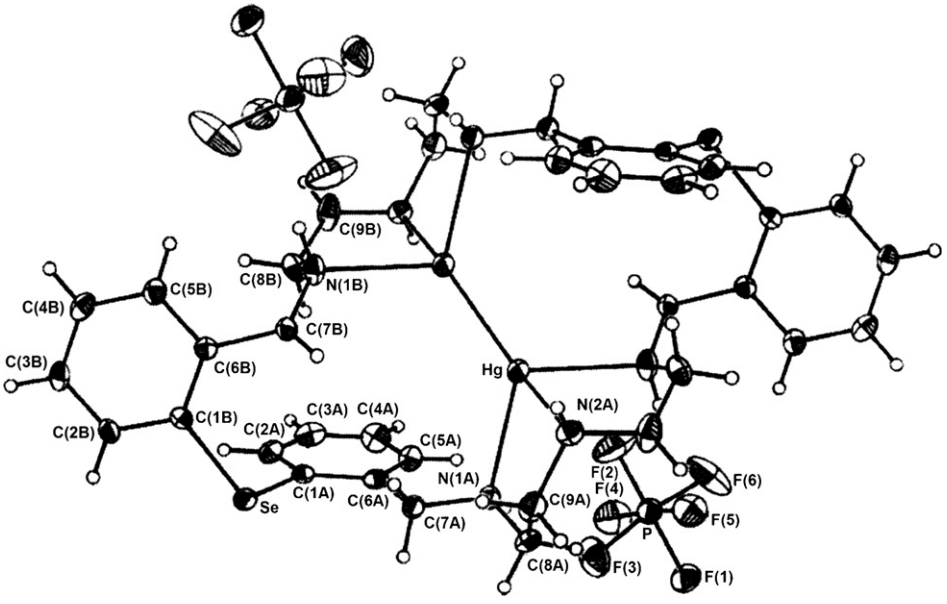

Fig. 52. ORTEP diagram of complex **65** cation. Taken from Ref. [82] with permission from the American Chemical Society.

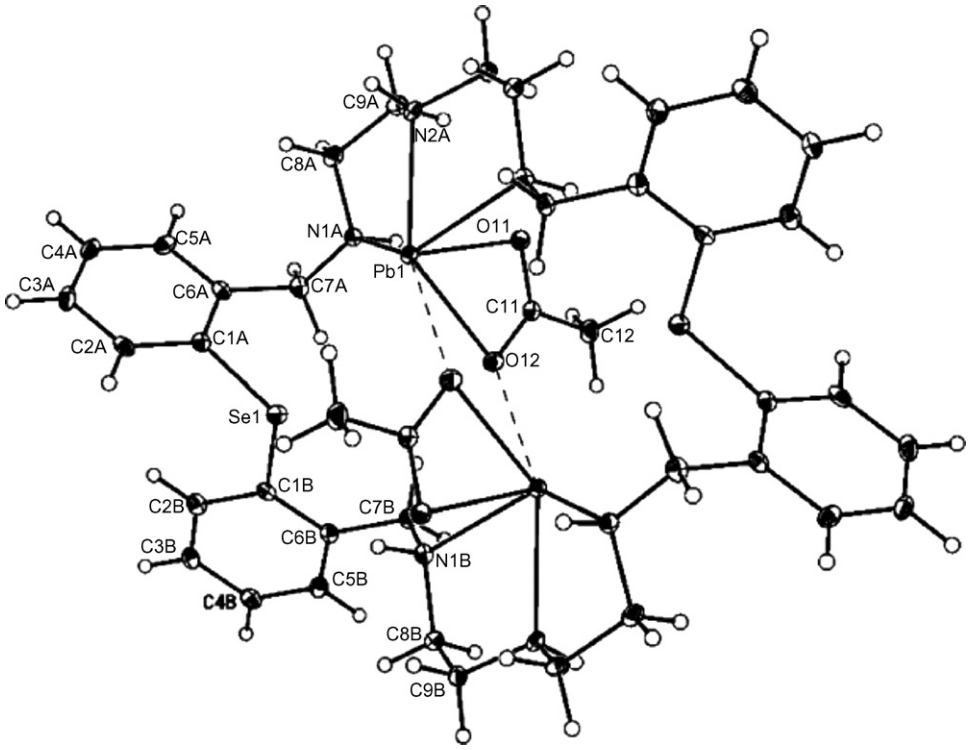

Fig. 53. Molecular structure of **66**. Taken from Ref. [82] with permission from the American Chemical Society.

as π stacking interactions between the molecules. The unit cell of **67c** consists of two discrete molecules with extensive hydrogen bonding among the neighbouring molecules [87]. The macrocyclic framework is highly puckered ellipsoid so as to suit the bonding pattern of the individual atoms. In **67c**, none of the bromide counter ions are situated inside the macrocyclic cavity, but one lies above the macrocyclic plane and forms intra-molecular hydrogen bonds with NH_2^+ and the hydrogen of a water molecule. One of the nitrogen atoms has bifurcated hydrogen bonding with two bromine atoms and the other nitrogen atom is bonded to one bromine and one water molecule (Fig. 54). The N–H···Br distances in **67c** show that the interaction of Br(1) atom with the macrocycle is the strongest.

In brief, the Schiff base macrocyles are suitable to bind to various transition metal ions but are prone to transmetalation and hydrolysis on treatment with metal salts leading to cleavage of the macrocycle. The selenaaza Schiff base macrocycle **50a** forms a hydrolyzed product with the Pd(II) cation [74] whereas the Te-analog forms transmetalated products with Pt(II) [78] and Hg(II) [77] cations. Reduction of the Schiff base components of these selenaaza macrocycles gives rise to more flexible macrocycles. These reduced Schiff base macrocycles show versatile and interesting coordination behavior towards a number of metal ions. Of particular interest is the Pd(II) complex of **55**, which coordinates through only nitrogen atoms as opposed to the N2Te2 coordination in the tellurium analog [81]. The coordination of Te to Pd(II) is due to the

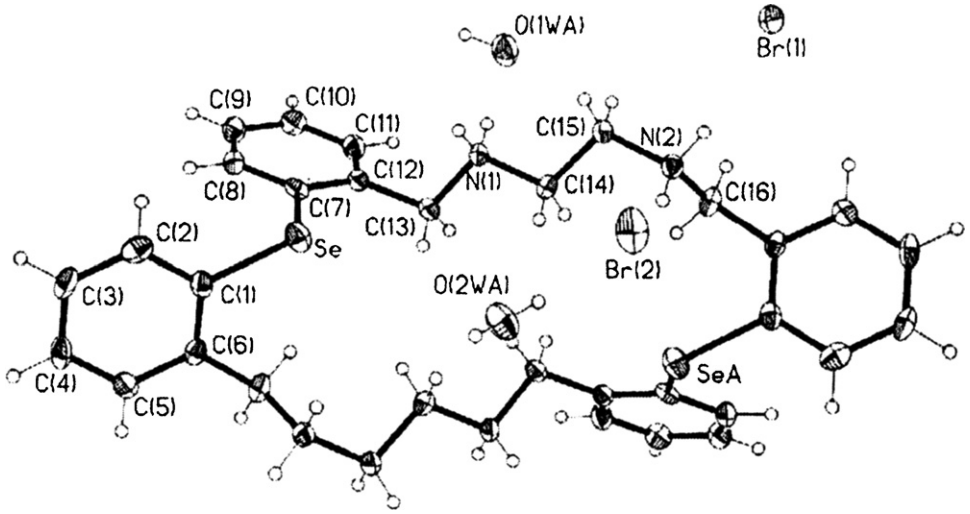

Fig. 54. Side view of compound **67c**. Reprinted from Ref. [87]. Copyright (2006), with permission from Elsevier.

greater σ-donor property of the Te over Se leading to soft–soft interaction and stabilization of the six-membered chelate ring. Also, the 28-membered diselenahexaaza macrocycle **62** shows potential to be used as an effective binuclear chelating ligand. The unusual non-interaction between selenium donor and metal atoms in all the complexes of **62** is attributed to the conformational requirement of the ligand around the metal atoms as well as the chelating ring effect.

Although much more is known about the recognition and binding of cations, anions are also an extremely important class to study. 70% of enzyme substrates are anionic. Due to the importance of anion recognition, there has been a boom in the design and synthesis of receptors for specific anion binding in the past decade. Hence, the protonation of the amino derivatives was carried out subsequently to study the binding of protonated derivatives with a variety of anionic substrates.

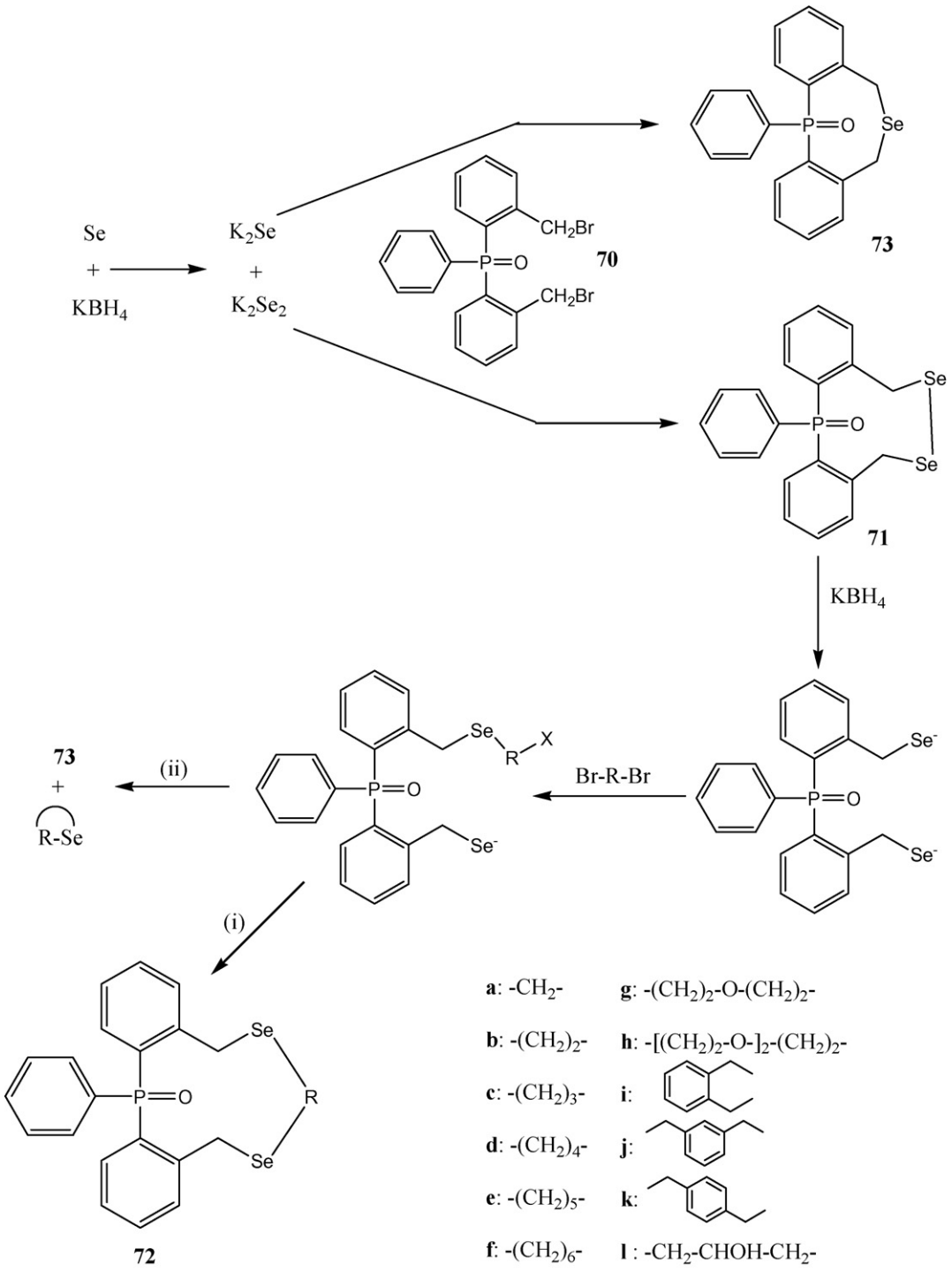

Scheme 20.

Also known are the 24- and 28-membered macrocyclic Schiff type ligands (**69**) with O, N and Se donor sets [83c].

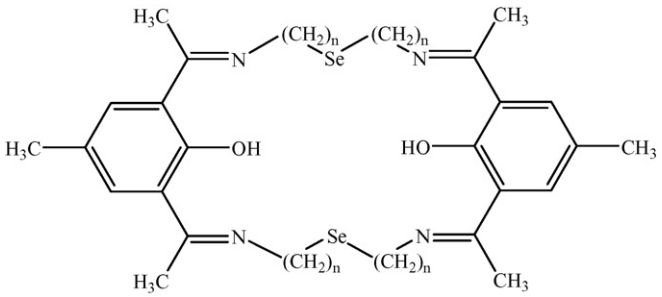

69a, n= 2; **69b**, n = 3

5.3. P/Se macrocycles

Ten to seventeen-membered macrocycles **72** having one phosphorus and two selenium atoms were synthesized by a one pot reaction as shown in Scheme 20 [83b]. In every case a side product 12-phenyl-7,12-dihydro-5H-12λ^5-dibenzo[*c*,*f*] [1,5] selenaphosphocin-12-one (**73**) is also isolated. In addition, two related macrocycles **74** and **75** containing two ethereal oxygen atoms in the cycle were reported (Scheme 21). For all three macrocycles (**72c**, **72f** and **75)** the phosphoryl P=O bond is directed upwards to the inside of the macrocycles. The unit cell of **72c** contains four sets of two independent molecules (I and II) which cannot be transformed into one another by either a symmetrical or translational operation (Fig. 55). There are no significant differences in bonding parameters between I and II except in the dihedral angles between the benzene ring planes. Reaction of these macrocyles with palladium(II) chloride gives 1:1 complexes except **74** which gives 2:1 complex.

The macrocyclic selenium-bridged hexamer [(Se=)P(μ-NtBu)$_2$P(μ-Se)]$_6$ (**77**) is obtained from the head-to-tail cyclization of the intermediate anion from the dimer [(Cl)(Se=)P(μ-NtBu)]$_2$ and sodium metal (Scheme 22) [88]. The formation of the P–Se–P bridge stems from the ambidentate nature of the intermediate anion. The $^{31}P\{^1H\}$ NMR spectrum and structural characterization of **76** suggests the presence of *cis* and *trans* isomers in a ratio of 7:1. The greater proportion of the *cis* isomer of **76** has an influence on the formation of a macrocyclic (rather than oligomeric or polymeric) product. Compound **77** is formed from six [(Se=)P(μ-NtBu)$_2$P(μ-Se)] units linked together into a macrocyclic arrangement through bridging Se atoms (Fig. 56). The molecule is only slightly distorted from overall planarity. The P_2N_2 ring units are approximately perpendicular to the mean plane of the macrocycle so that the molecules have a toroidal shape. Compound **77** represents a completely new type of Se macrocyclic arrangement, unique in possessing a rigid, crown-like arrangement combined with a large cavity size. Significantly, a cisoid geometry of the μ-Se atoms in **77** with respect to the P_2N_2 rings allows donor Se atoms to be available for potential metal coordination. In addition, there is a possibility of coordination to metal ions through *exo* Se atoms. The large size of the molecular cavity of the new Se macrocycle and its rigidity should make its host-guest chemistry of particular interest.

Recently Woollins and co-workers [89] reported the synthesis of large ring diselenides bearing the P–Se–Se–P linkage (Scheme 23). The structures of **78**–**80** confirm the presence of the 8-, 9- and 10-membered rings. Both R,R and S,S enantiomers are present in all the structures and no R,S/S,R diastereomers are observed. The macrocyclic framework is highly puckered with two phenyl rings on the opposite side of the heterocycle. The geometry around P(1) and P(2) is distorted tetrahedral. One of the representative crystal structures of **78** is given in Fig. 57.

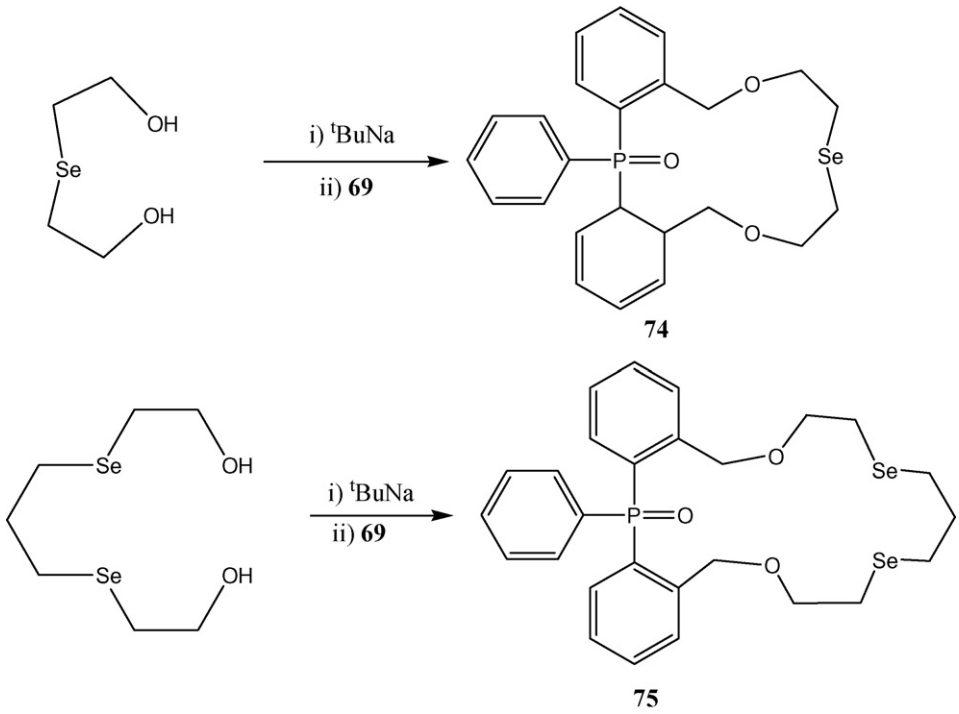

Scheme 21.

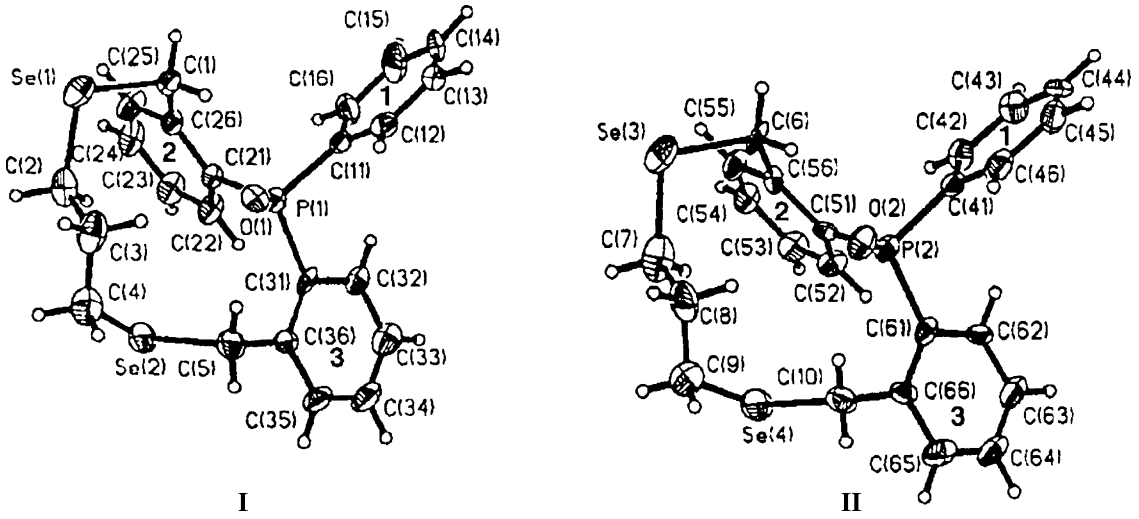

Fig. 55. The ORTEP plot for macrocycle **72c**. Taken from Ref. [83b]. Reproduced by permission of The Royal Society of Chemistry.

The P–Se heterocyclic diselenides **81** and **82** are also reported (Scheme 24). The structures of **81** and **82** are similar to the structures of **78**–**80**, although the P(1)–Se–Se angles for **81** and **82** are larger than those found in **78**–**80**.

6. Other macrocycles

Two novel organometallic macrocycles (**83**, **84**), which contain both the inorganic functionality of linear Cr≡Se≡Cr struc-

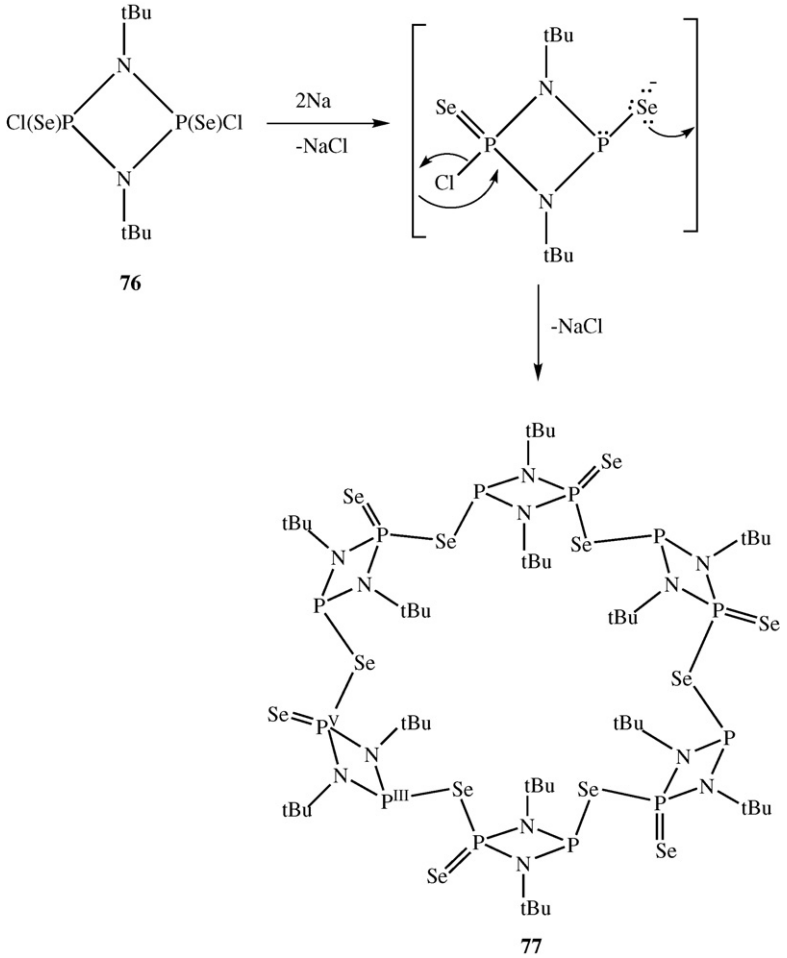

Scheme 22.

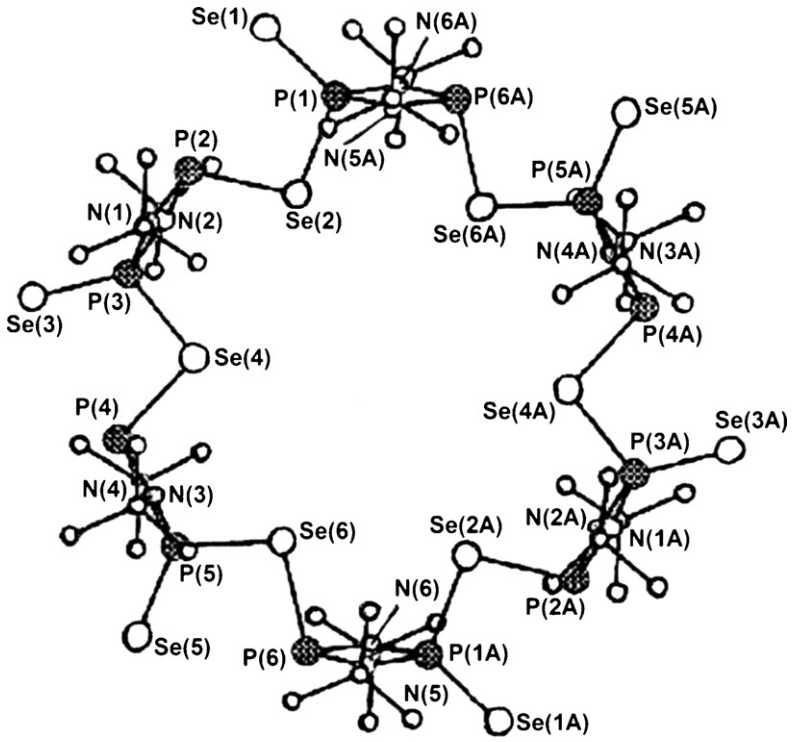

Fig. 56. Crystal structure of the macrocycle **77**. From Ref. [88]. Copyright Wiley-VCH Verlag GmbH and Co. KGaA. Reproduced with permission.

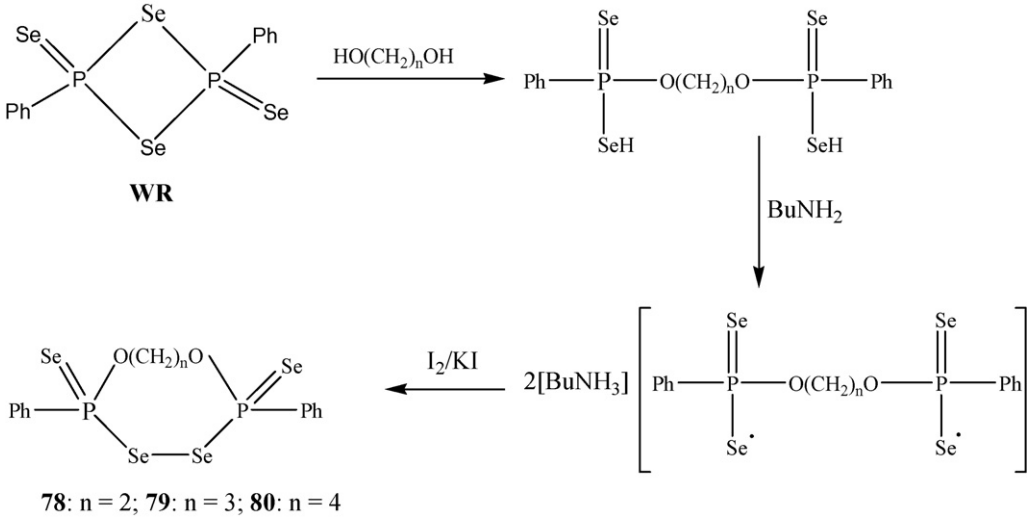

Scheme 23.

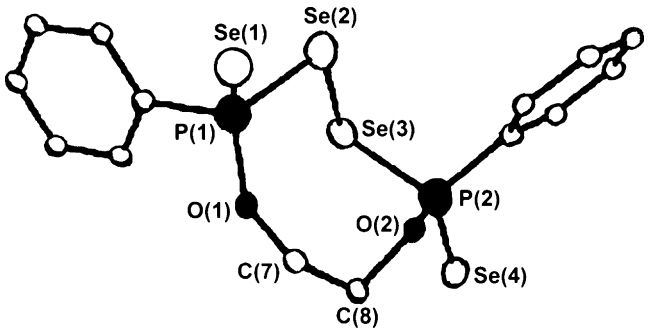

Fig. 57. Crystal structure of **78**. Taken from Ref. [89]. Copyright Wiley-VCH Verlag GmbH and Co. KGaA. Reproduced with permission.

tural moieties and organic diketo functionalities of succinoyl groups have been prepared *via* a facile "one pot" synthetic route (Scheme 25) [90]. In view of the rich chemistry of these functionalities, these macrocycles can be used as a new type of versatile synthon for preparing a wide variety of organometallic macrocycles. The molecule **83** consists of an essentially linear Cr–Se–Cr skeleton, four terminal carbonyls, and the succinoyl-bridged bis-(cyclopentadienyl) ligand (Fig. 58).

7. Cryptands

Before concluding, we shall consider data on cryptands containing selenium atoms. Incorporation of the larger Se atom should

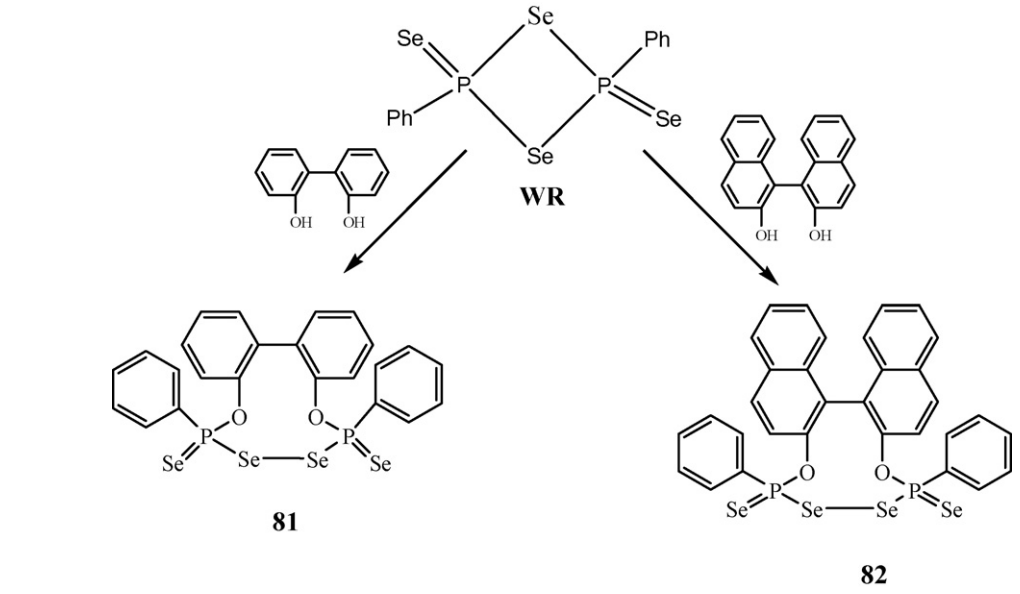

Scheme 24.

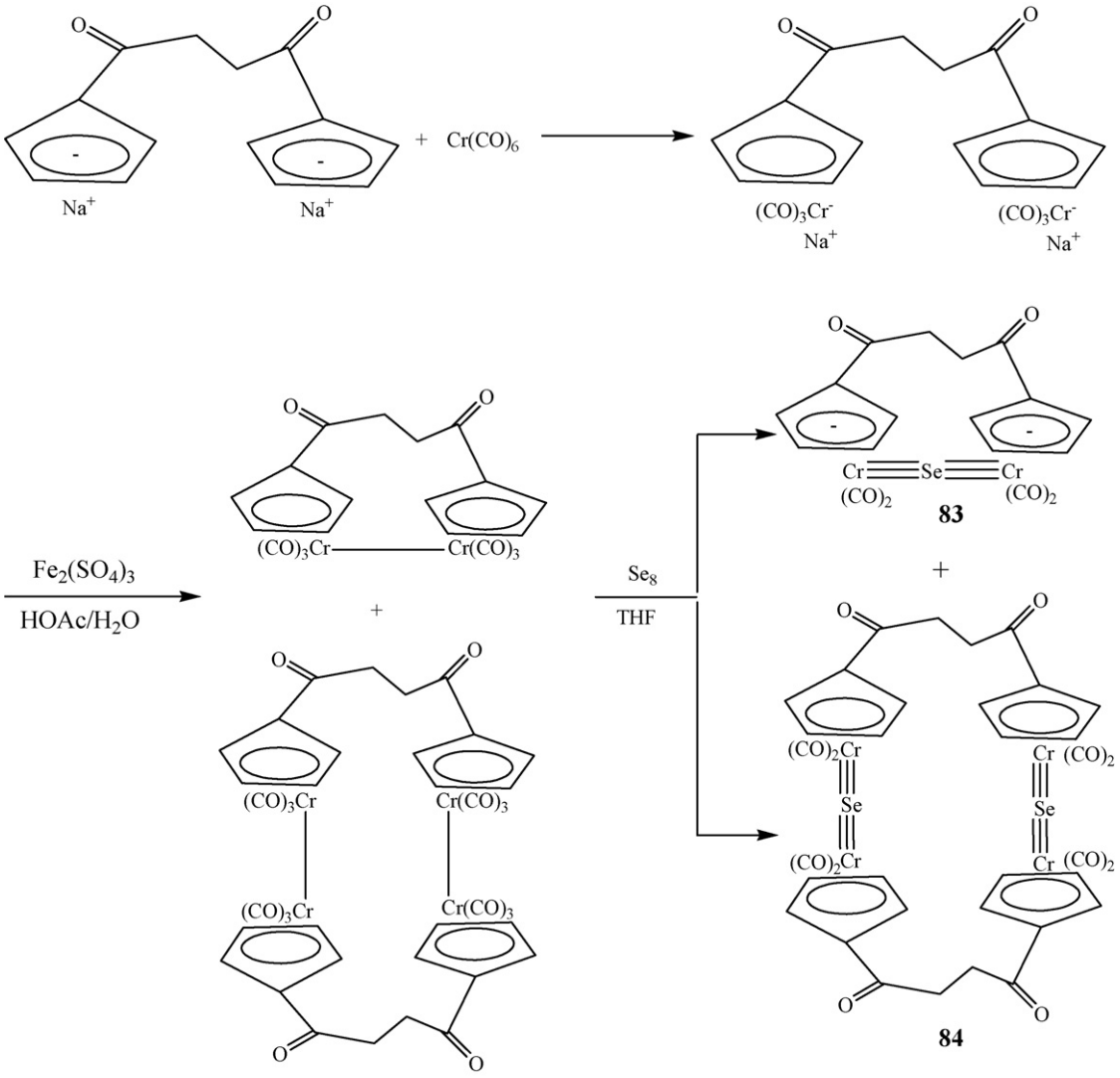

Scheme 25.

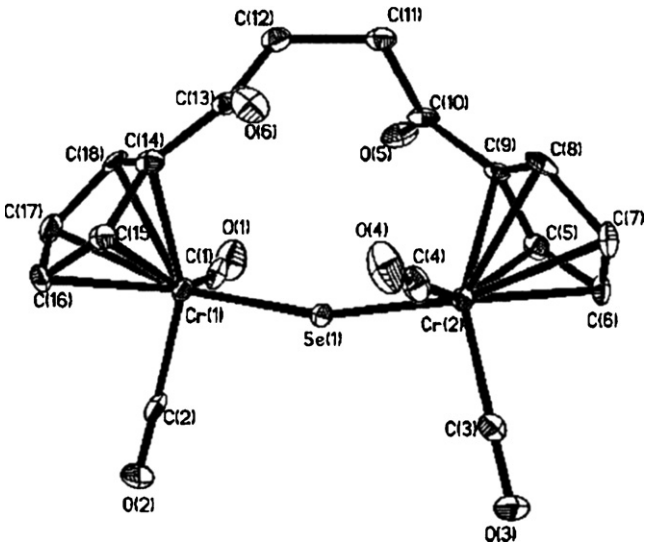

Fig. 58. ORTEP drawing of **83**. Reprinted with permission from Ref. [90]. Copyright (2004) American Chemical Society.

result in a change in size of the cage cavity and hence allow for some interesting coordination behavior. A nitro-capped cage **85** with N_3Se_3 donor set is known. A cobalt(III) complex of this sarcopagine ligand shows the encapsulated cobalt in a N_3Se_3 cage (Fig. 59) [91].

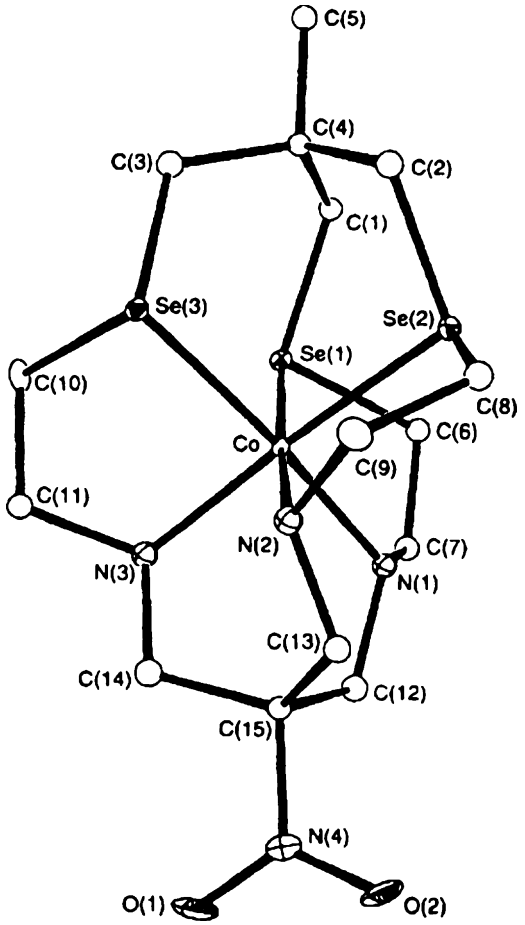

Fig. 59. Structure of the $[Co^{III}\mathbf{85}]^{3+}$ cation. Taken from Ref. [91]. Reproduced by permission of The Royal Society of Chemistry.

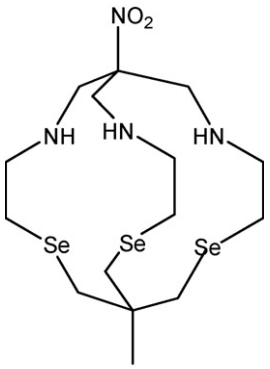

85

The cryptand **86** was synthesized from [2+3] condensation of tris(2-aminoehyl)amine and bis(*o*-formylphenyl) selenide using cesium ions as the template [75]. The formation of cryptand was confirmed from microanalysis and spectroscopic (IR, ^1H, ^{13}C, ^{77}Se NMR and FAB) data. A cryptand of the type **87** is also known [92].

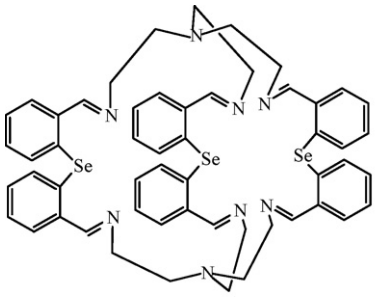

86

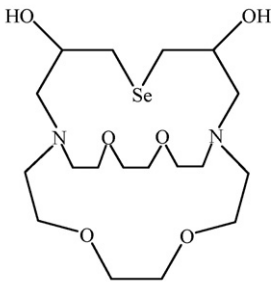

87

8. Overview

Following the discovery of sulfur coronands and their rich and interesting coordination chemistry, a similar development of the corresponding macrocyclic polyselena ethers was envisaged. Since the serendipitous discovery of selena-crown ethers by Pinto and co-workers, the synthesis and coordination chemistry studies of selena-macrocycles have received wide attention. Over the recent years, considerable effort has been directed towards the design and synthesis of new homo and mixed donor selenoether macrocyclic ligands to study their ligation properties toward transition and post-transition metal ions. Levason and co-workers have made a significant contribution in developing the chemistry of macrocyclic selenoethers by studying its (**8Se2**, **16Se4** and **24Se6**) coordination chemistry elaborately with d- and p-block elements and comparing the chemistry with cyclic polythiaethers and acyclic selenoethers. ^{77}Se-NMR spectroscopy, which is a major advantage, is exploited in predicting the structures of the selenium ligands/complexes in solution. To date most research on selena macrocycles has focused on exploratory synthetic work to determine the scope of their coordination chemistry. There is a need to expand the repertoire of available homo and mixed selenium macrocycles to exploit this class of macrocycles for other than metal coordination chemistry. Also, at present there are only a few examples in the literature of selena macrocycles being used as ligands for heavy and precious metals. Special attention should be given to the synthesis of macrocycles that can bind two or more different metal ions simultaneously and also to selenium-containing macropolycycles.

Acknowledgements

I gratefully acknowledge The Department of Science and Technology (India) for financial support under the scheme-"SERC Fast Track Proposals for Young Scientists" and BITS, Pilani-Goa Campus for supporting the research. I thank The Royal Chemical Society, American Chemical Society, Elsevier, Wiely InterSc. and Professor B. M. Pinto for permission to reproduce the figures. I would like to thank Prof. Lever and the referees for their helpful suggestions.

References

[1] (a) C.J. Pedersen, J. Am. Chem. Soc. 89 (1967) 7017;
(b) C.J. Pedersen, Angew. Chem. Int. Ed. Engl. 27 (1988) 1021.
[2] J.M. Lehn, Struct. Bond. (Berl.) 16 (1973) 1;
J.M. Lehn, Angew. Chem. Int. Ed. Engl. 27 (1988) 59.
[3] D.J. Cram, Angew. Chem. Int. Ed. Engl. 27 (1988) 1009.
[4] E.G. Hope, W. Levason, Coord. Chem. Rev. 122 (1993) 109.
[5] V.P. Litvinov, V.D. Dyachenko, Russ. Chem. Rev. 66 (1997) 923.
[6] W. Levason, S.D. Orchard, G. Reid, Coord. Chem. Rev. 225 (2002) 159.
[7] W. Levason, G. Reid, Compr. Coord. Chem. II 1 (2004) 399.
[8] A.K. Singh, S. Sharma, Coord. Chem. Rev. 209 (2000) 49.
[9] A. Ulman, J. Manassen, F. Frolow, D. Rabinovich, Tetrahedron Lett. 19 (1978) 167.
[10] (a) A. Ulman, J. Manassen, F. Frolow, D. Rabinovich, J. Am. Chem. Soc. 101 (1979) 7055;
(b) R.L. Hill, M. Gouterman, A. Ulman, Inorg. Chem. 21 (1982) 1450.
[11] (a) R.H. Mitchell, Can. J. Chem. (1980) 1398;
(b) R.H. Mitchell, K.S. Weerawarna, G.W. Busbnell, Tetrahedron Lett. 28 (1987) 5119.
[12] (a) H. Higuchi, S. Misumi, Tetrahedron Lett. 23 (1982) 5571;
(b) H. Higuchi, K. Tani, T. Otsubo, Y. Sakata, S. Misumi, Bull. Chem. Soc. Jpn. 60 (1987) 4027.
[13] L.R. Hanton, T. Kemmitt, Inorg. Chem. 32 (1993) 3648.
[14] (a) S. Muralidharan, M. Hojjatie, M. Firestone, H. Freiser, J. Org. Chem. 54 (1989) 393;
(b) M. Hojjatie, S. Muralidharan, H. Freiser, Tetrahedron 45 (1989) 1611.
[15] (a) B.M. Pinto, B.D. Johnston, R.J. Batchelor, F.W.B. Einstein, I.D. Gay, Can. J. Chem. 66 (1988) 2956;
(b) B.M. Pinto, B.D. Johnston, R.J. Batchelor, J.-H. Gu, J. Chem. Soc. Chem. Commun. (1988) 1087;
(c) B.M. Pinto, R.J. Batchelor, B.D. Johnston, F.W.B. Einstein, I.D. Gay, J. Am. Chem. Soc. 110 (1988) 2990;
(d) R.J. Batchelor, F.W.B. Einstein, I.D. Gay, J.-H. Gu, B.D. Johnston, B.M. Pinto, J. Am. Chem. Soc. 111 (1989) 6582;
(e) B.M. Pinto, B.D. Johnston, R. Nagelkerke, Heterocycles 28 (1989) 389.
[16] I. Cordova-Reyes, E. VandenHoven, A. Mohammed, B.M. Pinto, Can. J. Chem. 73 (1995) 113.
[17] R.J. Batchelor, F.W.B. Einstein, I.D. Gay, J.-H. Gu, S. Mehta, B.M. Pinto, X.-M. Zhou, Inorg. Chem. 39 (2000) 2558.
[18] I. Cordova-Reyes, H. Hu, J.-H. Gu, E. VandenHoven, A. Mohammed, S. Holdcroft, B.M. Pinto, Can. J. Chem. 74 (1996) 533.
[19] L.A. Ochrymowycz, C. Mak, J.D. Michna, J. Org. Chem. 39 (1974) 2079.
[20] H. Fujihara, M. Yabe, J.-J. Chiu, N. Furukawa, Tetrahedron Lett. 32 (1991) 4345.
[21] (a) H. Fujihara, M. Yabe, M. Ikemori, N. Furukawa, J. Chem. Soc. Perkin Trans. 1 (1993) 2145;
(b) H. Fujihara, M. Yabe, N. Furukawa, J. Chem. Soc. Perkin Trans. 1 (1996) 1783.
[22] R.D. Adams, K.T. McBride, Chem. Commun. (1997) 525.
[23] R.D. Adams, K.T. McBride, R.D. Rogers, Organometallics 16 (1997) 3895.
[24] R.D. Adams, J.L. Perrin, J.A. Queisser, J.B. Wolfe, Organometallics 16 (1997) 2612.
[25] D.G. Booth, W. Levason, J.J. Quirk, G. Reid, S.M. Smith, J. Chem. Soc. Dalton Trans. (1997) 3493.
[26] T. Kumagai, S. Akabori, Chem. Lett. (1989) 1667.
[27] M.K. Davies, M.C. Durrant, W. Levason, G. Reid, R.L. Richards, J. Chem. Soc. Dalton Trans. (1999) 1077.
[28] J. Connolly, M.K. Davies, G. Reid, J. Chem. Soc. Dalton Trans. (1998) 3833.
[29] W. Levason, J.J. Quirk, G. Reid, S.M. Smith, J. Chem. Soc. Dalton Trans. (1997) 3719.
[30] W. Levason, J.J. Quirk, G. Reid, J. Chem. Soc. Dalton Trans. (1996) 3713.
[31] D.J. Gulliver, E.G. Hope, W. Levason, S.G. Murray, G.L. Marshall, J. Chem. Soc. Dalton Trans. (1985) 1265.
[32] N.R. Champness, W. Levason, J.J. Quirk, G. Reid, C.S. Frampton, Polyhedron 14 (1995) 2753.
[33] W. Levason, J.M. Manning, P. Pawelzyk, G. Reid, Eur. J. Inorg. Chem. (2006) 4380.
[34] W. Levason, G. Reid, S.M. Smith, Polyhedron 16 (1997) 4253.
[35] P.F. Kelly, W. Levason, G. Reid, D.J. Willams, J. Chem. Soc. Chem. Commun. (1993) 1716.
[36] T.-F. Lai, C.-K. Poon, J. Chem. Soc. Dalton Trans. (1982) 1465.
[37] M.K. Davies, W. Levason, G. Reid, J. Chem. Soc. Dalton Trans. (1998) 2185.
[38] N.R. Champness, P.F. Kelly, W. Levason, G. Reid, A.M.Z. Slawin, D.J. Williams, Inorg. Chem. 34 (1995) 651.
[39] R.J. Batchelor, F.W.B. Einstein, I.D. Gay, J.-H. Gu, B.M. Pinto, X. Zhou, Inorg. Chem. 35 (1996) 3667.
[40] M.C. Durrant, R.L. Richards, S. Firth, J. Chem. Soc. Perkin Trans. 2 (1993) 445.
[41] W. Levason, J.J. Quirk, G. Reid, Inorg. Chem. 33 (1994) 6120.
[42] R.J. Batchelor, F.W.B. Einstein, I.D. Gay, J.-H. Gu, B.M. Pinto, X.-M. Zhou, J. Am. Chem. Soc. 112 (1990) 3706.
[43] V.B. Pett Jr., L.L. Diaddario, E.R. Dockal, P.W. Corfield, C. Ceccarelli, M.D. Glick, L.A. Ochrymowycz, D.B. Rorabacher, Inorg. Chem. 22 (1983) 3661.
[44] R.J. Batchelor, F.W.B. Einstein, I.D. Gay, J.-H. Gu, B.M. Pinto, X.-M. Zhou, Can. J. Chem. 78 (2000) 598.
[45] R.J. Batchelor, F.W.B. Einstein, I.D. Gay, J.-H. Gu, B.M. Pinto, J. Organomet. Chem. 411 (1991) 147.
[46] (a) E.R. Dockal, L.L. Diaddario, M.D. Glick, D.B. Rorabacher, J. Am. Chem. Soc. 99 (1997) 4530;
(b) P.W.R. Corfield, C. Ceccarelli, M.D. Glick, I.W.-Y. Moy, L.A. Ochrymowycz, D.B. Rorabacher, J. Am. Chem. Soc. 107 (1985) 2399;
(c) B. de Groot, S.J. Loeb, Inorg. Chem. 28 (1989) 3573;
(d) J.R. Hartman, S.R. Cooper, J. Am. Chem. Soc. 108 (1986) 1202;
(e) R.O. Gould, A.J. Lavery, M. Schröder, J. Chem. Soc. Chem. Commun. (1985) 1492.
[47] A.J. Barton, N.J. Hill, W. Levason, G. Reid, J. Am. Chem. Soc. 123 (2001) 11801.
[48] N.J. Hill, W. Levason, G. Reid, Inorg. Chem. 41 (2002) 2070.
[49] A.J. Barton, A.R.J. Genge, W. Levason, G. Reid, J. Chem. Soc. Dalton Trans. (2000) 2163.
[50] A.J. Barton, N.J. Hill, W. Levason, B. Patel, G. Reid, Chem. Commun. (2001) 95.
[51] A.J. Barton, N.J. Hill, W. Levason, G. Reid, J. Chem. Soc. Dalton Trans. (2001) 1621.
[52] W. Levason, M. Matthews, R. Patel, G. Reid, M. Webster, New J. Chem. 27 (2003) 1784.
[53] N.J. Hill, W. Levason, R. Patel, G. Reid, M. Webster, Dalton Trans. (2004) 980.
[54] W. Levason, G. Reid, J. Chem. Soc. Dalton Trans. (2001) 2953.
[55] (a) T. Tsuchiya, T. Shimizu, N. Kamigata, J. Am. Chem. Soc. 123 (2001) 11534;
(b) T. Tsuchiya, T. Shimizu, K. Hirabayashi, N. Kamigata, J. Org. Chem. 67 (2002) 6632;
(c) T. Tsuchiya, T. Shimizu, K. Hirabayashi, N. Kamigata, J. Org. Chem. 68 (2003) 3480.
[56] T. Shimizu, M. Kawaguchi, T. Tsuchiya, K. Hirabayashi, N. Kamigata, Org. Lett. 5 (2003) 1443.
[57] T. Shimizu, M. Kawaguchi, T. Tsuchiya, K. Hirabayashi, N. Kamigata, J. Org. Chem. 70 (2005) 5036.
[58] R. Pietschnig, S. Schäfer, K. Merz, Org. Lett. 5 (2003) 1867.
[59] F.C.J.M. Van Veggel, W. Verboom, D.N. Reinhoudt, Chem. Rev. 94 (1994) 279.
[60] S. Tomoda, M. Iwaoka, J. Chem. Soc. Chem. Commun. (1990) 231.
[61] A. Mazouz, P. Meunier, M.M. Kubicki, B. Hanquet, R. Amardeil, C. Bornet, A. Zahidi, J. Chem. Soc. Dalton Trans. (1997) 1043.
[62] W.P. Li, J. Wu, X.F. Liu, H.S. Xu, Chem. J. Chin. Univ. 16 (1995) 1559.
[63] V.W.-W. Yam, Y.-L. Pui, W.-P. Li, K.K.-W. Lo, K.-K. Cheung, J. Chem. Soc. Dalton Trans. (1998) 3615.
[64] D.W. Johnson, H.K. Mayer, J.P. Minard, J. Banaticla, C. Miller, Inorg. Chim. Acta 144 (1988) 167.
[65] A. Mazouz, J. Bodiguel, P. Meunier, B. Gautheron, Phosphorus, Sulfur Silicon Relat. Elem. 61 (1991) 247.
[66] C. Bornet, R. Amardeil, P. Meunier, J.C. Daran, J. Chem. Soc. Dalton Trans. (1999) 1039.
[67] (a) W. Li, X. Liu, H. Xu, Huaxue Xuebao 52 (1994) 1082;
W. Li, X. Liu, H. Xu, Chem. Abs. 122 (1994) 291007;
(b) X. Liu, W. Li, L. Zhang, X. Lu, H. Xu, Chin. Chem. Lett. 3 (1992) 255;
X. Liu, W. Li, L. Zhang, X. Lu, H. Xu, Chem. Abs. 117 (1992) 111767;
(c) X. Liu, W. Li, L. Zhang, X. Lu, H. Xu, Huaxue Xuebao 51 (1993) 575;
X. Liu, W. Li, L. Zhang, X. Lu, H. Xu, Chem. Abs. 119 (1993) 216159;
(d) W. Li, X. Liu, X. Lu, H. Xu, Gaodeng Xuexiao Huaxue Xuebao 15 (1994) 947;
W. Li, X. Liu, X. Lu, H. Xu, Chem. Abs. 122 (1994) 17798;
(e) W. Li, X. Liu, X. Lu, H. Xu, Chin. Chem. Lett. 5 (1994) 49;
W. Li, X. Liu, X. Lu, H. Xu, Chem. Abs. 121 (1994) 35714;
(f) W. Li, X. Liu, H. Xu, Y. Huang, S. Hu, Chin. J. Chem. 13 (1995) 47;
W. Li, X. Liu, H. Xu, Y. Huang, S. Hu, Chem. Abs. 122 (1995) 229227;
(g) J. Wu, X. Liu, H. Xu, Gaodeng Xuexiao Huaxue Xuebao 17 (1996) 1070;
J. Wu, X. Liu, H. Xu, Chem. Abs. 125 (1996) 211131.
[68] (a) Y. Liu, S.-P. Dong, Y. Inoue, T. Wada, J. Chem. Res.(S) (1999) 284;
(b) Y. Liu, H.-Y. Zhang, Chin. J. Chem. 18 (2000) 66;
(c) Y. Liu, H.-Y. Zhang, L.-X. Chen, X.-W. He, J. Chem. Res.(S) (2000) 216.
[69] M.J. Hesford, W. Levason, M.L. Matthews, G. Reid, Dalton Trans. (2003) 2852.
[70] X. Zeng, X. Han, L. Chen, Q. Li, F. Xu, X. He, Z.-Z. Zhang, Tetrahedron Lett. 43 (2002) 131.
[71] Y. Liu, J.-R. Han, Y.-L. Zhao, H.-Y. Zhang, Z.-Y. Duan, J. Incl. Phenom. Mac. Chem. 51 (2005) 191.
[72] (a) X. Wei, L. Xiufang, L. Xueran, X. Hansheng, Wuhan Univ. J. Nat. Sci. 2 (1997) 464;
(b) X. Hansheng, X. Guangya, W. Jun, L. Xiufang, Wuhan Univ. J. Nat. Sci. 4 (1999) 85.
[73] Y. Liu, J.-R. Han, Y. Chen, A. Yu, Z.-Y. Duan, H.-Y. Zhang, Supramol. Chem. 17 (2005) 623.
[74] A. Panda, S.C. Menon, H.B. Singh, C.P. Morley, R. Bachman, T.M. Cocker, R.J. Butcher, Eur. J. Inorg. Chem. (2005) 1114.
[75] A. Panda, S.C. Menon, H.B. Singh, R.J. Butcher, J. Organomet. Chem. 623 (2001) 87.

[76] U. Patel, H.B. Singh, R.J. Butcher, Eur. J. Inorg. Chem. (2006) 5089.
[77] S.C. Menon, H.B. Singh, R.P. Patel, S.K. Kulshreshtha, J. Chem. Soc. Dalton Trans. (1996) 1203.
[78] S.C. Menon, A. Panda, H.B. Singh, R.J. Butcher, Chem. Commun. (2000) 143.
[79] A. Panda, Novel organochalcogen derivatives: ligands, reagents and thiol peroxidase mimics, Ph.D. thesis, 2000.
[80] S. Panda, S.S. Zade, H.B. Singh, R.J. Butcher, Eur. J. Inorg. Chem. (2006) 172.
[81] S. Panda, H.B. Singh, R.J. Butcher, Chem. Commun. (2004) 322.
[82] S. Panda, H.B. Singh, R.J. Butcher, Inorg. Chem. 43 (2004) 8532.
[83] (a) K. Kobayashi, H. Izawa, K. Yamaguchi, E. Horn, N. Furukawa, Chem. Commun. (2001) 1428;
(b) J.L. Li, J.B. Meng, Y.M. Wang, J.T. Wang, T. Matsuura, J. Chem. Soc. Perkin Trans. 1 (2001) 1140;
(c) S.K. Tripathi, B.L. Khandelwal, S.K. Gupta, Phosphorus, Sulfur Silicon Relat. Elem. 177 (2002) 2285;
(d) M.J. Hesford, W. Levason, M.L. Matthews, S.D. Orchard, G. Reid, Dalton Trans. (2003) 2434.
[84] G.K. Anderson, in: E.W. Abel, F.G.A. Stone, G. Wilkinson (Eds.), Comprehensive Organometallic Chemistry II, 9, Pergamon, Oxford, 1995.
[85] C.M. Bates, P.K. Khanna, C.P. Morley, M.D. Vaira, Chem. Commun. (1997) 913.
[86] A. Bashall, M. Mcpartlin, B.P. Murphy, H.R. Powell, S. Waikar, J. Chem. Soc. Dalton Trans. (1994) 1383.
[87] S. Panda, S.S. Zade, A. Panda, H.B. Singh, R.J. Butcher, J. Organomet. Chem. (2006) 2793.
[88] S. González-Calera, D.J. Eisler, J.V. Morey, M. McPartlin, S. Singh, D.S. Wright, Angew. Chem. Int. Ed. 47 (2008) 1111.
[89] G. Hua, Y. Li, A.M.Z. Slawin, J.D. Woollins, Angew. Chem. Int. Ed. 47 (2008) 2857.
[90] L.-C. Song, H.-W. Cheng, X. Chen, Y.-J. Hua, S.-X. Lou, Q.-M. Hu, Organometallics 23 (2004) 3366.
[91] R. Bhula, A.P. Arnold, G.J. Gainsford, W.G. Jackson, Chem. Commun. (1996) 143.
[92] N.G. Luk'yanenko, A.S. Reder, Zh. Obshch. Khim 59 (1989) 1690.